A control-theoretic approach to dynamic optimization of metabolic networks

A dissertation submitted for the degree of

Doctor of Philosophy

by

Diego Antonio Oyarzún Rodríguez

Supervisor: Prof. Peter Wellstead
Co-supervisor: Dr. Dimitrios Kalamatianos

Hamilton Institute

National University of Ireland Maynooth

Ollscoil na hÉireann, Má Nuad

February 2010

Contents

Abstract

The characterization of general control principles that underpin metabolic dynamics is an important part of systems analysis in biology. It has been long argued that many biological regulatory mechanisms have evolved so as to optimize cellular adaptation in response to external stimuli. In this thesis we use an optimal control framework to solve dynamic optimization problems associated with metabolic dynamics. The analysis is based on a nonlinear control-affine model of a metabolic network with the enzyme concentrations as control inputs.

We consider the optimization of time-dependent enzyme concentrations to activate an unbranched network and reach a prescribed metabolic flux. The solution accounts for time-resource optimality under constraints in the total enzymatic abundance. We identify a temporal pattern in the solution that is consistent with previous experimental and numerical observations. Our analysis suggests that this behaviour may appear in a broader class of networks than previously considered.

In addition, we address the optimization of time-dependent enzyme expression rates for a metabolic network coupled with a model of enzyme dynamics. The formulation accounts for the transition between two metabolic steady states in networks with arbitrary stoichiometries and enzyme kinetics. We consider a finite horizon quadratic cost function that weighs the deviations of metabolites, enzymes and their expression rates from their target values, together with the time-derivative of the expression rates. The problem is recast as an iterative sequence of Linear Quadratic Tracking problems, and we derive conditions under which the iterations converge to a suboptimal solution of the original problem. Additionally, if constant metabolite concentrations are enforced, the nonlinear system can be written as a linear Differential-Algebraic system. In the infinite horizon case the problem can be recast as a standard Linear Quadratic Regulator problem for a lower-dimensional system, the solution of which is readily available.

Acknowledgements

My supervisors, Prof. Peter Wellstead and Dr. Dimitrios Kalamatianos, deserve my sincere gratitude for their incredible patience and for trusting in my ability to pursue this project. Dimitrios' enduring support was critical in the tough times of this project, and Prof. Wellstead's wise guidance has always encouraged me to push the ideas further.

The expert eye of Prof. Rick Middleton has been an important source of ideas for several problems in this thesis. Prof. Brian Ingalls (University of Waterloo, Canada) was the one that suggested the starting idea for this project, and I also thank his invitation for a fruitful research internship at his Department. My thanks also go to Ben-Fillippo Krippendorff for introducing me to an interesting research topic that was carried out in parallel to this thesis.

A number of people have made my stay in Ireland an enjoyable experience, especially Dirk Fey, Miriam Rodríguez, Jesus Valcárcel and Max von Kleist. I am grateful to Steven Strachan, Rade Stanojević, Mark Verwoerd and Oliver Mason for welcoming me at the Hamilton Institute and easing my adaptation to the new environment. I also thank Rosemary Hunt and Kate Moriarty for their willingness to help in all sorts of administrative matters.

I must acknowledge the role of Prof. Mario Salgado (Universidad Federico Santa María, Chile). He introduced me to academic research in the first place, and I feel sure that many signs of his rigour and teachings can be found throughout this work.

Nothing of this would be possible without the never-ending support of my family: Carmen Gloria, Eduardo, and my brother Orlando. Perhaps they do not notice it, but they have been constantly present and I have always felt them backing me up.

Finally, I thank Andrea Weiße for her warm support in these three years while en-

during the obstacles and the painful experience of proofreading this whole manuscript.

Dedicado a mi madre, Carmen Gloria.

Chapter 1

Introduction

1.1 Motivation

A fundamental property of organisms is their ability to self-regulate and sustain their functions under variable environmental conditions [1]. The regulatory mechanisms that enable this robustness are complex and largely unknown, but their functioning can be conceptually compared to man-made control systems [2]. As scientists gain more knowledge on the mechanisms that underlie cellular regulation, intricate arrays of feedback structures are being revealed. An attractive idea is to analyze these systems with methods from Systems and Control theory, the use of which has gained strength in the field of Systems Biology [3, 4, 5] and, more recently, with the emergence of Synthetic Biology [6].

The use of control-theoretic principles to analyze biological systems is certainly not new and dates back several decades. In fact, some of the seminal works in Systems and Control theory by N. Wiener [2], L. von Bertalanffy [7] and M. Mesarović [8] were inspired by biological problems. The resurgence of this trend has been fostered by the availability of experimentally validated models, which is thanks to the tremendous progress made in modern experimental methods. These models not only provide a solid ground for carrying out control-theoretic analyses, but some of their unique features also pose challenging new problems for Systems and Control theory [9].

Since cellular processes rely on complex regulatory architectures, an important goal is the identification of design principles that underlie this complexity [10, 11, 12]. One of the basic principles in evolutionary theory is that mutation and natural selection favour phenotypes that benefit the fitness of an organism [13]. The idea that biological regulation has evolved so as to improve fitness is the basis for using optimization theory to understand the observed properties of organisms [14, 15].

Traditional approaches have mostly aimed at macroscopic properties such as organ sizes or feeding behaviour in animals [16, 17]. However, with the recent advent of detailed mathematical models at a biochemical level, optimization techniques are also being used for analyzing the biochemical "circuitry" that underpins cellular dynamics [18].

1.2 Topic of the thesis

Cellular activity is determined by the interaction among a large number of chemical species. These biochemical reactions do not occur in isolation and are interconnected by sharing species as reactants or products. A collection of interacting reactions is referred to as a *biochemical network*. Different types of chemical compounds take part in these networks, with proteins being by far the most abundant [19]. Proteins contribute to nearly all cellular functions and are synthesized via gene expression according to the information encoded in the DNA [20].

Many cellular functions are commanded by changes in gene expression in response to environmental stimuli. As illustrated in Figure 1.1, external stimuli are sensed by receptor molecules in the cell membrane and trigger the transmission of a signal to the nucleus. This information modulates gene expression so as to induce specific cellular responses [20].
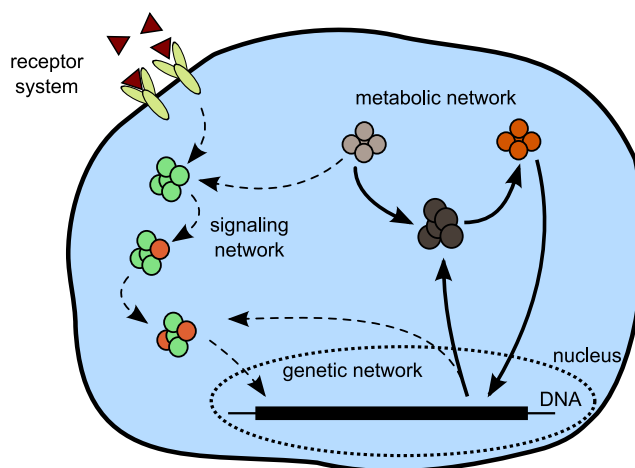
Figure 1.1. Biochemical networks in the cellular response to environmental stimuli. In this thesis we study metabolic networks controlled by gene expression (solid lines).

The interaction among the different networks in Figure 1.1 allows the regulation of cellular activity according to the environmental conditions. In this thesis we focus on the regulation of *metabolic networks*. These convert nutrients into usable energy and synthesize a variety of chemical species required by the cell [20]. The chemical species involved in a metabolic network are generally known as *metabolites*. Metabolic networks support many cellular functions and their dynamics play a major role in cell fitness. In addition, specific functions can be realized by alternative networks [21], but it is not clear why a particular metabolic design is preferred over the different alternatives [22]. This has led to postulate that present-day metabolic systems have been optimized through evolutionary processes [18, 23, 24, 25]. In this context, the fundamental premise of this thesis is that metabolic systems can be rationalized as solutions of optimization problems which are coherent with the cellular functions they support.

Metabolic reactions are enabled by a special type of proteins known as *enzymes*. Enzymes are subject to degradation processes and hence their dynamics are governed by the balance between gene expression and protein degradation. Although this is a simplified view that overlooks relevant subprocesses of gene expression (such as transcriptional and translational dynamics [20]), it facilitates the use of a Systems and Control approach to treat metabolic dynamics. Moreover, some metabolites can affect gene expression by interacting with intermediate molecules that are able to attenuate or amplify the rate at which an enzyme is synthesized [26]. With this in mind, we can regard metabolic networks as systems subject to feedback control from gene expression, as shown in Figure 1.2.
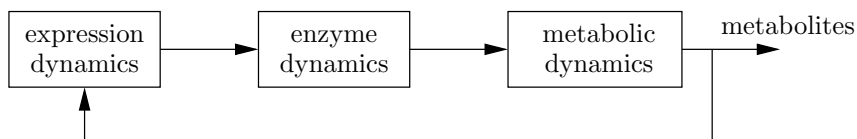
Figure 1.2. Genetic regulation of metabolic networks as a feedback control system.

Most studies in metabolic optimization neglect enzyme dynamics and consider enzymatic concentrations as *fixed parameters* of the metabolic model. This simplification is founded on the fact that genetic and enzyme dynamics occur in a considerably slower time-scale than their metabolic counterpart [27]. Several recent studies, however, have emphasized the importance of enzyme dynamics in the con-

3

text of metabolic optimization, e.g. [28, 29]. The effect of gene expression becomes important in cellular decisions subject to environmental changes. These may induce a "genetic reprogramming" so as to adapt the metabolic activity by suppressing and activating specific networks. An example of this is the adaptation of bacteria *E. coli* to diverse nutritional conditions, either to avoid starvation under nutrient depletion [30], maximize growth under nutrient abundance [31], or to choose a specific nutrient source from a mixed medium [32].

In this thesis we address metabolic optimization within an optimal control framework. A distinctive feature is the use of a *nonlinear control-affine* model to describe the dynamics of metabolite concentrations in response to *time-dependent* enzyme concentrations. This is done in two alternative ways:

(a) by regarding the enzymes as control inputs to the metabolic network, as shown in Figure 1.3 (top),

(b) by regarding the enzyme expression rates as control inputs to a system composed of a metabolic network coupled with a model for enzyme dynamics, as illustrated in Figure 1.3 (bottom).
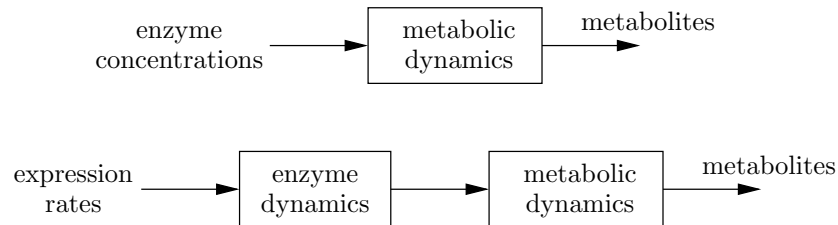
Figure 1.3. Top: metabolic network with enzyme concentrations as control inputs. Bottom: coupled system for a metabolic network and enzyme dynamics, with the enzyme expression rates as control inputs.

1.3 Contributions and outline of the thesis

In **Chapter 2** we review ideas behind dynamic modeling of metabolic networks. Most of this material is standard in the literature, but one contribution should be remarked:

- The standard linear stoichiometric model is rewritten explicitly in terms of the reaction kinetics with the enzyme concentrations as control inputs, as in

Figure 1.3 (top). This yields a novel *nonlinear control-affine* model that is amenable to control-theoretic analysis.

In **Chapter 3** we review the main existing methods for static and dynamic optimization of metabolic networks. Dynamic optimization approaches are not abundant, and with the exception of few cases, optimal control methods have not been used in their full potential.

The main results of this thesis are presented throughout Chapters 4, 5 and 6, where we use the nonlinear control-affine model introduced in Chapter 2 for the analysis of optimal control problems associated with metabolic dynamics.

In **Chapter 4** we address a nonlinear optimal control problem for the activation of unbranched networks under simplex-type constraints on the enzyme concentrations. We use the setup of Figure 1.3 (top) and consider time-dependent enzyme concentrations to minimize a combination of the time taken by the activation and the integral of the enzyme trajectories. The contributions of this chapter are:

- The derivation of the general bang-bang form of the solution. The use of Pontryagin's Minimum Principle reveals a sequential pattern in the time courses of the optimal enzyme profiles that is consistent with previous experimental and numerical observations [28, 29]. In contrast to previous studies, the solution is obtained for a general class of irreversible monomolecular enzyme kinetics that includes, but is not limited to, the common Mass Action, Michaelis-Menten, and Hill kinetics.

- An equivalent static nonlinear optimization problem that can be used to obtain numerical solutions of the original optimal control problem.

- The derivation of a formula for the achievable supremum flux, which arises as a consequence of the saturable enzyme kinetics and the enzymatic constraints.

- The sensitivity analysis of the optimal solution via numerical investigations of cases studies. The sensitivity is shown to be consistent with the common assertion that unbranched networks are more sensitive to those reactions located toward the end of the reaction chain.

- A novel framework for integrating enzyme dynamics into the metabolic model. This is realized by coupling the nonlinear control-affine system with a linear

model that describes the balance between gene expression and enzyme degradation. As in Figure 1.3 (bottom), the enzyme expression rates are regarded as control inputs.

The coupled model is used in Chapters 5 and 6 for the optimization of time-dependent enzyme expression rates in networks with arbitrary topologies and kinetics. In both chapters we use the setup of Figure 1.3 (bottom) and consider the minimization of a quadratic cost associated to the transition between two prescribed steady states. The cost weighs the deviation of the state trajectories from their target values, together with the time-derivative of the expression rates representing the genetic effort for enzyme synthesis.

In **Chapter 5** we address the general nonlinear problem for a finite horizon cost function. The contributions of this chapter are:

- An iterative algorithm for computing a suboptimal solution of the nonlinear problem. The method is based on a global approximation of the nonlinear dynamics by means of a sequence of linear time-variant systems. The original problem can then be approximated by a sequence of Linear Quadratic Tracking problems, the solution of which can be readily computed using well-known results. As opposed to previous studies [33], the iterative scheme relies on the solution of a differential Lyapunov equation at each iteration. This may provide computational advantages over the traditional Riccati equation approach for high-dimensional networks.

- The convergence analysis of the algorithm. Provided that the optimization horizon is sufficiently small, the iterations are shown to converge to a unique fixed-point for a broad range of kinetics and arbitrary stoichiometries.

In **Chapter 6** we study a special case of the previous problem. We consider an infinite horizon cost function and impose the additional constraint of constant metabolite concentrations along the whole optimization interval. The contributions of the chapter are:

- An equivalent Differential-Algebraic Equation (DAE) model for the enzyme dynamics. It is shown that imposing constant metabolites translates into algebraic constraints on the enzyme trajectories and expression rates.

- The reformulation of the problem as a Linear Quadratic Regulator (LQR) problem for an unconstrained lower-dimensional linear system. We use a state

transformation to decouple the algebraic and differential parts of the DAE system. This allows for a parameterization of all controls that satisfy the algebraic constraint in terms of a lower-dimensional control variable. Provided that the weight matrices are positive definite, this problem is shown to satisfy the stabilizability and detectability conditions of the standard LQR problem, and thus its solution can be readily obtained.

We conclude in **Chapter 7** summarizing the main ideas of the thesis and pointing out some open questions for future research. Some of the technical results used in the thesis are briefly presented in the appendices: classic optimal control results are described in **Appendix A**, and a fixed-point theorem that is used in Chapter 5 is presented in **Appendix B**.

Some of the results of this thesis have been presented in invited talks at the *3rd Biennial Regional Meeting on Nonlinear Control and its Applications* (University of Waterloo, Canada, 2008), *Stats & Control Meeting* (Université de Montréal, Canada, 2008), and *3rd Conference of Young Chilean Scientists* (Max Planck Institute for Experimental Medicine, Göttingen, Germany, 2009). In addition, this thesis has led to the following peer-reviewed publications:

- D. A. Oyarzún, B. P. Ingalls, R. H. Middleton, and D. Kalamatianos. Sequential activation of metabolic pathways: a dynamic optimization approach. *Bulletin of Mathematical Biology*, vol. 71, no. 8, pp. 1851–1872, 2009.

- D. A. Oyarzún, B. P. Ingalls, R. H. Middleton, and D. Kalamatianos. Optimal metabolic pathway activation. In *Proceedings of the 17th IFAC World Congress*, pp. 12587–12592, Seoul, Korea, 2008.

- D. A. Oyarzún, B. P. Ingalls, and D. Kalamatianos. Optimal metabolic regulation by time varying enzyme activities: a control theoretic approach. In *Proceedings of Foundations of Systems Biology & Engineering*, pp. 491–496, Stuttgart, Germany, 2007.

1.4 Related work

As part of a collaboration with Ben-Fillippo Krippendorff and Dr. Wilhelm Huisinga from the Computational Physiology Group at the Hamilton Institute, we have studied the dynamics of cell membrane receptor systems in response to inhibitory protein

drugs. Therapeutic protein drugs have an increasing role in the treatment of cancer and other complex diseases [34]. They repress signal transmission from the extracellular medium to the nucleus (see Figure 1.1) by competitive binding to receptor molecules, so as to prevent the natural ligand from triggering undesirable cellular responses (such as uncontrolled growth in the case of cancer).

This research has been focused on the analysis of receptor dynamics at a single cell level and their interaction with whole-body pharmacokinetic models. The results have been omitted from this thesis to avoid redundancies with the Ph.D. Thesis of Ben-Fillippo Krippendorff [35]. Some of them have been presented in:

B. F. Krippendorff, D. A. Oyarzún, and W. Huisinga. Ligand accumulation counteracts therapeutic inhibition in receptor systems. In *Proceedings of Foundations of Systems Biology & Engineering*, pp. 173–176, Denver, USA, 2009.

B. F. Krippendorff, D. A. Oyarzún, and W. Huisinga. Optimizing the inhibition of Receptor Tyrosine Kinases in cancer treatment. In *BioSysBio Conference*, University of Cambridge, UK, 2009.

Chapter 2

Dynamic models of metabolic networks

2.1 Introduction

As with any physical system, biochemical models are an approximation of the real system and their accuracy will depend on the assumptions made in the model construction. In the case of metabolic networks, the standard approach is to use deterministic models in the form of Ordinary Differential Equations (ODE)[36, 37]. Deterministic models perform generally well because the chemical species appear in large molecular numbers and hence the stochastic effects average out [38].

In this chapter we present the main ideas behind ODE models of metabolic networks. In these models the state variable is composed by the concentrations of the different chemical species interacting in the network. The models are based on the *law of mass action*, which is a basic principle for modeling biochemical systems. The aim is to describe a metabolic network with models that are amenable for control-theoretic analyses. We shall distinguish between models that only describe the network topology, called *stoichiometric models*, and models that also include the (possibly) nonlinear behaviour of each reaction, called *kinetic models*. We also stress the importance of genetic regulation of metabolic networks, whereby gene expression can be regarded as a feedback "controller" that drives the network between different operating points.

The chapter is organized as follows: we begin in Section 2.2 by introducing the law of mass action and deriving the models of saturable enzyme kinetics for single biochemical reactions. These ideas are extended to whole reaction networks in Section 2.3, where we also present some illustrative examples. We conclude in Section 2.4 with a discussion on the regulation of metabolic network and its control-

9

theoretic interpretation.

2.2 Models of single biochemical reactions

2.2.1 The law of mass action

Consider the following reaction with n reactants and m products

$$\sum_{i=1}^{n} \alpha_i R_i \xrightarrow{v} \sum_{i=1}^{m} \beta_i P_i. \tag{2.2.1}$$

The constants $\alpha_i, \beta_i \in \mathbb{N}$ denote the stoichiometric coefficients of the reactants and products, respectively. The variables of interest are the time-dependent concentrations of the different species, denoted as $R_i(t)$ and $P_i(t)$, together with the rate at which the reaction occurs, denoted as v. We write the reactant and product concentration vectors as

$$
\begin{aligned}
R &= \begin{bmatrix} R_1 & R_2 & \dots & R_n \end{bmatrix}^T, \\
P &= \begin{bmatrix} P_1 & P_2 & \dots & P_n \end{bmatrix}^T,
\end{aligned} \tag{2.2.2}
$$

respectively. The concentrations are measured in molarity units [M] or [mol/l] and the rate in units of molarity per time. The reaction rate can be expressed as a function of the species concentrations, i.e. $v = v(R, P)$, so that the rate of change of the species concentrations is given by

$$
\begin{aligned}
\frac{\mathrm{d}R_i}{\mathrm{d}t} &= -\alpha_i v(R, P), \quad i = 1, 2, \dots, n, \\
\frac{\mathrm{d}P_i}{\mathrm{d}t} &= \beta_i v(R, P), \quad i = 1, 2, \dots, m.
\end{aligned} \tag{2.2.3}
$$

The reaction rate can be decomposed into forward (v_+) and backward (v_-) rates as

$$v(R, P) = v_+(R) + v_-(P). \tag{2.2.4}$$

Assuming that the species are present in large molecular numbers and a spatially homogeneous medium (also known as a "well-stirred" medium), the reaction rates

are proportional to the product of the reactant concentrations. Thus we write

$$v_+(R) = k_+ \prod_{i=1}^{n} R_i^{\alpha_i},$$
$$v_-(P) = k_- \prod_{i=1}^{m} P_i^{\beta_i}. \qquad (2.2.5)$$

This is known as the *law of mass action* for biochemical reactions, see e.g. [36, 37]. The constants $k_+ > 0$ and $k_- > 0$ are known as the forward and backward *kinetic* constants, respectively. When $v = 0$, it is said that the reaction is in *chemical equilibrium* and

$$K_{\mathrm{eq}} = \frac{k_+}{k_-} = \frac{\prod_{i=1}^{m} P_{i\,\mathrm{eq}}^{\beta_i}}{\prod_{i=1}^{n} R_{i\,\mathrm{eq}}^{\alpha_i}}, \qquad (2.2.6)$$

is called the equilibrium constant of the reaction. $R_{i\,\mathrm{eq}}$ and $P_{i\,\mathrm{eq}}$ are the species concentrations when the equilibrium is reached. The equilibrium should be understood in the sense that the forward and backward reaction rates are equal, and thus the net rate is zero (this does not imply that the forward and backward reactions are not occurring). Although all biochemical reactions are *reversible* (composed by a forward and a backward reaction), when $K_{\mathrm{eq}} \gg 1$ the forward reaction is strongly favoured. In those cases, it is said that the reaction is *irreversible* and it is common to assume that $v_- = 0$ and write reaction (2.2.1) as

$$\sum_{i=1}^{n} \alpha_i R_i \xrightarrow{v} \sum_{i=1}^{m} \beta_i P_i, \qquad (2.2.7)$$

with rate

$$v(R) = k_+ \prod_{i=1}^{n} R_i^{\alpha_i}. \qquad (2.2.8)$$

A broad range of biochemical reactions can be described with the law of mass action. The transient behaviour of the reaction can then be obtained by solving the ODEs in (2.2.3) for given initial conditions. In the context of metabolic networks we are interested in a special class of reactions, namely those that are catalyzed by specific enzymatic molecules. Although these can be readily described with the law of mass action, their particular features demand the use of specialized dynamic models.

2.2.2 Enzymatic reactions

Many of the biochemical reactions in a cell do not occur spontaneously in the environment (that is, they have a very small equilibrium constant K_{eq}). These "improbable" reactions can occur inside a cell due to enzyme molecules that catalyze them with a high degree of specificity. Enzymes are proteins that remain unchanged by the reactions they catalyze. The catalytic effect leads to rate accelerations of typically about 10^6 to 10^{12} fold as compared to the spontaneous reaction [37]. The thermodynamic basis for this effect is related to the ability of an enzyme to decrease the *free energy* of the reaction, the details of which can be found in standard textbooks such as [20]. The simplest mechanism for an enzymatic reaction is the following

$$E + S \xrightarrow{k_1} E + P. \tag{2.2.9}$$

Reaction (2.2.9) is an irreversible monomolecular reaction that converts a substrate S into a product P and is catalyzed by an enzyme E. Since the concentration of E is unaffected by the reaction, the model for (2.2.9) is simply

$$\begin{aligned}
\frac{\mathrm{d}S}{\mathrm{d}t} &= -v(S), \\
\frac{\mathrm{d}P}{\mathrm{d}t} &= v(S),
\end{aligned} \tag{2.2.10}$$

and $E(t) = E_T$ is the constant enzyme concentration. Using the law of mass action we can write the reaction rate as a linear function of the substrate

$$v(S) = k_1 E_T S. \tag{2.2.11}$$

Enzymes have a specific number of sites to which the reactants can bind. When all the binding sites are taken by molecules of S, the catalytic effect reaches a saturation point and the enzyme cannot further accelerate the reaction. This saturation is not captured by the mass action model in (2.2.11), and therefore a more detailed analysis is required. Consider the following extended model of reaction (2.2.9)

$$E + S \overset{v_1}{\longleftrightarrow} E_S \overset{v_2}{\longrightarrow} E + P, \tag{2.2.12}$$
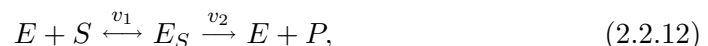
where the intermediate reactions follows the mass action law, i.e. $v_1 = k_1 E \cdot S - k_{-1} E_S$ and $v_2 = k_2 E_S$. Reaction (2.2.12) extends (2.2.9) by explicitly considering the enzyme-substrate binding. The compound E_S denotes the enzyme-substrate complex that forms after the binding of S to a substrate-specific site of the enzyme. Assuming a *quasi* steady state of the complex E_S, that is,

$$\frac{\mathrm{d}E_S}{\mathrm{d}t} = 0, \tag{2.2.13}$$

it can be shown [39] that reaction (2.2.12) is equivalent to

$$S \xrightarrow{v} P, \tag{2.2.14}$$

with reaction rate

$$v(S) = k_2 E_\mathrm{T} \frac{S}{S + K_\mathrm{m}}. \tag{2.2.15}$$

The constant K_m is defined as

$$K_\mathrm{m} = \frac{k_{-1} + k_2}{k_1}, \tag{2.2.16}$$

and $E_\mathrm{T} = E + E_S$ denotes the total concentration of enzyme (free and bound to the substrate). Equation (2.2.15) is known as the *Michaelis-Menten* equation and its plot can be seen in Figure 2.1 (left). The Michaelis-Menten model is a better representation than the mass action model in (2.2.11) because it accounts for enzyme saturation. In fact, as it can be seen from (2.2.15), for low substrate concentrations ($S \ll K_\mathrm{m}$) the rate behaves linearly as

$$v(S) \approx \frac{k_2 E_\mathrm{T}}{K_\mathrm{m}} S, \tag{2.2.17}$$

whereas for high substrate concentrations it saturates to $v \approx k_2 E_\mathrm{T}$.

Remark 2.1: *In the literature, e.g. [39, 27, 36], it is common to find the rate (2.2.15) written as*

$$v(S) = V_\mathrm{max} \frac{S}{S + K_\mathrm{m}}, \tag{2.2.18}$$

where $V_\mathrm{max} = k_2 E_\mathrm{T}$ is the saturation rate or maximum reaction velocity. *In this*

thesis we do not adopt this convention because, as it will be clear later in this chapter, the enzymatic concentrations are regarded as time-dependent variables rather than fixed parameters of the model.

The specific mode of action of an enzyme is referred to as the *enzyme kinetics*. Michaelis-menten kinetics in (2.2.15) are one of most common descriptions, but depending on the particular properties of the enzyme, different expressions for the reaction rate can be found. For example, some enzymes exhibit a phenomenon known as *cooperativity*, which can be described by the so-called Hill kinetics

$$v(S) = k_{\mathrm{h}} E_{\mathrm{T}} \frac{S^h}{1 + k_{\mathrm{h}} S^h}, \tag{2.2.19}$$

with $k_{\mathrm{h}} > 0$ and $h > 0$. As it can be seen in Figure 2.1 (right), Hill kinetics exhibit sigmoidal behaviour, leading to a switch-like behaviour for sufficiently high h.
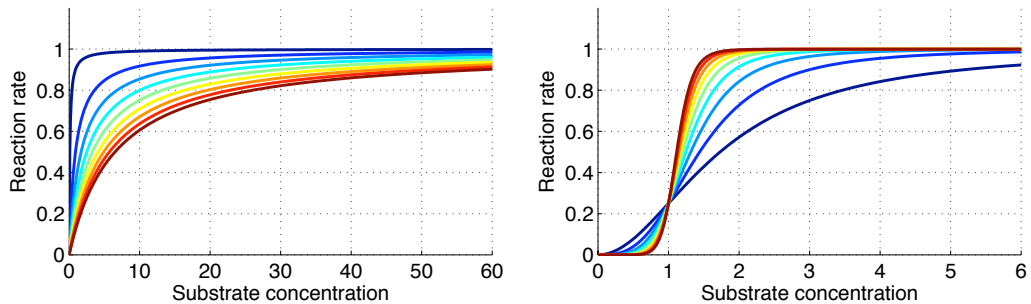
Figure 2.1. Nonlinear enzyme kinetics. Left panel: Michaelis-Menten kinetics with $k_2 = 1$, $E_{\mathrm{T}} = 1$ and $K_{\mathrm{m}} = 0.1$ (blue) up to $K_{\mathrm{m}} = 6.4$ (dark red). Right panel: Hill kinetics with $k_{\mathrm{h}} = 1/3$, $E_{\mathrm{T}} = 1$ and Hill coefficient $h = 2$ (blue) up to $h = 10$ (dark red).

The reaction rate of an enzymatic reaction is generally a nonlinear function of the reactants (see [39] for a good presentation of different enzyme kinetics and their corresponding rate equations). The exception are linear kinetics following the mass action law as in (2.2.11), but as discussed before, those models are very crude since they do not account for enzyme saturation. Throughout the thesis we will make the following assumption.

Assumption 2.1: *The reaction rates are linear functions of the enzyme concentra-*

tion. Thus for the reaction

$$S \xrightarrow{v} P, \tag{2.2.20}$$

we write

$$v = v(S, e) = g(S)e. \tag{2.2.21}$$

The variable $e = e(t)$ is the time-dependent enzyme concentration and the continuous nonlinear function $g(S)$ satisfies $g(0) = 0$ and is called the turnover rate, *i.e. the rate per unit of enzyme concentration.*

This assumption is met by most commonly used enzyme kinetics, but exceptions can be found as discussed in [39, 40]. The turnover rate describes the saturating behaviour of the enzyme and, for example, in the case of Michaelis-Menten kinetics in (2.2.15) is given by

$$g(S) = \frac{k_2 S}{K_{\mathrm{m}} + S}. \tag{2.2.22}$$

Equation (2.2.21) is important for the purposes of this work. As it will be seen in the next section, it allows us to regard a metabolic network as a control-affine dynamical system with the enzyme concentrations as control inputs.

2.3 Metabolic network modeling

2.3.1 Stoichiometric and kinetic models

In the previous section we showed how to obtain dynamic models of single biochemical reactions. We now extend this idea to whole networks of enzymatic reactions. The reactions in a metabolic network share chemical species either as reactants or products, and therefore it is not convenient to distinguish between these two classes. We thus consider a network of n *metabolites* $s_1, s_2, \ldots, s_n$ interacting in m reactions with reaction rates $v_1, v_2, \ldots, v_m$. The chemical equation for the jth reaction is

$$\sum_{i=1}^{n} \alpha_{ij} s_i \xleftrightarrow{v_j} \sum_{i=1}^{n} \beta_{ij} s_i, \quad j = 1, 2, \ldots, m, \tag{2.3.1}$$

where $\alpha_{ij}, \beta_{ij} \in \mathbb{N}$ are the stoichiometric coefficients of metabolite s_i in the jth reaction. The rate of change of s_i is given by the balance between those reactions that have s_i as a product and reactant. The ODE for the ith metabolite then reads

$$\frac{\mathrm{d}s_i}{\mathrm{d}t} = \sum_{j=1}^{m} N_{ij} v_j, \quad i = 1, 2, \ldots, n, \tag{2.3.2}$$

where

$$N_{ij} = \beta_{ij} - \alpha_{ij}. \tag{2.3.3}$$

Metabolite s_i is consumed (produced) in the jth reaction whenever $N_{ij} < 0$ ($N_{ij} > 0$). Equation (2.3.2) is also known as the *mass balance* equation for s_i and can be written in vector form as

$$\frac{\mathrm{d}s}{\mathrm{d}t} = \boldsymbol{N} v, \tag{2.3.4}$$

where $s = \begin{bmatrix} s_1 & s_2 & \ldots & s_n \end{bmatrix}^T$, $v = \begin{bmatrix} v_1 & v_2 & \ldots & v_m \end{bmatrix}^T$ and $\boldsymbol{N} \in \mathbb{Z}^{n \times m}$ is the *stoichiometric matrix* of the network defined as

$$[\boldsymbol{N}]_{ij} = N_{ij}. \tag{2.3.5}$$

We shall refer to (2.3.4) as the *stoichiometric model* of the network. If the reaction rates are considered as control inputs and the metabolite concentration as state vector, then (2.3.4) is a linear time-invariant system with zero state matrix (which in turn can be seen as a network of integrators). For simplicity of notation, in the sequel we will write $\dot{s} = \frac{\mathrm{d}s}{\mathrm{d}t}$. The rate vector v depends on the metabolites of the network and the enzyme concentrations. From the definitions in Remark 2.1, we can write each reaction rate as

$$v_i(s, e_i) = g_i(s) e_i, \quad i = 1, 2, \ldots, m, \tag{2.3.6}$$

where $e_i = e_i(t)$ denotes the concentration of enzyme catalyzing the ith reaction. Combining (2.3.4) and (2.3.6) we can write the model in vector form as

$$\dot{s} = \boldsymbol{N}\boldsymbol{G}(s)e, \qquad (2.3.7)$$

where $e = \begin{bmatrix} e_1 & e_2 & \dots & e_m \end{bmatrix}^T$ and

$$\boldsymbol{G}(s) = \begin{bmatrix} g_1(s) & 0 & \cdots & 0 \\ 0 & g_2(s) & \ddots & 0 \\ 0 & \ddots & \ddots & \vdots \\ 0 & \cdots & 0 & g_m(s) \end{bmatrix} \qquad (2.3.8)$$

Equation (2.3.7) is known as the *kinetic model* of the network. If the enzyme concentrations are taken as control inputs, the model (2.3.7) corresponds to a control-affine nonlinear dynamical system.

2.3.2 Steady state analysis

Metabolic networks exchange mass with their surrounding and hence in steady state the reactions do not reach their chemical equilibrium. Instead each metabolic reaction reaches a so-called *dynamic equilibrium*, whereby the metabolites and reaction rate have constant nonzero values [27].

The steady state of a metabolic network can be identified by inspecting the stoichiometric matrix $\boldsymbol{N}$ [36, 41]. From the stoichiometric model in (2.3.4) it follows that $\dot{s} = 0$ is attained by any rate vector $\bar{v} \in \mathbb{R}^m$ such that $\bar{v} \in \ker\{\boldsymbol{N}\}$. Therefore, if $\boldsymbol{K}$ is a matrix such that its columns span the nullspace of $\boldsymbol{N}$, i.e. $\boldsymbol{K} \in \mathbb{R}^{m \times (m-d)}$ such that $\boldsymbol{N}\boldsymbol{K} = \boldsymbol{0}$ with $d = \mathrm{rank}\{\boldsymbol{N}\}$, any steady state rate vector can be written as

$$\bar{v} = \boldsymbol{K}\phi, \qquad (2.3.9)$$

where $\phi \in \mathbb{R}^{m-d}$. The rate vector $\bar{v}$ is referred to as the *steady state flux* of the network and depends solely on the network structure (represented by the stoichiometric matrix $\boldsymbol{N}$). The stoichiometric model (2.3.4) does not include information on the reversibility of the reactions, and therefore the vector ϕ may need to satisfy additional constraints to guarantee that $\bar{v}$ is compatible with the irreversible reac-

tions. If the specific enzyme kinetics are known, as in the kinetic model (2.3.7), then for each flux $\bar{v}$ the steady state metabolites ($\bar{s}$) and enzymes ($\bar{e}$) are given by the solution of

$$\boldsymbol{G}(\bar{s})\bar{e} = \bar{v}. \tag{2.3.10}$$

Equation (2.3.10) is a system of nonlinear algebraic equations. This system is underdetermined ($n + m$ unknowns and m equations) and therefore the steady state concentrations cannot be fully identified unless n unknowns are given. If $\bar{s}$ is known, then $\bar{e}$ is given by

$$\bar{e} = \boldsymbol{G}^{-1}(\bar{s})\bar{v}. \tag{2.3.11}$$

Conversely, if n components of $\bar{e}$ are known, one can compute the corresponding steady state metabolite concentrations. In this case, however, depending on the nonlinearities in the model (included in the matrix $\boldsymbol{G}(s)$), the system (2.3.10) can also have multiple or no solutions.

2.3.3 Examples

We present two examples to illustrate the main ideas discussed so far.

Stoichiometric model

Consider the following network of irreversible reactions composed of $n = 7$ metabolites, two products (P_1 and P_2), and $m = 7$ reactions:

$$
\begin{aligned}
&S \xrightarrow{v_1} s_1 && s_3 + s_5 \xrightarrow{v_5} s_4 + s_6 \\
&s_1 \xrightarrow{v_2} s_2 && s_4 \xrightarrow{v_6} P_2 \\
&s_2 \xrightarrow{v_3} P_1 && s_6 \xrightarrow{v_7} s_5 \\
&s_1 \xrightarrow{v_4} 2s_3
\end{aligned}
\tag{2.3.12}
$$
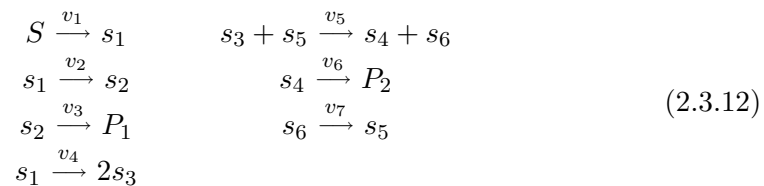
This network can be represented by the diagram in Figure 2.2.

The substrate S and the products are not included in the model so as to represent the transfer of mass between the network and its surroundings. Moreover, it is common to assume that the dynamics of the substrate S are much slower than those of the network under consideration, and hence S is assumed constant. From
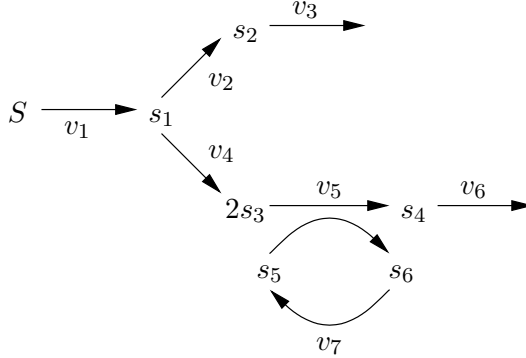
Figure 2.2. Example metabolic network.

the mass balance equation in (2.3.2) we obtain the stoichiometric matrix

$$
\boldsymbol{N} =
\begin{bmatrix}
1 & -1 & 0 & -1 & 0 & 0 & 0 \\
0 & 1 & -1 & 0 & 0 & 0 & 0 \\
0 & 0 & 0 & 2 & -1 & 0 & 0 \\
0 & 0 & 0 & 0 & 1 & -1 & 0 \\
0 & 0 & 0 & 0 & -1 & 0 & 1 \\
0 & 0 & 0 & 0 & 1 & 0 & -1
\end{bmatrix}.
\tag{2.3.13}
$$

The rank of $\boldsymbol{N}$ is $d = 5$ and the nullspace of $\boldsymbol{N}$ is spanned by the columns of

$$
\boldsymbol{K} =
\begin{bmatrix}
1 & 1 & 1 & 0 & 0 & 0 & 0 \\
0.5 & 0 & 0 & 0.5 & 1 & 1 & 1
\end{bmatrix}^T.
\tag{2.3.14}
$$

Therefore, the steady state flux can be computed as $\bar{v} = \boldsymbol{K}\phi$ with $\phi = \begin{bmatrix} \phi_1 & \phi_2 \end{bmatrix}^T$, that is

$$
\bar{v} =
\begin{bmatrix}
\phi_1 + 0.5\phi_2 \\
\phi_1 \\
\phi_1 \\
0.5\phi_2 \\
\phi_2 \\
\phi_2 \\
\phi_2
\end{bmatrix},
\tag{2.3.15}
$$

for any $\phi_1 > 0$, $\phi_2 > 0$ (the positivity of ϕ_1 and ϕ_2 ensures that $\bar{v}$ is compatible with irreversible reactions). For $\phi_1 \neq 0$ and $\phi_2 = 0$, the flux $\bar{v}$ represents a steady state flux through branch $\{v_1, v_2, v_3\}$, whereas if $\phi_1 = 0$ and $\phi_2 \neq 0$ the flux goes through branch $\{v_1, v_4, v_5, v_6, v_7\}$.

Kinetic model

We consider the simple unbranched network in Figure 2.3 to illustrate the nonlinear behaviour of metabolic dynamics. We assume a constant substrate S with mass

$$S \xrightarrow{\;\;v_1\;\;} s_1 \xrightarrow{\;\;v_2\;\;} s_2 \xrightarrow{\;\;v_3\;\;}$$
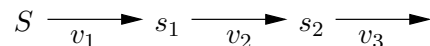
Figure 2.3. Example unbranched metabolic network.

action kinetics for v_1 and Michaelis-Menten kinetics for v_2 and v_3:

$$v_1 = k_{\text{cat}\,1} S e_1, \tag{2.3.16}$$

$$v_2 = \frac{k_{\text{cat}\,2} s_1}{K_{\text{m}\,2} + s_1} e_2, \tag{2.3.17}$$

$$v_3 = \frac{k_{\text{cat}\,3} s_2}{K_{\text{m}\,3} + s_2} e_3. \tag{2.3.18}$$

The saturation of enzyme kinetics is an important source of nonlinearities. To illustrate this, Figure 2.4 shows unit step responses of the network for different initial conditions. As it was discussed in Section 2.2.2, Michaelis-Menten kinetics are approximately linear for low metabolite concentrations and the saturation becomes important only for higher concentrations, see (2.2.17) and Figure 2.1 (left). This behaviour is verified in Figure 2.4, where it can be seen that for large initial conditions, the trajectories have nearly constant slopes for prolonged time intervals. Linear-like behaviour (i.e. approximately exponential trajectories) appears only when the initial conditions are chosen sufficiently small.
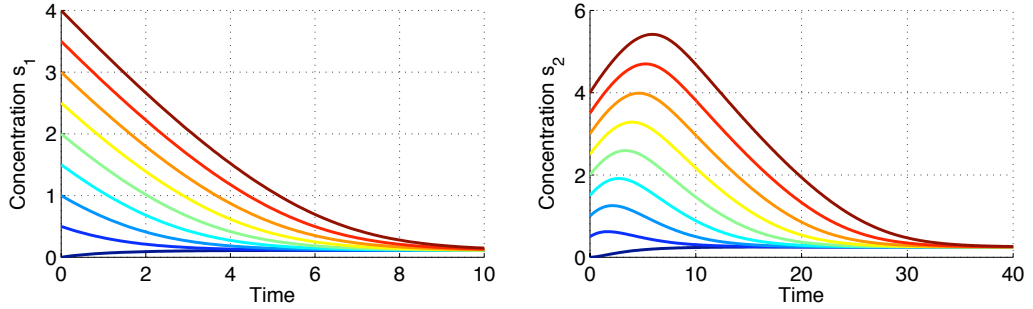
Figure 2.4. Metabolite responses of the network in Figure 2.3 for $e_i(t) = 1, \forall t \geq 0, i = 1, 2, 3$, and different initial conditions from $s_i(0) = 0$ (blue) up to $s_i(0) = 4$ (dark red), $i = 1, 2$. The parameter values are $\{k_{\text{cat} 1}, k_{\text{cat} 2}, k_{\text{cat} 3}\} = \{0.1, 1, 0.5\}$, $\{K_{\text{m} 1}, K_{\text{m} 2}\} = \{1, 1\}$ and $S = 1$.

2.4 Regulation of metabolic networks

The regulation of metabolic networks is implemented by a number of mechanisms which, from a Control Engineering viewpoint, can be regarded as several nested feedback loops. These work via different biochemical mechanisms and in a range of time-scales[27, Section 1.3]. Two important types of regulation are *metabolic* and *genetic* control of metabolic networks. Although this thesis is related to genetic regulation, we first briefly describe the regulation at a metabolic level.

Regulation at a metabolic level

This regulatory action arises from biochemical interactions between an enzyme and some metabolites that do not participate in the corresponding reaction. Specific metabolites in the network can interact with an enzyme and have an effect on its catalytic behaviour. A common example of this phenomenon are the so-called *allosteric enzymes*. Consider a metabolite s and an allosteric enzyme that can be modified by an inhibitor I and an activator A, which are both metabolites of the network. In the irreversible case [37] the turnover rate of the reaction is modeled as

$$g(s, I, A) = \left(\frac{k_{\text{cat}} s}{1 + K_{\text{R}} s} \right) \left(\frac{K_{\text{R}} + K_{\text{T}} L(I, A) f(s)^{q-1}}{1 + L(I, A) f(s)^q} \right), \qquad (2.4.1)$$

21

where

$$f(s) = \frac{1 + K_{\mathrm{T}}s}{1 + K_{\mathrm{R}}s}, \tag{2.4.2}$$

$$L(I, A) = L^* \left(\frac{1 + K_{\mathrm{I}}I}{1 + K_{\mathrm{A}}A} \right)^q. \tag{2.4.3}$$

All the parameters are positive and depend on the particular properties of the enzyme. The turnover rate $g(s, I, A)$ in (2.4.1) can be understood as the combination of Michaelis-Menten kinetics (compare the first factor of (2.4.1) with the Michaelis-Menten equation in (2.2.15)) and a regulatory effect caused by the inhibitor and activator metabolites. In general, there are various mechanisms for enzyme regulation with different degrees of complexity [39]. However, for the purposes of this thesis it suffices to note that these mechanisms, regardless their specific mode of action, introduce additional nonlinearities to the kinetic model in (2.3.7).

Regulation at a genetic level

The enzymatic concentrations catalyzing a metabolic network are controlled by gene expression mechanisms. Genetic regulation occurs at much slower time-scales than regulation at the metabolic level; in fact, the time constants of genetic regulation are of the order of minutes to hours, whereas those of metabolic interactions are within seconds [27]. In addition, some metabolites can promote or repress the expression of an enzyme, and hence in many cases gene regulation corresponds to a feedback mechanism.
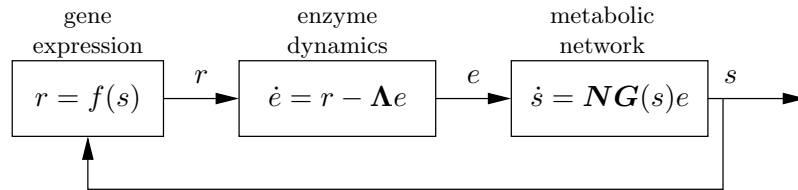
Figure 2.5. Closed-loop genetic regulation of metabolic networks.

This form of feedback control can be described by the block diagram in Figure 2.5, whereby enzyme concentrations are regarded as inputs to the control-affine kinetic model in (2.3.7). We describe enzyme dynamics with a mass balance model for enzyme expression and degradation. If the degradation rates are assumed pro-

portional to the enzyme concentration, then we can write

$$\dot{e} = r - \mathbf{\Lambda}e, \tag{2.4.4}$$

where $r \in \mathbb{R}^m$ is the vector of enzyme expression rates and

$$\mathbf{\Lambda} = \begin{bmatrix} \lambda_1 & 0 & \cdots & 0 \\ 0 & \lambda_2 & \ddots & 0 \\ 0 & \ddots & \ddots & \vdots \\ 0 & \cdots & 0 & \lambda_m \end{bmatrix}. \tag{2.4.5}$$

The constants $\lambda_i > 0$ can account not only for enzyme degradation, but also for dilution effects due to cell growth.

The expression rates r can depend on the metabolites in the network. This dependency is very complex and can be modeled with different degrees of detail. Gene expression can be described, for example, via ODE models, piecewise linear differential equations or boolean models [42]. The particular choice depends largely on the phenomenological knowledge of the system under study. In some cases, such as the Lac operon model [26], the biochemical mechanisms behind gene regulation have been identified and one could integrate an ODE model for gene expression with one for metabolic dynamics. However, in most cases the mechanisms are not known and authors have proposed the use of empirical static models [43]. The expression rate can then be described as a saturable Hill-type algebraic function of intermediate *effector* molecules, the activation of which is triggered by specific metabolites. For example, if metabolite s_j activates an effector R, then according to [29] its concentration can be described by

$$R = \frac{R_\mathrm{T}}{K_\mathrm{R} + s_j}, \tag{2.4.6}$$

with $R_\mathrm{T}, K_\mathrm{R} > 0$. Depending on whether the effector activates or represses the

expression of enzyme e_i, its effect can be modeled as

$$f_i(R) = \beta_i \frac{R^h/\alpha_i}{1 + R^h/\alpha_i} \quad \text{(activation)},$$

$$(2.4.7)$$

$$f_i(R) = \frac{\beta_i}{1 + R^h/\alpha_i} \quad \text{(repression)}.$$

The parameter $\beta_i > 0$ is the maximal expression rate, $\alpha_i > 0$ is the strength of the regulation, and $h > 0$ is the Hill coefficient. Note that the models (2.4.6)–(2.4.7) can be lumped into a single expression of the form $r_i = f_i(s_j)$.

Following the analogy between genetic regulation and feedback control, the relation $r = f(s)$ in Figure 2.5 can be seen as a nonlinear feedback "controller" with parameters α_i, β_i and h. Genetic regulation of metabolic networks can adjust enzymatic concentrations and drive the metabolic network between different operating points. As will be seen later in Chapters 4–6, the main results of this thesis are the solution of open loop optimal control problems for the system in Figure 2.5.

Chapter 3

Metabolic network optimization

3.1 Introduction

In this chapter we review different approaches for metabolic network optimization available in the literature. These are diverse in terms of their purposes: some approaches aim at understanding metabolic dynamics, whereas others are concerned with the intervention of metabolic systems. Studies on metabolic optimization also differ in terms of the mathematical tools they use, and we shall classify them as *static* or *dynamic* approaches depending on whether they address steady state or transient properties, respectively. Recent reviews [44, 45] underline this diversity and shows a number of different techniques and applications where optimization has been used for the analysis and design of biochemical systems. We put special attention on dynamic optimization, which is the core topic of this thesis and has a straightforward control-theoretic interpretation. In particular, the articles by Klipp *et al.* [28] and Zaslaver *et al.* [29] are the basis for the results presented later in Chapter 4, and thus we shall discuss them in more detail.

The chapter is organized as follows: in Section 3.2 we briefly discuss the motivation and rationale behind metabolic optimization. The most relevant static optimization approaches are presented in Section 3.3. We conclude in Section 3.4 by presenting some dynamic optimization techniques and, especially, the results in [28, 29] which serve as preamble for next chapter.

3.2 Rationale behind metabolic optimization

The use of optimization techniques in metabolic networks has a two-fold motivation. The first aims at understanding the structure and dynamics of metabolic systems, also referred to as *reverse engineering* of metabolic networks. As discussed in Chapter 1, metabolic networks enable many cellular functions and their dynamics play

a major role in cell fitness. It has been argued that, from an evolutionary perspective, present-day metabolic systems are the outcome of stepwise improvements in their operation [23]. In addition, specific cellular functions can be supported by alternative metabolic networks [22], the implementation of which uses different topologies, kinetics and/or regulatory mechanisms. It is not clear why a particular metabolic design is preferred over the possible alternatives. These ideas have led to the postulate that metabolic networks in organisms have been optimized through evolutionary processes so as to improve their adaptation to environmental conditions [18, 24]. The reader is referred to the reviews in [13, 14] for good presentations of the drawbacks and advantages of optimization theory in general biological systems. Nevertheless, in this context the idea is to solve optimization problems in an attempt to understand the properties of metabolic networks [23].

The second motivation behind metabolic optimization aims at the design of metabolic networks for biotechnological purposes. This is the prime objective of *Metabolic Engineering* [46, 47], whereby genetic alterations are introduced so as to over-express or knock out enzymes in living cells and modify their existing networks [48, 49]. A typical goal of metabolic design is to increase the rate at which a cell synthesizes or secretes a commercially important compound, or even to enable the synthesis of a substance that would not be produced by the wild-type cell. The role of optimization theory is then to aid the analysis and design of metabolic interventions by using quantitative criteria [50, 51].

In the following sections we review different metabolic optimization ideas that have been reported in the literature. Regardless the purpose they were developed for, we classify them according to whether they use static or dynamic optimization techniques.

3.3 Static optimization approaches

3.3.1 Flux Balance Analysis

An optimization technique that has been successfully applied to metabolic networks is Flux Balance Analysis (FBA), whereby the steady state flux of a stoichiometric model is chosen to optimize a linear objective function [52]. Any vector that lies in the nullspace of the stoichiometric matrix is a valid steady state flux (recall (2.3.9) in the previous chapter). The steady state flux is, therefore, not uniquely determined and the idea behind FBA is to single out a flux vector that optimizes a quantity

representing the network's function.

Consider a network with m reactions and the stoichiometric model

$$\dot{s} = \boldsymbol{N}v. \tag{3.3.1}$$

In the FBA framework [53] the optimal flux distribution v^* is computed as the solution of the following linear program:

$$
\begin{aligned}
&v^* = \arg\max_{v \in \mathbb{R}^m} c^T v, \\
&\text{subject to} \\
&\boldsymbol{N}v = 0, \\
&v_{\min} \le v \le v_{\max}.
\end{aligned}
\tag{3.3.2}
$$

The vector $c \in \mathbb{R}^m$ defines the weight of each flux in the cost function, and the vectors $v_{\min}, v_{\max} \in \mathbb{R}^m$ specify bounds for the flux (the inequality should be understood component-wise). The constraints in (3.3.2) are the steady state condition and the physical bounds that limit the flux. The bounds $v_{\min}$ and $v_{\max}$ arise from the limited enzymatic availability and their corresponding saturating behaviour (as discussed in Section 2.2.2).

Since the FBA formulation does not require knowledge of the reaction kinetics, it is particularly useful in cases when only the stoichiometry of the network is known. One of the major advantages of FBA is that it relies on a linear programming framework, and therefore solutions can be efficiently computed even for systems of very high dimensions. In [54], for example, FBA was used to analyze the metabolic network of the yeast *S. cerevisiae* with $m = 1175$ metabolic reactions.

The selection of an appropriate cost function in (3.3.2) has a major impact on the properties of the solution and is subject of active research [55, 56, 57]. In the case of bacterial networks, a common choice is the maximization of the cellular growth rate, which is assumed to be a function of certain fluxes [58]. Growth maximization has been experimentally verified in a number of studies, see e.g. [59]. In this setup, FBA has provided useful predictions of fluxes and growth in the bacterium *E. coli* under different environmental conditions [60, 31].

With a slightly different formulation, the work in [24] presented an FBA-based approach for the computation of the steady state fluxes in a metabolic network. In this work the concept of *flux minimization* was introduced, whereby the flux vector

is partitioned into an "internal" and a "target" component. The latter is defined as those fluxes that have a direct effect on the network function, or in other words, those fluxes that can be regarded as outputs of the network. The rationale is that metabolic fluxes require an energy expenditure by the cell, and thus it is reasonable to assume that the internal fluxes should be kept minimal, while the target fluxes should be kept close to the nominal levels that are enough to sustain the network function.

A number of other applications of the FBA framework have also been reported, see the review in [61] and the references therein for a list of landmark works in the development of FBA theory. A shortcoming is that FBA-based optimization is based on models that do not include kinetic information, which makes them unable to predict metabolite concentrations. An alternative to FBA is the S-system formulation described next, which also relies on linear programming but allows the approximate computation of metabolite concentrations.

3.3.2 S-system formulation

A number of optimization approaches are based on the so called *S-system* (from "synergistic") formalism. It was first introduced within the Biochemical Systems Theory developed by Savageau [22] as a systematic tool for modeling biochemical networks. Unlike the stoichiometric description in (2.3.4), S-system models do not have a mechanistic interpretation, but are rather a *power-law* approximation to the mass balance equations [62]. An important advantage of this approach is that the steady state metabolite concentrations can be obtained as a solution of a linear system of algebraic equations (compare with the nonlinear system that describes the steady state of the kinetic model in (2.3.10)). This feature has been exploited by several groups, especially in the biotechnology community, for solving a range of optimization problems, see e.g. [47]. In particular, in [63] the authors used a mixed-integer linear optimization program to determine regulatory mechanisms that yield a substantial increase in metabolite concentrations, which is a typical goal of metabolic engineering applications. Using similar ideas as in the FBA theory, the authors in [64] proposed linear programming within the S-system formalism to optimize a metabolic network according to multi-objective criteria, which accounts for the fact that no single optimization criterion can be of general validity.

3.3.3 Other optimization approaches

The FBA and S-system approaches are frameworks under which a number of static optimization problems can be explored in a systematic fashion. There are also other optimization studies that do not use a common framework for their formulation. These are manifold and rather problem-specific in terms of the optimization criteria and the decision variables to be optimized. Good reviews of other optimization problems that have been proposed can be found in [18, 23]. A list of different cost functions that have been used can also be found in [65, Section 1].

Different studies have addressed the optimization of enzyme kinetics, e.g. [23, 66, 67, 68]. In addition, since gene expression requires certain cellular effort, it has been argued that observed enzyme concentrations can be understood as the outcome of an optimization process. On the theoretical side, this problem has been treated in [69] and [65], where optimal enzyme concentrations were determined under a constraint on the total enzyme availability. On the experimental side, the remarkable work in [70] showed that the observed expression levels of the enzyme LacZ in *E. coli* matches the solution of a cost/benefit optimization problem. LacZ is responsible for the uptake of lactose and its use for cellular growth. The cost was measured as the reduction in cell growth due to the burden imposed by the synthesis and maintenance of LacZ, whereas the benefit was defined as the gain in growth rate due to the utilization of lactose. Optimal expression levels of LacZ were theoretically computed, and experimental results showed that under different extracellular lactose concentrations, the expression levels of LacZ evolved to match their predicted optimal values.

3.4 Dynamic optimization approaches

A common feature of static optimization approaches is that they address the network behaviour under static enzyme concentrations. However, the temporal distribution of enzymatic activity affects pathway behaviour and thus metabolic responses can be modulated by the timing of enzyme expression. Zaslaver *et al.* observed well defined temporal patterns in enzyme expression data in the Serine, Methionine and Arginine pathways in *E. coli* under extracellular medium shift [29, 71]. Additional experimental evidence revealing temporal modulation in the Lysine pathway has been recently reported in [72]. These experiments provide metabolic instances of the generally accepted fact that specific temporal patterns in gene expression appear in

the operation of a range of cellular functions, including complex molecular assemblies [73] and organism development [74].

The work in [29] suggested that the temporal patterns observed in enzyme expression can be understood in terms of optimization principles. Any rigorous attempt to further investigate this idea requires the use of dynamic optimization theory. However, as pointed out in [47, p. 165], to date there have been relatively few studies on dynamic optimization of metabolic networks. Next we review some of the approaches that can be found in the literature.

3.4.1   Optimization of reaction rates

The works in [75, 76] present a dynamic optimization algorithm for homeostatic regulation of metabolic networks. The formulation is based on the the so-called *cybernetic* modeling framework [77]. The algorithm optimizes time-dependent reaction rates for an appropriate regulation of the metabolites in the central nitrogen metabolism of *S. cerevisiae*. The optimization was carried out by time discretization and numerical solution of a nonlinear static optimization problem at each time step. From a Control Engineering viewpoint this scheme is implemented as a tracking controller that ensures that the metabolite concentrations follow the desired steady state values.

Dynamic extensions of the FBA principle have also been reported in the literature. Notably, the work in [78] presents two optimization algorithms for growth maximization in *E. coli*. Both approaches optimize the reaction rates and metabolite concentrations such that the cell attains maximal growth under mixed nutritional conditions of glucose and acetate. The first approach is similar to that in [75, 76] in the sense that, after a time discretization, a collection of static optimization problems is solved in each time step. It also allows for constraints on the time-derivative of the reactions rates and relies on a sequence of linear programming problems (which, as in FBA, makes it scalable to larger networks). The second approach corresponds to a dynamic optimization algorithm *per se* that can be solved by numerical routines with an orthogonal point collocation method [79]. The results showed good agreement with experimental data, supporting the idea that growth maximization is a valid objective in bacterial metabolism not only under steady state conditions (as in the application of FBA in [31]), but also when transient phenomena are considered.

The works in [80, 81] address optimal homeostatic regulation within a Linear

Quadratic Regulator framework (see Appendix A.2). The authors define the home-ostatic objective function as a quadratic functional of the deviations of metabolites and reaction rates from their steady state values. This approach has the considerable advantage of having an analytical solution via the Riccati equation, but on the other hand it cannot account for constraints and requires a linear model.

3.4.2 Optimization of enzymatic concentrations

All the aforementioned studies on dynamic optimization [75, 76, 78, 80, 81] consider the metabolites as state variables and the reaction rates as control inputs to be optimized. This is useful since it only requires a stoichiometric model for the network and, moreover, these models are linear in the reaction rates (recall the model in (2.3.4)). However, as discussed in Section 2.2.2, the reaction rates are nonlinear functions of the metabolites, and thus it is not accurate to regard the rates as independent variables. A more precise approach is to directly optimize the enzymatic concentrations for the kinetic model (2.3.7). In principle, the ideas presented in [78, 80, 81] could be used for models that include reaction kinetics, but this has not been explored so far.

Dynamic optimization of enzymatic concentrations was considered by Klipp and co-workers in [28]. The problem under study was the activation of an unbranched network from an "off" state, where only the network's substrate is present, to a state where all substrate has been converted into product. The authors computed time-dependent enzyme profiles that drive the network between these two conditions with minimal *transition time*. The transition time of a metabolic network is defined as the average time needed to reach the steady state [82, 83]. A constraint in the total enzyme concentration was included as a way of accounting for the limited gene expression capabilities of a cell. The formulation considered mass action kinetics and was numerically solved by approximating the enzyme profiles as piecewise constant functions. It was found that the optimal enzyme profiles switch from zero to maximal concentration and back to an intermediate level. The switching sequence of the enzymes followed the same ordering as the reactions they catalyze in the network. In addition, the optimal transition time was found to be always smaller than the one achieved by choosing optimal constant enzyme concentrations, which stresses the fact that dynamic manipulation of the enzymes can improve the pathway performance.

The findings of [28] are in agreement with the experimental observations of

Zaslaver *et al.* in [29]. There, a sequential or "just-in-time" pattern in enzyme expression was found in unbranched pathways responsible for amino acid synthesis. In order to explain these experimental results, the authors studied a model for an unbranched network with three reactions exhibiting Michaelis-Menten kinetics. The enzyme concentrations were assumed to be regulated by gene expression by a repressor molecule, the activation of which was a function of the pathway product. This corresponds to the genetic regulation mechanism described by Figure 2.5 in the previous chapter. The gene regulatory parameters were computed so as to minimize a mixed cost function accounting for the effort required by enzyme expression and the deviation of the reaction rates from a target steady state flux. The optimized parameters are equivalent to α_i and β_i in (2.4.7) and, interestingly, their optima were such that the enzyme profiles showed a hierarchical structure. The optimal enzyme profiles were found to be ordered in the same sequence as they act in the pathway. This is illustrated in Figure 3.1, which shows the optimal enzymatic responses of [29, Fig. 6].
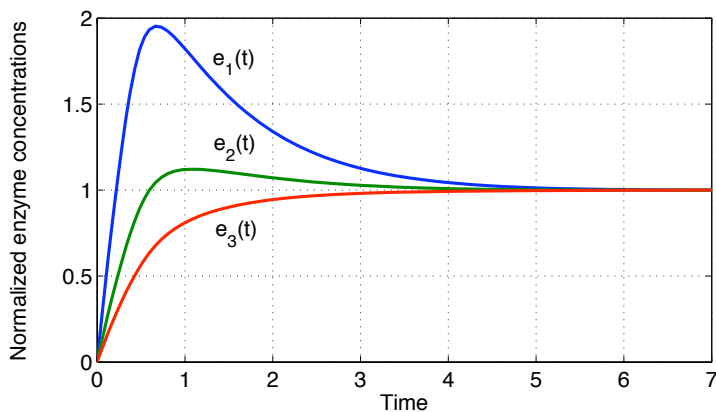
Figure 3.1. Optimal enzyme profiles computed in [29] normalized with respect to their steady state values. Parameters values are the same as in [29, Fig. 6], with the exception of the substrate $S = 1$ and $R_T = 1$, which are not specified in the paper.

The sequential behaviour in the optimal enzymatic responses agrees qualitatively with the gene expression data presented by the same authors. Their results support the idea that genetic regulation of some metabolic networks may be underpinned by an optimality principle. Conversely, the notion that sequential enzyme expression in unbranched pathways arises from an optimality criterion is in accordance with what had already been suggested in [28]. These observations motivate the development of

a rigorous approach to the dynamic optimization of enzyme concentrations, which is the topic of the next chapter.

Chapter 4

Optimal activation of unbranched networks

4.1 Introduction

The cellular response to environmental disturbances may include the activation or inactivation of appropriate metabolic networks. As discussed in Chapter 3, experimental observations of *sequential* enzyme expression patterns in the activation of unbranched networks have been reported in the literature [29]. In these patterns, enzymes are synthesized one after another following the same order as they act in the network. Moreover, the analyses in [29, 28] suggest that this sequential behaviour may be the outcome of an optimality principle underlying metabolic activation. These analyses were carried out numerically, so it is unclear whether the sequential patterns are inherent properties of metabolic activation or rather consequences of specific kinetics and parameter values.

The purpose of this chapter is to examine the properties of optimal metabolic activation in more general unbranched networks. To that end, we adopt a control-theoretic framework and pose an optimal control problem that accounts for time-resource minimization in metabolic activation under a constrained total enzyme abundance. This constraint represents the limited capacity of the cell to synthesize the enzymes. The optimized inputs are time-dependent enzyme concentrations that rapidly drive the network to a prescribed steady state flux with moderate enzyme usage.

By identifying the form of the optimal solution, we show that sequential activation is a feature that indeed arises in a broad class of unbranched networks. The analysis is based on the application of Pontryagin's Minimum Principle (see Appendix A.1), which allows us to analytically characterize the form of the solution.

The solution is a switching sequence that matches the topology of the network, thus suggesting that the sequential activation appears in more general instances than previously considered. In fact, the results hold for unbranched networks of arbitrary length with a class of irreversible kinetics that includes (but is not limited to) mass action, Michaelis-Menten and Hill kinetics.

In addition, the structure of the switching sequence can be used to construct an equivalent static optimization problem, the solution of which allows the computation of the optimal switching times. Other features of the optimized activation are also explored. Feasibility is addressed by deriving a general formula for the upper bound on the achievable target flux in terms of the saturation velocities of the individual reactions. Sensitivity analysis of the optimal solution is carried out numerically by considering two case studies.

Finally, since gene expression dynamics are relatively slow, switching enzyme concentrations are not realistic from a biological viewpoint. We explore the numerical solution of a similar optimal control problem for a metabolic model coupled with enzyme dynamics. Although such a numerical solution does not allow for generalizations, the results show a temporal sequence that agrees with our theoretical analysis.

The chapter is organized as follows: the problem formulation and the form of the optimal solution are presented in Section 4.2 and Section 4.3, respectively. The derivation of the equivalent static optimization problem is discussed in Section 4.4, and further results are presented in Section 4.5. We conclude with a discussion of the results in Section 4.6.

4.2 Problem formulation

We consider unbranched metabolic networks with n metabolites and $(n + 1)$ irreversible reactions as the one shown in Figure 4.1. In that scheme s_0 denotes the concentration of the substrate that feeds the pathway. As discussed in Chapter 2, the pathway activity is presumed to have a negligible effect on the concentration of substrate, so s_0 is considered constant.

$$s_0 \xrightarrow{\quad v_0 \quad} s_1 \xrightarrow{\quad v_1 \quad} \cdots \xrightarrow{\quad v_{n-1} \quad} s_n \xrightarrow{\quad v_n \quad}$$
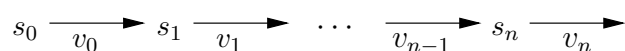
Figure 4.1. Unbranched metabolic pathway.

The kinetics of each reaction are assumed to be linear in the enzyme concentrations (see Assumption 2.1 in Chapter 2), i.e.

$$v_i(s_i, e_i) = g_i(s_i)e_i, \qquad (4.2.1)$$

where $s_i = s_i(t)$ and $e_i = e_i(t)$ are the concentrations of the ith metabolite and enzyme, respectively. We consider a class of nonlinear monomolecular enzyme kinetics satisfying the following assumption.

Assumption 4.1: *The turnover rate functions $g_i(s_i)$ in (4.2.1) satisfy*

$$\frac{\partial g_i(s_i)}{\partial s_i} > 0, \text{ for } s_i > 0, \ i = 0, 1, \ldots, n, \qquad (4.2.2)$$

Assumption 4.1 states that an increase in substrate s_i yields an increase in the reaction rate, which can saturate for large substrate concentrations. This monotonicity condition is satisfied by a broad class of enzyme dynamics that includes Mass Action, Michaelis-Menten and Hill kinetics. The irreversibility of the reactions also implies that $g_i(s_i) \geq 0$ for all s_i. In particular, as stated in Assumption 2.1, it also holds that

$$g_i(0) = 0. \qquad (4.2.3)$$

As in (2.3.2), the dynamic model for the unbranched network in Figure 4.1 is given by mass balance as

$$\dot{s}_i = v_{i-1}(s_{i-1}, e_{i-1}) - v_i(s_i, e_i), \ i = 1, 2, \ldots, n. \qquad (4.2.4)$$

The kinetic model is given by (2.3.7)

$$\dot{\boldsymbol{s}} = \boldsymbol{N}\boldsymbol{G}(s)e, \qquad (4.2.5)$$

where the state and control are $s = \begin{bmatrix} s_1 & s_2 & \ldots & s_n \end{bmatrix}^T$ and $e = \begin{bmatrix} e_0 & e_1 & \ldots & e_n \end{bmatrix}^T$, respectively, and $\boldsymbol{G}(s) = \text{diag}\,\{g_0(s), g_1(s), \ldots, g_n(s)\}$. The stoichiometric matrix

$N \in \mathbb{Z}^{n \times (n+1)}$ is given by

$$N = \begin{bmatrix} 1 & -1 & 0 & \cdots & 0 \\ 0 & 1 & -1 & \cdots & 0 \\ \vdots & \ddots & \ddots & \ddots & \vdots \\ 0 & 0 & \cdots & 1 & -1 \end{bmatrix}. \tag{4.2.6}$$

We are interested in optimizing time-dependent enzyme concentrations that activate the network from the origin (i.e. when the network is "off") to a steady state with a given metabolic flux. For clarity, we first give a precise definition of the notion of pathway activation and then we describe each element of the optimization problem itself: the cost function, the input constraints, and the terminal condition.

Metabolic pathway activation

Assuming that the pathway is initially inactive, i.e. $e(0) = 0$, $s(0) = 0$, we aim at obtaining temporal enzymatic profiles that drive the pathway to a steady state characterized by a pre-specified constant flux $V > 0$. From Figure 4.1 and (4.2.4), the pathway reaches a steady state at $t = t_f$ when

$$v_i(t) = V, \text{ for } t \geq t_f, \ i = 0, 1, \ldots, n. \tag{4.2.7}$$

The time t_f is the duration of the activation process and its value is regarded as an outcome of the optimization.

Cost function

If the pathway to be activated has a critical impact on cellular fitness, then the metabolic product has to be built rapidly and with efficient enzyme usage. To quantitatively express this principle, the control $e(t)$ should minimize a cost function of the form

$$\mathcal{J} = \int_0^{t_f} \left(1 + \alpha^T e(t)\right) \, \mathrm{d}t, \tag{4.2.8}$$

with a weighting vector $\alpha \in \mathbb{R}^{n+1}_{\geq 0}$. The minimization of $\mathcal{J}$ implies a combined optimization of: (i) the time taken to reach the new steady state, and (ii) a measure of the enzyme usage. The weight vector α can be appropriately tuned to reflect the relative biosynthetic cost of specific enzymes. If we choose $\alpha = 0$ then $\mathcal{J} = t_f$,

which corresponds to the total activation time.

Input constraints

A cell can expend only a limited set of resources on the activation of any given pathway. A simple and convenient way of taking those limitations into account is to consider an upper bound on the total enzyme abundance [69, 28]. For that purpose, we consider a control that is constrained as $e(t) \in \mathcal{U}$ for all $t \in [0, t_f)$, where $\mathcal{U}$ is the simplex defined as

$$\mathcal{U} = \left\{ e \in \mathbb{R}_{\geq 0}^{n+1} : \sum_{i=0}^{n} e_i \leq E_{\mathrm{T}} \right\}. \tag{4.2.9}$$

The constant $E_{\mathrm{T}} > 0$ is the upper bound on the total enzymatic concentration that can be allocated for the pathway activation.

Terminal condition

In principle, the terminal condition for the optimization problem is specified solely by enforcing the steady state after time t_f, which is described by (4.2.7). Once the pathway has reached the steady state (i.e. after time t_f), the enzyme concentrations must maintain the pathway flux. Combining the steady state condition in (4.2.7) with the form of the reaction rates in (4.2.1), we get the required steady state enzyme levels as

$$e_i(t) = \frac{V}{g_i(s_i^f)}, \text{ for } t \geq t_f, \ i = 0, 1, \ldots, n, \tag{4.2.10}$$

where $s_i^f = s_i(t_f)$ is the ith component of the steady state metabolite vector $s^f = s(t_f)$. Equation (4.2.10) specifies the steady state enzymatic concentrations that are needed to sustain the target flux. However, this condition alone does not ensure that those enzymatic levels are within the constraint set $\mathcal{U}$ *after* the optimization period. Using the definition of $\mathcal{U}$ in (4.2.9) together with (4.2.10), it follows that the steady state metabolite concentrations must satisfy $s^f \in \mathcal{S}$ with

$$\mathcal{S} = \left\{ s^f \in \mathbb{R}_{>0}^{n} : \frac{V}{g_0(s_0)} + \sum_{i=1}^{n} \frac{V}{g_i\left(s_i^f\right)} \leq E_{\mathrm{T}} \right\}. \tag{4.2.11}$$

The terminal set $\mathcal{S}$ guarantees that the steady state is compatible with the upper bound on total enzyme abundance. Rather than specifying the steady state as a single point, $\mathcal{S}$ defines a surface where the terminal state must lie.

In summary, the optimal control problem for the metabolic network activation reads as follows.

Problem 4.1: *Consider the kinetic model* (4.2.5) *with $\boldsymbol{N}$ defined in* (4.2.6), *$\boldsymbol{G}(s)$ satisfying Assumption 4.1, initial condition $s(0) = 0$ and a prescribed target flux $V > 0$. Find a final time t_f and a piecewise continuous control $e(t) : [0, t_f) \rightarrow \mathcal{U}$ that minimizes*

$$\mathcal{J} = \int_0^{t_f} \left(1 + \alpha^T e(t)\right) \, \mathrm{d}t,$$

for a given $\alpha \in \mathbb{R}_{\geq 0}^{n+1}$, and drives the system to a steady state $s(t_f) \in \mathcal{S}$ with $\mathcal{S}$ defined in (4.2.11).

Problem 4.1 is a nonlinear optimal control problem with free final time, the solution of which is described in the next section.

4.3 Optimal network activation

4.3.1 Form of the optimal activation

A suitable framework for solving optimal control problems such as Problem 4.1 is provided by Pontryagin's Minimum Principle (PMP), see Appendix A.1. Application of PMP typically results in the statement of a two-point boundary value problem (BVP), so that any solution of the original optimization problem also solves the BVP. In general, solving this BVP for systems with nonlinear dynamics can be very challenging, and the analysis is typically carried out on a case-by-case basis.

An explicit solution to Problem 4.1 is not attainable through PMP since the BVP does not admit a general solution. Even in a particular instance of the problem in which the pathway length and kinetics were specified, the nonlinear dynamics would typically lead to a BVP which can only be treated numerically. The main result of this chapter is stated in the next theorem and describes properties of the solution that can be used to compute the full solution without solving the associated BVP. The proof is presented in Section 4.3.2.

Theorem 4.1: *There exists a set of* switching times $\{t_0, t_1, \ldots, t_{n-1}\}$, *with* $0 < t_i < t_j$ *for* $i < j$ *and* $t_{n-1} = t_f$ *that partition the optimization interval as*

$$[0, t_f) = \bigcup_{i=0}^{n-1} T_i, \tag{4.3.1}$$

with $T_0 = [0, t_0)$ *and* $T_i = [t_{i-1}, t_i)$ *for* $i = 1, 2, \ldots, n-1$, *such that the solution* $e^*(t)$ *to Problem 4.1 satisfies*

$$e_i(t) = \begin{cases} E_{\mathrm{T}}, & \text{for } t \in T_i, \\ 0, & \text{for } t \notin T_i, \end{cases} \tag{4.3.2}$$

Equation (4.3.2) shows that the optimal control is a switching sequence between 0 and the maximal level E_{T}. These "bang-bang" controls are a common feature of solutions in classical time optimal control [84]. The bang-bang quality of the solutions to Problem 4.1 is a consequence of the geometry of the constraint region $\mathcal{U}$ and the fact that the dynamics and the cost depend linearly on the control $e(t)$. It is also observed that the form of the optimal solution does not depend on the weight α. Therefore, variations in the biosynthetic costs for enzyme production will be reflected only in the activation duration of the individual reactions, without any effect in the activation sequence. The result of Theorem 4.1 can also be interpreted as follows:

1) at any time $t \in [0, t_f)$, only one enzyme is active (i.e. has a nonzero concentration);

2) the active enzyme is present at maximum concentration;

3) each enzyme is active over a single time interval;

4) the order of enzyme activation matches the order of reactions in the pathway.

This means that the optimal activation follows a *sequential* pattern, whereby the reactions are activated one after another in the same order as they appear in the network. The sequential behaviour holds for arbitrary pathway lengths (n) and a broad class of irreversible monomolecular reaction kinetics, namely those that satisfy the monotonicity condition in Assumption 4.1. Moreover, we find that the activation sequence is a consequence of both the pathway structure and the reaction kinetics.

From an intuitive point of view, the "pipeline" structure of the pathway implies the ith metabolite cannot be produced unless the upstream portion of the pathway has been activated. Moreover, the monotonicity condition on the kinetics (4.2.2) precludes the optimality of activating an upstream reaction after the ith one has already been activated (a fact that arises from (4.3.30) and (4.3.31) in the proof).

We also observe that the description of the optimal solution provided by Theorem 4.1 considerably simplifies the numerical computation of the optimal solutions. Since the optimal control can be fully parameterized in terms of $\{t_0, t_1, \ldots, t_{n-1}\}$, one needs only to optimize over the n switching times, rather than over the whole class of admissible controls. This will be used later in Section 4.4 to obtain an equivalent nonlinear static optimization problem that gives the complete numerical solution of Problem 4.1.

The bang-bang solution of Theorem 4.1 resembles the previous results in [28], whereby optimal enzyme inputs were numerically determined for networks with mass action kinetics. It should be pointed out, however, that in [28] the authors consider a thermodynamically closed network, i.e. the model does not include a constant substrate pool. In that case the network reaches a nil steady state flux, and therefore the problem is of different nature and our solution cannot be directly applied. The reader is referred to [85] for an optimal control approach to the problem in [28].

4.3.2   Proof of Theorem 4.1

The proof is based on Pontryagin's Minimum Principle, the details of which are presented in Appendix A.1. In what follows we use the standard control-theoretic notation and define the state and control as $x = s$ and $u = e$, respectively.

For Problem 4.1, the Hamiltonian in (A.1.3) is given by

$$\mathcal{H}\left(x(t), u(t), p(t)\right) = 1 + \alpha^T u(t) + p(t)^T \dot{x}(t), \tag{4.3.3}$$

where $p(t) = \begin{bmatrix} p_1(t) & p_2(t) & \ldots & p_n(t) \end{bmatrix}^T$ is the co-state vector. From PMP the co-state satisfies (A.1.5), and thus using the mass balance equations in (4.2.4) and the property $v_i(x_i, u_i) = g_i(x_i)u_i$, the ODE for the ith co-state is

$$\dot{p}_i(t) = (p_i(t) - p_{i+1}(t))\frac{\partial g_i}{\partial x_i}u_i(t), \quad i = 1, 2, \ldots, n. \tag{4.3.4}$$

In addition, the Hamiltonian can be written as

$$\mathcal{H}\left(x(t), u(t), p(t)\right) = 1 + \sum_{i=0}^{n} h_i(t) u_i(t),$$ (4.3.5)

The function $h_i(t)$ is called the ith switching function and is given by

$$h_i(t) = \alpha_i + (p_{i+1}(t) - p_i(t)) g_i\left(x_i(t)\right), \quad i = 0, 1, \dots, n,$$ (4.3.6)

with $p_0(t) = 0$ and $p_{n+1}(t) = 0$.

For clarity, the proof is split in three parts. Firstly, we use geometric arguments to show that the solution lies on a face of the simplex $\mathcal{U}$ for all $t \in [0, t_f)$. Secondly, we define some notation and derive a link between the values of the switching functions and the optimal solution. Finally, by examining properties of $\dot{h}_i(t)$ we show that the optimal solution satisfies the claim.

Part 1:

Denote the set of vertices of the set $\mathcal{U}$ as $\mathcal{V} = \{\mathbf{v_0}, \mathbf{v_1}, \dots, \mathbf{v_n}\} \cup \{\mathbf{0}\}$, where $\mathbf{v_i}$ has E_{T} in its $(i+1)^{\text{st}}$ entry and 0 elsewhere. Similarly, the set of n-dimensional faces of $\mathcal{U}$ is defined as

$$\mathcal{F} = \{F_0, F_1, \dots, F_n\} \cup \{\mathcal{P}\},$$ (4.3.7)

where F_i and $\mathcal{P}$ are the faces defined by the hyperplanes

$$F_i = \{u \in \mathcal{U} : u_i = 0\},$$ (4.3.8)

$$\mathcal{P} = \left\{ u \in \mathcal{U} : \sum_{i=0}^{n} u_i = E_{\text{T}} \right\}.$$ (4.3.9)

In what follows we denote the optimal control that solves Problem 4.1 as $u^*(t)$. From condition (A.1.6) in PMP we know that the optimal control must minimize the Hamiltonian. We notice in (4.3.5) that $\mathcal{H}\left(x(t), u(t), p(t)\right)$ is a linear function defined over the simplex $\mathcal{U}$. Therefore it follows that the optimal control is located in the boundary of $\mathcal{U}$ for all $t \in [0, t_f)$. Moreover, this implies that $u^*(t) \in \mathcal{V}, \forall t \in [0, t_f)$ and hence the optimal control can always be found at the vertices of $\mathcal{U}$. As a consequence, if the optimal control is not unique then it has to lie on a face of the

$\mathcal{U}$, i.e. the convex hull of a subset of $\mathcal{V}$. We next present a simple fact that will be used to preclude the optimality of the face $F_i, i = 0, 1, \ldots, n$.

Lemma 4.1: *Let $f(u) : \mathcal{U} \to \mathbb{R}$ be a linear function of u with $\mathcal{U}$ defined in (4.2.9). Assume that the minimum of $f(u)$ is not attained at vertex $\mathbf{v_j}$, then $f(u)$ cannot attain its minimum at any face of $\mathcal{U}$ that contains $\mathbf{v_j}$.*

Proof:

The proof follows by contradiction. Let Q be any r-dimensional face of $\mathcal{U}$ with vertex set $\mathcal{V}_Q \subseteq \mathcal{V}$ and $r \leq n + 1$. Suppose $\mathcal{V}_Q$ is partitioned as $\mathcal{V}_Q = \mathcal{V}_{Q+} \cup \mathcal{V}_{Q-}$, where the subset $\mathcal{V}_{Q+}$ contains the vertices where $f(u)$ is minimal and $\mathcal{V}_{Q-} = \mathcal{V}_Q \setminus \mathcal{V}_{Q+}$. Let $\mathbf{v_j} \in \mathcal{V}_{Q-}$ and assume that there exists $y \in Q$ such that $f(y)$ is minimal. Then, if we define the index sets $\mathbb{I}_{Q+} = \{i : \mathbf{v_i} \in \mathcal{V}_{Q+}\}$ and $\mathbb{I}_{Q-} = \{i : \mathbf{v_i} \in \mathcal{V}_{Q-}\}$, there exists $\beta_i \geq 0$ such that

$$y = \sum_{i \in \mathbb{I}_{Q-}} \beta_i \mathbf{v_i} + \sum_{i \in \mathbb{I}_{Q+}} \beta_i \mathbf{v_i}, \tag{4.3.10}$$

with

$$\sum_{i \in \mathbb{I}_{Q-} \cup \mathbb{I}_{Q+}} \beta_i = 1. \tag{4.3.11}$$

Linearity of $f(u)$ implies that $f(y) = f(\mathbf{v_i}), \forall i \in \mathbb{I}_{Q+}$, and (4.3.10) yields

$$\left(1 - \sum_{i \in \mathbb{I}_{Q+}} \beta_i\right) f(y) = \sum_{i \in \mathbb{I}_{Q-}} \beta_i f(\mathbf{v_i}),$$
$$\sum_{i \in \mathbb{I}_{Q-}} \beta_i f(y) = \sum_{i \in \mathbb{I}_{Q-}} \beta_i f(\mathbf{v_i}), \tag{4.3.12}$$

which is a contradiction because $f(y) < f(\mathbf{v_i})$ for all $i \in \mathbb{I}_{Q-}$.

□□□

The condition (A.1.8) in PMP implies that $\mathcal{H}$ must vanish along the optimal trajectory, so that (4.3.5) implies $u^*(t) \neq \mathbf{0}, \forall t \in [0, t_f)$. This precludes the optimality of the origin, and thus we can use Lemma 4.1 to conclude that $u^*(t) \notin F_i \setminus \mathcal{V}, \forall i$.

This implies that $u^*(t) \in \mathcal{P}$ and therefore the optimal solution satisfies

$$\sum_{i=0}^{n} u_i^*(t) = E_\mathrm{T}. \qquad (4.3.13)$$

Part 2:

Now suppose that we partition the interval $[0, t_f)$ in subintervals $\{T_0, T_1, \ldots, T_q\}$ such that $T_0 = [0, t_0)$ and $T_i = [t_{i-1}, t_i)$, $\forall i = 1, 2, \ldots, q$, with $t_i < t_j$, $\forall i < j$ and $t_q = t_f$. Define the index set

$$\mathbb{I}_\ell = \{i : u_i^*(t) \neq 0, \forall t \in T_\ell\} \qquad (4.3.14)$$

so that the set

$$U_\ell^* = \{u_i^* : i \in \mathbb{I}_\ell\}, \qquad (4.3.15)$$

contains all the components of u^* that are nonzero during interval T_ℓ. Note that since $x(0) = 0$ and $x(t_f) \neq 0$ (recall the definition of the set $\mathcal{S}$ in (4.2.11)), the set U_ℓ^* is nonempty. Note that, without loss of generality, the partition $\{T_0, T_1, \ldots, T_q\}$ is chosen so that $U_i^* \neq U_{i+1}^*$ for $i = 0, 1, \ldots, q-1$.

From (4.3.5), the condition (A.1.8) in PMP translates into

$$1 + \sum_{i=0}^{n} h_i(t) u_i^*(t) = 0, \forall t \in [0, t_f). \qquad (4.3.16)$$

During interval T_ℓ, the above equation becomes

$$1 + \sum_{i \in \mathbb{I}_\ell} h_i(t) u_i^*(t) = 0, \forall t \in T_\ell. \qquad (4.3.17)$$

In addition, the result in (4.3.13) implies that for all $i \in \mathbb{I}_\ell$, u_i satisfies

$$\sum_{i \in \mathbb{I}_\ell} u_i^*(t) = E_\mathrm{T}, \forall t \in T_\ell, \qquad (4.3.18)$$

which can also be written as

$$1 - \sum_{i \in \mathbb{I}_\ell} \frac{1}{E_\mathrm{T}} u_i^*(t) = 0, \forall t \in T_\ell. \qquad (4.3.19)$$

44

Note also that because of the linear Hamiltonian, if for any time $t \in [0, t_f)$ a point $u_a \in \mathcal{P} \setminus \mathcal{V}$ is optimal, then any $u_b \neq u_a$ such that $u_b \in \mathcal{P} \setminus \mathcal{V}$ is also optimal. This means that equations (4.3.17) and (4.3.19) must be satisfied by any $u^* \in \mathcal{P}$, which is only possible when

$$h_j(t) = -\frac{1}{E_\mathrm{T}} < 0, \, \forall\, j \in \mathbb{I}_\ell, \, \forall\, t \in T_\ell. \tag{4.3.20}$$

Equation (4.3.20) allows to identify the elements of U_ℓ^* (i.e. the nonzero controls in interval T_ℓ) by examining the trajectories of the switching functions.

Part 3:

With the previous definitions, the proof follows by showing that

$$U_\ell^* = \{u_\ell\}, \, \forall\, \ell = 0, 1, \ldots, q, \tag{4.3.21}$$

$$q = n - 1. \tag{4.3.22}$$

The claim can be proven with an inductive procedure based on the following lemma.

Lemma 4.2: *Consider interval T_ℓ, $\ell \geq 2$, and assume that*

$$x_i(t_\ell) = 0, \, \forall\, i > \ell + 1, \tag{4.3.23}$$

$$U_j^* = \{u_j\}, \, \forall\, j \leq \ell. \tag{4.3.24}$$

Then,

$$U_{\ell+1}^* = \{u_{\ell+1}\}. \tag{4.3.25}$$

Proof:

We first note that since $x(0) = 0$ and $g_i(0) = 0$, then (4.3.24) implies

$$x_j(t) = 0, \, \forall\, t \in \bigcup_{i=0}^{j-2} T_i, \, \forall\, 2 \leq j \leq \ell,$$

which combined with (4.3.6) yields

$$h_j(t) = \alpha_j, \, \forall t \in \bigcup_{i=0}^{j-2} T_i, \, \forall \, 2 \leq j \leq \ell. \tag{4.3.26}$$

From (4.2.4), (4.3.6), and (4.3.4), for all j it holds

$$\dot{h}_j(t) = (\dot{p}_{j+1}(t) - \dot{p}_j(t)) \, g_j \, (x_j(t)) + (p_{j+1}(t) - p_j(t)) \frac{\partial g_j}{\partial x_j} \dot{x}_j(t)$$

$$= (p_{j+1}(t) - p_{j+2}(t)) \frac{\partial g_{j+1}}{\partial x_{j+1}} g_j \, (x_j(t)) \, u_{j+1}(t) \; -$$

$$(p_j(t) - p_{j+1}(t)) \frac{\partial g_j}{\partial x_j} g_{j-1} \, (x_{j-1}(t)) \, u_{j-1}(t), \tag{4.3.27}$$

where we define $g_{-1} = 0$. Since $u_j(t) = 0, \, \forall \, j \neq \ell, \, \forall \, t \in T_\ell$, (4.3.27) yields

$$\dot{h}_j(t) = 0, \, \forall \, j \notin \{\ell - 1, \ell + 1\}, \, \forall \, t \in T_\ell. \tag{4.3.28}$$

On the other hand, if $j = \ell - 1$ then $u_{j+1}(t) = E_{\mathrm{T}}$, $u_{j-1}(t) = 0, \, \forall \, t \in T_\ell$, which after substituting in (4.3.27) yields

$$\dot{h}_{\ell-1}(t) = (p_\ell(t) - p_{\ell+1}(t)) \frac{\partial g_\ell}{\partial x_\ell} g_{\ell-1} \, (x_{\ell-1}(t)) \, E_{\mathrm{T}}, \, \forall \, t \in T_\ell. \tag{4.3.29}$$

Combining (4.3.29) and (4.3.6) with $i = \ell$ leads to

$$\dot{h}_{\ell-1}(t) = \left(\frac{\alpha_\ell - h_\ell(t)}{g_\ell(x_\ell(t))} \right) \frac{\partial g_\ell}{\partial x_\ell} g_{\ell-1} \, (x_{\ell-1}(t)) \, E_{\mathrm{T}}, \, \forall \, t \in T_\ell. \tag{4.3.30}$$

Equation (4.3.6) with $i = \ell$ implies that $g_\ell(t) > 0, \, \forall \, t \in T_\ell$, since otherwise $h_\ell(t) = \alpha_\ell \geq 0$ for some $t \in T_\ell$ and (4.3.20) cannot be satisfied. This guarantees that $\dot{h}_{\ell-1}(t)$ in (4.3.30) is well defined in the interval T_ℓ. Similarly, (4.3.24) implies that $g_{\ell-1} \, (x_{\ell-1}(t)) > 0, \, \forall \, t \in T_{\ell-1}$ and $\dot{x}_{\ell-1}(t) = 0, \, \forall \, t \in T_\ell$. Then, $g_{\ell-1} \, (x_{\ell-1}(t)) > 0, \, \forall \, t \in T_\ell$ and thus, using (4.2.2) and (4.3.20) in (4.3.30) yields

$$\dot{h}_{\ell-1}(t) > 0, \, \forall \, t \in T_\ell. \tag{4.3.31}$$

Equations (4.3.20), (4.3.26), (4.3.28) and (4.3.31) provide information on the

trajectory of the jth switching function. These can be summarized as

$$h_j(t) = \begin{cases} \alpha_j & , \forall\, 2 \leq j \leq \ell,\ \forall\, t \in \bigcup_{i=0}^{j-2} T_i, \\ -\frac{1}{E_T} & , \forall\, j \leq \ell,\ \forall\, t \in T_j, \end{cases} \tag{4.3.32}$$

$$\dot{h}_j(t) > 0,\ \forall\, j < \ell,\ \forall\, t \in T_{j+1}, \tag{4.3.33}$$

$$\dot{h}_j(t) = 0,\ \forall\, j < \ell,\ \forall\, t \in \bigcup_{i=j+2}^{\ell} T_i. \tag{4.3.34}$$

In order to clarify the idea, a schematic plot of the switching functions $h_{\ell-2}(t)$, $h_{\ell-1}(t)$ and $h_\ell(t)$ is depicted in Figure 4.2.
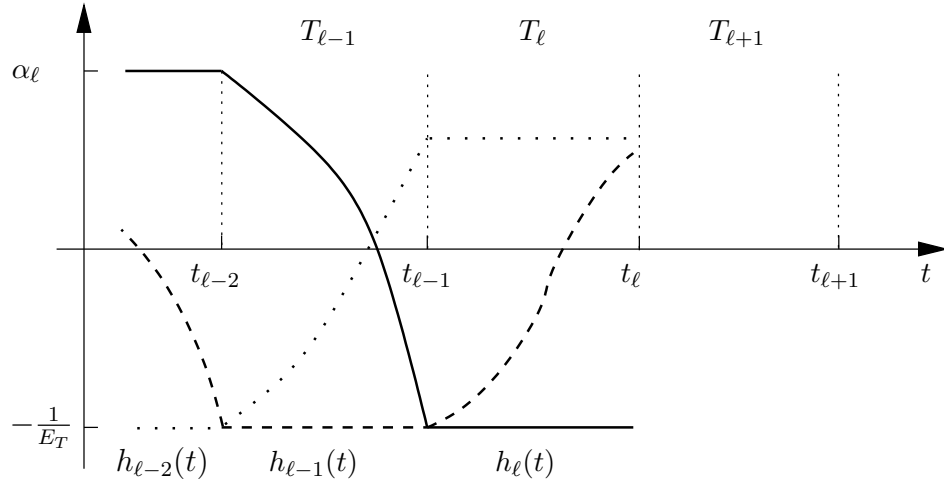
Figure 4.2. Sketch plot of switching functions $h_{\ell-2}(t)$, $h_{\ell-1}(t)$ and $h_\ell(t)$ satisfying equations (4.3.32)–(4.3.34).

The idea is then to show that the form of the trajectories in Figure 4.2 implies that the only enzyme that can be nonzero in $T_{\ell+1}$ is $u_{\ell+1}$ (as expressed in (4.3.25)). We proceed by analyzing the effect of enzyme u_j being nonzero in interval $T_{\ell+1}$.

- Case $j < \ell$:

  Assume that $u_j \in U_{\ell+1}^*$ for some $j < \ell$. Then in order to satisfy (4.3.20), (4.3.32)–(4.3.34) imply that $h_j(t)$ must be discontinuous at $t = t_\ell$ (see Figure 4.2), which from (4.3.6) is not possible since both $x(t)$ and $p(t)$ are continuous.

Hence, it follows that

$$u_j \notin U^*_{\ell+1}, \; \forall\, j < \ell. \tag{4.3.35}$$

- Case $j > \ell + 1$:

From (4.3.23) we have that $x_i(t_\ell) = 0$, $\forall\, i > \ell + 1$ and hence using (4.2.4) we conclude that $x_i(t) = 0$, $\forall\, i > \ell + 1$, $\forall\, t \in T_{\ell+1}$. The switching function in (4.3.6) then becomes

$$h_i(t) = \alpha_i \geq 0, \; \forall\, i > \ell + 1, \; \forall\, t \in T_{\ell+1}, \tag{4.3.36}$$

which contradicts (4.3.20) and hence

$$u_j \notin U^*_{\ell+1}, \; \forall\, j > \ell + 1. \tag{4.3.37}$$

- Case $j \in \{\ell, \ell + 1\}$:

Assume that $U^*_{\ell+1} = \{u_\ell, u_{\ell+1}\}$. Using (4.3.35)–(4.3.37) in (4.3.27) yields

$$\dot{h}_\ell(t) = (p_{\ell+1}(t) - p_{\ell+2}) \frac{\partial g_{\ell+1}}{\partial x_{\ell+1}} g_\ell\left(x_\ell(t)\right) u_{\ell+1}(t), \; \forall\, t \in T_{\ell+1}, \tag{4.3.38}$$

$$\dot{h}_{\ell+1}(t) = -(p_{\ell+1}(t) - p_{\ell+2}) \frac{\partial g_{\ell+1}}{\partial x_{\ell+1}} g_\ell\left(x_\ell(t)\right) u_\ell(t), \; \forall\, t \in T_{\ell+1}. \tag{4.3.39}$$

Substituting (4.3.6) with $i = \ell + 1$ in (4.3.38)–(4.3.39) leads to

$$\dot{h}_\ell(t) = \left(\frac{\alpha_{\ell+1} - h_{\ell+1}(t)}{g_{\ell+1}\left(x_{\ell+1}(t)\right)} \right) \frac{\partial g_{\ell+1}}{\partial x_{\ell+1}} g_\ell\left(x_\ell(t)\right) u_{\ell+1}(t), \; \forall\, t \in T_{\ell+1}, \tag{4.3.40}$$

$$\dot{h}_{\ell+1}(t) = -\left(\frac{\alpha_{\ell+1} - h_{\ell+1}(t)}{g_{\ell+1}\left(x_{\ell+1}(t)\right)} \right) \frac{\partial g_{\ell+1}}{\partial x_{\ell+1}} g_\ell\left(x_\ell(t)\right) u_\ell(t), \; \forall\, t \in T_{\ell+1}. \tag{4.3.41}$$

Since $x_{\ell+1}(t) \neq 0$, $\forall\, t \in T_{\ell+1}$, the right hand sides of (4.3.40)–(4.3.41) do not have singularities. From (4.3.20), $U^*_{\ell+1} = \{u_\ell, u_{\ell+1}\}$ implies that $\dot{h}_\ell(t) = \dot{h}_{\ell+1}(t) = 0$, $\forall\, t \in T_{\ell+1}$, but in view of (4.3.40)–(4.3.41), this can only hold if $u_\ell(t) = u_{\ell+1}(t) = 0$, $\forall\, t \in T_{\ell+1}$, which contradicts the assumption that $U^*_{\ell+1} = \{u_\ell, u_{\ell+1}\}$. Moreover, if $U^*_{\ell+1} = \{u_\ell\}$, then $U^*_{\ell+1} = U^*_\ell$, contradicting the fact that $U^*_i \neq U^*_{i+1}$, $\forall\, i = 0, 1 \ldots, q - 1$. Thus, $u_\ell \notin U^*_{\ell+1}$ and since $U^*_\ell \neq \emptyset$, we get the result in (4.3.25).

□□□

To conclude the argument, next we show that $U_0^* = \{u_0\}$ and $U_1^* = \{u_1\}$. These imply that conditions (4.3.23)–(4.3.24) in Lemma 4.2 are satisfied for $\ell = 1, 2$, and hence the lemma can be used inductively to prove the claim in (4.3.21).

Consider interval T_0 and assume that vertex $\mathbf{v_j}$, $j > 0$, is optimal in T_0, then since $x(0) = 0$ it follows from (4.2.4) that $x(t) = 0$, $\forall t \in T_0$. From (4.2.3) and (4.3.6), this yields $h_j(t) = \alpha_i \geq 0$, $\forall i > 0$, which contradicts (4.3.20) and therefore $\mathbf{v_j}, j > 0$, cannot be optimal in interval T_0. Lemma 4.1 then yields

$$U_0^* = \{u_0\}. \tag{4.3.42}$$

We now consider interval T_1. Assume $\mathbf{v_j}$, $\forall j > 1$, is optimal in interval T_1, then (4.3.42) implies $x_i(t_0) = 0$, $\forall i > 1$ and hence (4.2.4) yields $x_i(t) = 0$, $\forall i > 1$, $\forall t \in T_1$. The switching function in (4.3.6) becomes

$$h_i(t) = \alpha_i \geq 0, \ \forall i > 1, \tag{4.3.43}$$

which contradicts (4.3.20) and therefore $\mathbf{v_j}, j > 1$, cannot be optimal in interval T_1. Thus, from Lemma 4.1 we conclude that $u_j \notin U_1^*$, $\forall j > 1$.

Now suppose that $\mathbf{v_0}$ and $\mathbf{v_1}$ are optimal in interval T_1, then similarly as in case $j \in \{\ell, \ell + 1\}$ in the proof of Lemma 4.2 (take (4.3.38)–(4.3.41) with $\ell = 0$), it can be shown that $\dot{h}_0(t) = \dot{h}_1(t) = 0$, $\forall t \in T_1$ only when $u_0(t) = u_1(t) = 0$, $\forall t \in T_1$, which contradicts the optimality of $\mathbf{v_0}$ and $\mathbf{v_1}$. Moreover, if $\mathbf{v_0}$ is optimal in T_1, then $U_1^* = U_0^*$, contradicting our hypothesis that $U_i^* \neq U_{i+1}^*$, $\forall i = 0, 1, \ldots, q$. Thus, we conclude that $u_0 \notin U_1^*$, which together with the non-emptiness of U_1^* yields

$$U_1^* = \{u_1\}. \tag{4.3.44}$$

Equations (4.3.42) and (4.3.44) imply that $x_i(t_1) = 0$, $\forall i > 1$ and therefore, we can inductively use Lemma 4.2, to get the result (4.3.21).

To prove (4.3.22) it suffices to show that $q \neq n$. Assume that $q = n$ and consider interval T_n, so that from (4.3.21) it holds that $U_n^* = \{u_n\}$. From (4.3.32)–(4.3.34) it follows that there is no switching function h_i such that condition (4.3.20) holds for $\ell > n$ (this can also be seen from the trajectories for the switching functions in Figure 4.2). Thus, $U_n^* = \{u_n\}$ implies that $\dot{x}_n(t) < 0$, $\forall t \geq t_{n-1}$, which cannot hold (if it were true, then $\lim_{t \to \infty} x_n(t) = 0$ and thus $x(t_f) \notin \mathcal{S}$). This leads to the

conclusion that $q \neq n$ and (4.3.22) follows.

4.3.3 Example

As an illustrative example of the result in Theorem 4.1, we consider a network as in Figure 4.1 of length $n = 3$, where all the reactions exhibit Michaelis-Menten kinetics of the form

$$v_i(s_i, e_i) = \frac{k_{\text{cat}\,i} s_i(t)}{K_{\text{m}\,i} + s_i(t)} e_i(t). \tag{4.3.45}$$

The model parameters are $\{k_{\text{cat}\,1}, k_{\text{cat}\,2}, k_{\text{cat}\,3}, k_{\text{cat}\,4}\} = \{1, 2, 4, 3\}$, $K_{\text{m}\,i} = 1$ for all i, $s_0 = 5$ and we set the enzymatic weights to $\alpha_i = 1$ for all i. The maximum enzyme concentration is $E_{\text{T}} = 1$. The solution of Problem 4.1 with $V = 0.2$ is shown in Figure 4.3. The optimal switchings occur at $t_0 = 1.5$, $t_1 = 2.1$ and $t_2 = 2.4$, and the steady state concentrations of the metabolites are $s_1^f = 0.65$, $s_2^f = 0.32$ and $s_3^f = 0.29$. The optimal solution is a sequence of switches that agrees with the result of Theorem 4.1 and guarantees that the steady state is maintained after the activation time ($t \geq t_2$). The terminal steady state enzyme levels are computed directly from (4.2.10). We also notice that the last enzyme needs to be present only after the activation period, which is required to achieve the steady state flux.

The numerical solution was obtained via an equivalent nonlinear static optimization problem and the gradient-based routine `fmincon` available in the Optimization Toolbox for Matlab®. For clarity, the details of this equivalent optimization problem are presented in the next section.

4.4 Equivalent nonlinear optimization problem

The result of Theorem 4.1 allows us to fully characterize the solution to Problem 4.1 in terms of the n switching times $\{t_0, t_1, \ldots, t_{n-1}\}$. Numerical solutions can thus be obtained by considering the switching times as decision variables of an equivalent static optimization problem. In this section we show how to translate Problem 4.1 into a static nonlinear optimization problem which can be solved with standard software packages.
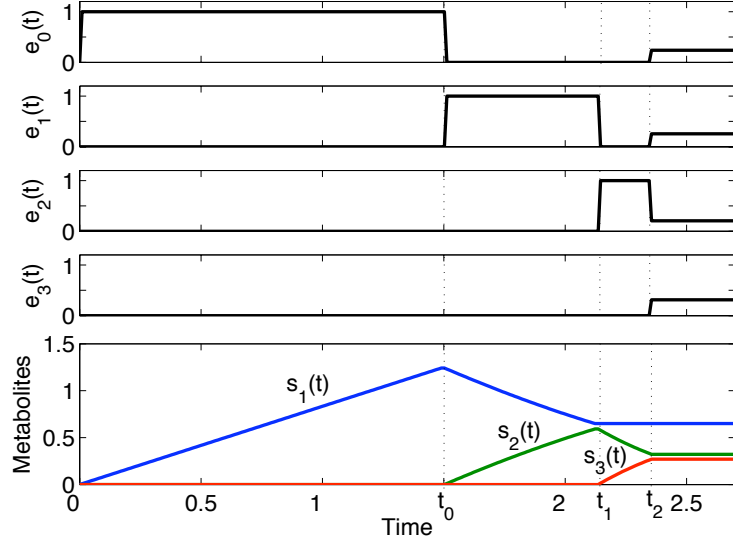
Figure 4.3. Optimal activation for pathway of length $n = 3$ with Michaelis-Menten kinetics.

Equivalent cost

Consider the statement of Theorem 4.1 and write the cost function in (4.2.8) as

$$\mathcal{J} = \int_0^{t_0} \left(1 + \alpha^T e(t)\right) \mathrm{d}t + \sum_{i=1}^{n-1} \int_{t_{i-1}}^{t_i} \left(1 + \alpha^T e(t)\right) \mathrm{d}t. \tag{4.4.1}$$

Substitution of the optimal control (4.3.2) in (4.4.1) yields

$$\mathcal{J} = \sum_{i=0}^{n-1} \beta_i \Delta_i, \tag{4.4.2}$$

where Δ_i is the *switching period* of the ith control, i.e. $\Delta_0 = t_0$ and $\Delta_i = t_i - t_{i-1}$. The weights β_i are defined as

$$\beta_i = 1 + \alpha_i E_{\mathrm{T}}, \tag{4.4.3}$$

so that the original cost function can be simply written as a linear function of the switching periods. In vector form (4.4.2) reads

$$\mathcal{J} = \beta^T \Delta, \tag{4.4.4}$$

where $\Delta = \begin{bmatrix} \Delta_0 & \Delta_1 & \cdots & \Delta_{n-1} \end{bmatrix}^T$ and $\beta = \begin{bmatrix} \beta_0 & \beta_1 & \ldots & \beta_{n-1} \end{bmatrix}^T$.

Explicit formulae for the switching periods

The optimization of (4.4.4) with the switching periods as decision variables requires writing the nonlinear constraint (4.2.11) in terms of Δ. This is a difficult task, but as it will be shown next, we can derive explicit formulae for the switching periods in terms of the final state. This allows to carry out the optimization with the final state as the decision variable and use the constraint (4.2.11) as it is.

Let $\{T_0, T_1, \ldots, T_{n-1}\}$ be the partition of the interval $[0, t_f)$ described in Theorem 4.1. We first note that substitution of the optimal control (4.3.2) in the dynamics (4.2.4) yields

$$\dot{s}_j = \begin{cases} E_T g_0(s_0), & j = 1, \\ 0, & j \neq 1, \end{cases} \tag{4.4.5}$$

for all $t \in T_0$ and

$$\dot{s}_j = \begin{cases} -E_T g_i(s_i), & j = i, \\ E_T g_i(s_i), & j = i + 1, \\ 0, & j \notin \{i, i+1\}, \end{cases} \tag{4.4.6}$$

for all $t \in T_i, i > 0$. Thus, given a set of intervals $\{T_0, T_1, \ldots, T_{n-1}\}$, the solution of (4.4.5)–(4.4.6) with initial condition $s(0) = 0$ is the state trajectory of system in (4.2.4) under the optimal bang-bang control. Let us now introduce a new state variable

$$z = \boldsymbol{T}s, \tag{4.4.7}$$

with $\mathbf{T} \in \mathbb{R}^{n \times n}$ defined as

$$\boldsymbol{T} = \begin{bmatrix} 1 & 1 & \cdots & 1 \\ 0 & 1 & \cdots & 1 \\ \vdots & \ddots & \ddots & \vdots \\ 0 & 0 & \cdots & 1 \end{bmatrix}. \tag{4.4.8}$$

Since the original state variable s is given by

$$s_i = z_i - z_{i+1}, \tag{4.4.9}$$

the dynamics (4.4.5)–(4.4.6) can be written as

$$\dot{z}_j = \begin{cases} E_{\mathrm{T}} g_0(s_0), & j = 1, \\ 0, & j \neq 1, \end{cases} \tag{4.4.10}$$

for all $t \in T_0$, whereas

$$\dot{z}_j = \begin{cases} E_{\mathrm{T}} g_i(z_i - z_{i+1}), & j = i + 1, \\ 0, & j \neq i + 1, \end{cases} \tag{4.4.11}$$

for all $t \in T_i, i > 0$ and with initial condition $z(0) = 0$. The system (4.4.10)–(4.4.11) has a simpler structure than (4.4.5)–(4.4.6). In fact, during the interval T_i every component of z remains constant, except for z_{i+1}. This also implies that

$$z_j(t) = \begin{cases} z_j^f, & j \leq i, \\ 0 & j > i + 1, \end{cases} \tag{4.4.12}$$

for all $t \in T_i, i \geq 0$ and with $z^f = \boldsymbol{T} s^f$.

As shown next, equations (4.4.10)–(4.4.12) allow the explicit computation of the switching periods as a function of the final state z^f. In the sequel we write $\Delta_i = \Delta_i(z^f)$ to denote the dependence of Δ_i on the final state. Integrating (4.4.10) from $t = 0$ up to $t = t_1$ leads to

$$\Delta_0(z^f) = \frac{z_1^f}{E_{\mathrm{T}} g_0(s_0)}. \tag{4.4.13}$$

The remaining switching periods can be computed as follows. Equation (4.4.12) implies that $z_i(t) = z_i^f$ for all $t \in T_i$, which can be substituted in (4.4.11) to obtain

$$\dot{z}_{i+1}(t) = E_{\mathrm{T}} g_i(z_i^f - z_{i+1}(t)), \tag{4.4.14}$$

for all $t \in T_i, i > 0,$. Integration of (4.4.14) on the interval T_i yields

$$\Delta_i(z^f) = \frac{1}{E_{\mathrm{T}}} \int_{z_{i+1}(t_{i-1})}^{z_{i+1}(t_i)} \frac{1}{g_i(z_i^f - \tau)} \, \mathrm{d}\tau, \quad i > 0. \tag{4.4.15}$$

In addition, from (4.4.12) we have $z_{i+1}(t_{i-1}) = 0$ and $z_{i+1}(t_i) = z_{i+1}^f$, so that the above equation becomes

$$\Delta_i(z^f) = \frac{1}{E_{\mathrm{T}}} \int_0^{z_{i+1}^f} \frac{1}{g_i(z_i^f - \tau)} \, \mathrm{d}\tau, \quad i > 0. \tag{4.4.16}$$

Equations (4.4.13) and (4.4.16) are explicit formulae for computing the switching period Δ_i in terms of the final state z^f. We point out that since $s_i^f > 0$, the change of variables in (4.4.7) guarantees that $z_i^f > z_{i+1}^f$ and thus the integrand in (4.4.16) has no singularities on the integration interval.

Equivalent optimization problem

The formulae for Δ_i can be used to compute the equivalent cost (4.4.4) as a function of the final state z^f instead of the switching times. Using (4.4.9), the terminal set $\mathcal{S}$ in (4.2.11) can be written in terms of z^f as

$$\mathcal{S}_z = \left\{ z^f \in \mathbb{R}_{>0}^n : \frac{V}{g_0(s_0)} + \sum_{i=1}^n \frac{V}{g_i\left(z_i^f - z_{i+1}^f\right)} \leq E_{\mathrm{T}}, \ z_i^f > z_{i+1}^f \right\}. \tag{4.4.17}$$

From the results in the previous section, the following lemma holds.

Lemma 4.3: *Given $s^f \in \mathbb{R}_{>0}^n$, there exists a set of switching times $\{t_0, t_1, \ldots, t_{n-1}\}$ such that the optimal control in (4.3.2) drives the state from $s(0) = 0$ to $s(t_f) = s^f$.*

Proof:

For a given $z^f = \boldsymbol{T} s^f \in \mathcal{S}_z$, a unique set of switching periods $\{\Delta_0, \Delta_1, \ldots, \Delta_{n-1}\}$ can be computed with (4.4.13) and (4.4.16). Thus, given an arbitrary $s^f \in \mathbb{R}_{>0}^n$ we

can always find a set of switching times $\{t_0, t_1, \ldots, t_{n-1}\}$ such that $s(t_f) = s^f$.

$\square\square\square$

Lemma 4.3 guarantees that for any $z^f \in \mathcal{S}_z$, there is a set of switching times that drive the state s from the origin to $s^f = \boldsymbol{T}^{-1} z^f$. Therefore, the minimization of the equivalent cost in(4.4.4) can be carried out with the final state z^f as the decision variable. In addition, we have the next lemma.

Lemma 4.4: *Let $s^{f*} \in \mathbb{R}^n_{>0}$ be the final state associated to the solution of Problem 4.1, then*

$$\frac{V}{g_0\left(s_0\right)} + \sum_{i=1}^{n} \frac{V}{g_i\left(s_i^{f*}\right)} = E_{\mathrm{T}}. \tag{4.4.18}$$

Proof:

The proof follows by contradiction. Since s^{f*} is the terminal state of the optimal solution, we have that $s^{f*} \in \mathcal{S}$ with $\mathcal{S}$ defined in (4.2.11). Suppose that

$$\frac{V}{g_0\left(s_0\right)} + \sum_{i=1}^{n} \frac{V}{g_i(s_i^{f*})} < E_{\mathrm{T}}, \tag{4.4.19}$$

then there exists $\varepsilon > 0$ such that

$$\frac{V}{g_0\left(s_0\right)} + \sum_{i=1}^{n} \frac{V}{g_i(s_i^{f*})} + \varepsilon = E_{\mathrm{T}}. \tag{4.4.20}$$

By taking the last term out of the sum, (4.4.20) can be written as

$$\frac{V}{g_0\left(s_0\right)} + \sum_{i=1}^{n-1} \frac{V}{g_i(s_i^{f*})} + \frac{V}{g_n(s_n^{\varepsilon})} = E_{\mathrm{T}}, \tag{4.4.21}$$

where $s_n^{\varepsilon} > 0$ is such that

$$g_n(s_n^{\varepsilon}) = \frac{g_n(s_n^{f*})}{1 + \frac{\varepsilon}{V} g_n(s_n^{f*})}. \tag{4.4.22}$$

From (4.4.22) it can be seen that $g_n\left(s_n^{\varepsilon}\right) < g_n\left(s_n^{f*}\right)$, which using the monotonicity condition in Assumption 4.1 implies $s_n^{\varepsilon} < s_n^{f*}$. The optimal control (4.3.2) applied

to system (4.2.4) implies that $\dot{s}_n(t) > 0, \forall t \in [t_{n-2}, t_{n-1})$, so that there exists $t^\varepsilon < t_{n-1}$ such that $s_n(t^\varepsilon) = s_n^\varepsilon$, which in turn from (4.4.4) means that a lower cost is achieved, and hence s^{f*} cannot be the terminal state for the optimal solution.

$$\square\square\square$$

Equation (4.4.18) in Lemma 4.4 implies that the optimal solution enforces full enzyme usage not only during the optimization interval $[0, t_{n-1})$, as stated by Theorem 4.1, but also after the activation time (i.e. for $t \geq t_{n-1}$). We can thus rewrite the set $\mathcal{S}_z$ in (4.4.17) as

$$\mathcal{S}_z = \left\{ z^f \in \mathbb{R}_{>0}^n : \frac{V}{g_0(s_0)} + \sum_{i=1}^n \frac{V}{g_i\left(z_i^f - z_{i+1}^f\right)} = E_{\mathrm{T}}, \, z_i^f > z_{i+1}^f \right\}. \qquad (4.4.23)$$

We are now able to state the original optimal control problem as an equivalent nonlinear static optimization problem.

Problem 4.2 (Equivalent static optimization problem) *Find*

$$z^{f*} = \arg\min_{z^f} \beta^T \Delta(z^f) \qquad (4.4.24)$$

subject to $\qquad\qquad\qquad\qquad\qquad\qquad\qquad\qquad\qquad\qquad\quad (4.4.25)$

$$z^f \in \mathcal{S}_z, \qquad\qquad\qquad\qquad\qquad\qquad\qquad\qquad (4.4.26)$$

where $\mathcal{S}_z$ is defined in (4.4.23) and the switching periods $\Delta(z^f)$ are computed from (4.4.13) and (4.4.16).

The solution of Problem 4.2 can be obtained with standard routines for constrained nonlinear optimization. Once the solution z^{f*} is found, the optimal switching periods can be obtained from (4.4.13) and (4.4.16), while the final state can be computed from (4.4.9).

Remark 4.1: *In order to recast Problem 4.1 as a static nonlinear optimization problem, we introduced the change of variables $z = \boldsymbol{T}s$ defined in (4.4.7). This simplifies the analysis, as seen in the system (4.4.10)–(4.4.11), and leads to simple expressions for the switching periods in terms of the final state z^f. However, the change of variables is not mandatory and a similar analysis can be carried out in the original state variable s, leading to slightly more complicated formulae for the switching periods.*

4.5 Further analyses

4.5.1 Limit steady state flux

In the statement of Problem 4.1 we assumed that the network can reach any prescribed flux $V > 0$. However, the flux achievable by the network is constrained by the bound on the total enzyme abundance (4.2.9) and the saturating rates of the reaction steps. From the form of the reaction rates in (4.2.1), we define the saturating turnover rates $\hat{g}_i$ as

$$\hat{g}_i = \sup_{s_i > 0} g_i(s_i) = \sup_{s_i > 0} v_i(s_i, 1). \tag{4.5.1}$$

Note that since s_0 is constant, $\hat{g}_0 = g_0$. The constraint (4.4.18) implies that a flux $V > 0$ is achievable provided that

$$\frac{V}{g_0(s_0)} + \sum_{i=1}^{n} \frac{V}{g_i(s_i^f)} = E_{\mathrm{T}}, \tag{4.5.2}$$

has a solution $s^f \in \mathbb{R}_{>0}^n$. If we denote as $\hat{V}$ the supremum flux such that (4.5.2) has a positive solution, then it follows

$$
\begin{aligned}
\hat{V} &= E_{\mathrm{T}} \left(\inf_{s^f \in \mathbb{R}_{>0}^n} \frac{1}{g_0(s_0)} + \sum_{i=1}^{n} \frac{1}{g_i\left(s_i^f\right)} \right)^{-1}, \\
&= E_{\mathrm{T}} \left(\sum_{i=0}^{n} \frac{1}{\hat{g}_i} \right)^{-1}, \tag{4.5.3}
\end{aligned}
$$

where we interpret $\frac{1}{\infty} = 0$ for the case of non-saturating kinetics (e.g. Mass Action kinetics—such reactions do not constrain the achievable flux). Equation (4.5.3) gives the maximal flux under which the optimization problem is feasible. This formula also indicates how the total enzyme pool should be distributed to achieve maximal flux. The flux $\hat{V}$ will be reached only if the ratio $\frac{E_{\mathrm{T}}}{\hat{g}_i} \left(\sum_{i=0}^{n} \frac{1}{\hat{g}_i} \right)^{-1}$ of enzymatic activity is dedicated to enzyme e_i. In the typical case that the saturating turnover rates in (4.5.1) are not attained at finite metabolite concentrations, the upper bound $\hat{V}$ is not an achievable target. As shown in the next lemma, when the target flux V approaches the value $\hat{V}$, the optimal cost becomes arbitrarily large.

Lemma 4.5: *Denote the value of the optimal cost (as a function of V) as*

$$\mathcal{J}^*(V) = \min_{e(\cdot) \in \mathcal{U}} \mathcal{J}(V), \tag{4.5.4}$$

then

$$\lim_{V \to \hat{V}} \mathcal{J}^*(V) = \infty, \tag{4.5.5}$$

where $\hat{V}$ is the supremum flux given in (4.5.3).

Proof:

Let the target steady state flux be $V = \hat{V} - \delta$, $\delta > 0$, so that the terminal constraint (4.4.18) becomes

$$\frac{\hat{V}}{g_0(s_0)} + \sum_{i=1}^{n} \frac{\hat{V}}{g_i\left(s_i^{f*}\right)} - \delta \sum_{i=0}^{n} \frac{1}{g_i\left(s_i^f\right)} = E_{\mathrm{T}}. \tag{4.5.6}$$

Substituting $\hat{V}$ in (4.5.3) in the above equation and rearranging terms we obtain

$$E_{\mathrm{T}} \sum_{i=1}^{n} \left(\frac{1}{g_i\left(s_i^f\right)} - \frac{1}{\hat{g}_i} \right) = \delta \sum_{i=0}^{n} \frac{1}{\hat{g}_i} \left(\frac{1}{g_0(s_0)} + \sum_{i=1}^{n} \frac{1}{g_i\left(s_i^f\right)} \right). \tag{4.5.7}$$

By definition $\hat{g}_i \geq g_i\left(s_i^f\right)$ for all $s_i^f > 0$, which together with $g_i\left(s_i^f\right) > 0$ implies that the left hand side of (4.5.7) is nonnegative. Therefore, when $\delta \to 0$ the terminal set $\mathcal{S}$ is equal to set of positive solutions of the equation

$$\sum_{i=0}^{n} \left(\frac{1}{g_i\left(s_i^f\right)} - \frac{1}{\hat{g}_i} \right) = 0. \tag{4.5.8}$$

All the terms of the sum in (4.5.8) are positive and hence, the only positive solution to (4.5.8) is obtained when

$$g_i\left(s_i^f\right) = \hat{g}_i, \tag{4.5.9}$$

which implies that each reaction must be saturated. From the monotonicity condition in Assumption 4.1, this means that the unique positive solution to (4.5.8) is

$s_i^f = \infty$ for all i. Thus, we concluded that if $V \to \hat{V}$ then the set $\mathcal{S}$ degenerates into a single point at infinity. The claim (4.5.5) follows from the definition of $\mathcal{J}$ in (4.2.8), where it is clear that the state can be driven to infinity only when $t_f = \infty$.

$$\square\square\square$$

The result of Lemma 4.5 implies that the maximal flux can only be reached by saturating all the reactions in the pathway, which in turn would require an infinite activation period.

4.5.2 Sensitivity of the solution

In this section we study the sensitivity properties of the optimal solution in Theorem 4.1 via two numerical case studies. We consider pathways of length $n = 6$ with $s_0 = 1$ and assume that all the reactions follow Michaelis-Menten kinetics of the form (4.3.45). We adopt as nominal model parameters $k_{\text{cat}\,i} = 1$ and $K_{\text{m}\,i} = 1$. The nominal values for the enzyme weights are chosen as $\alpha_i = 5$ and the numerical solutions are obtained with the equivalent nonlinear optimization problem described in Section 4.4 and the routine `fmincon` available in the Optimization Toolbox for Matlab$^{\circledR}$.

Sensitivity to kinetic parameters

In order to study the effect of kinetic parameters on the optimal activation, we compare the sensitivity of the optimal cost with respect to parameters $k_{\text{cat}\,i}$ and $K_{\text{m}\,i}$ of each reaction. Varying one constant at a time and setting the others to their nominal values, we obtain optimal solutions for different values of $k_{\text{cat}\,i}$ and $K_{\text{m}\,i}$ in a range of $\pm 90\%$ of their nominal values. The target flux is chosen as 80% of the maximal flux $\hat{V}$ (see (4.5.3)) for the parameter range. The results are shown in Figure 4.4, where the optimal cost normalized with respect to its nominal value is shown for $k_{\text{cat}\,i}$ between 10% and 25% of the nominal value, and $K_{\text{m}\,i}$ from 10% to 100% of its nominal value.
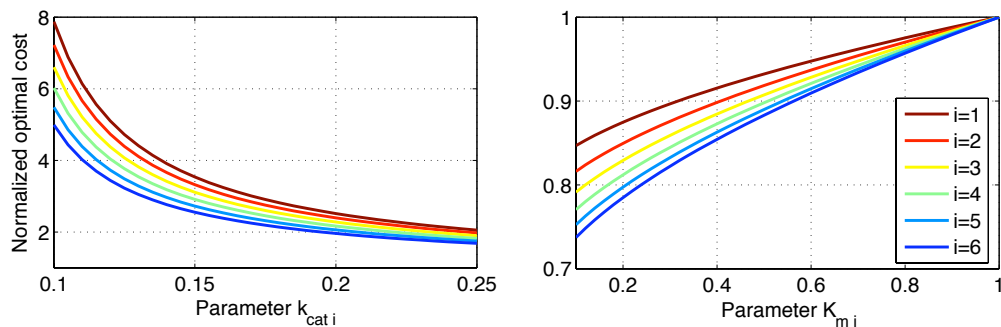
Figure 4.4. Normalized optimal cost as a function of the kinetic parameters.

As expected the optimal activation takes longer as parameters $k_{\mathrm{cat}\,i}$ decrease. As shown in Figure 4.4, the optimal activation is less sensitive to the k_{cat} parameter of those reactions that are located toward the end of the pathway. For example, reducing $k_{\mathrm{cat}\,6}$ to 10% of its nominal value yields a five-fold increase in the optimal cost, whereas the same reduction in $k_{\mathrm{cat}\,1}$ yields almost an eight-fold increase. This is a consequence of the fact that early reactions must process more material in order to reach steady state. The overall trend is consistent with the commonly accepted assertion [37] in the literature on Metabolic Control Analysis that the sensitivity of the steady state flux with respect to a particular $k_{\mathrm{cat}\,i}$ decreases as the reaction is located toward the end of the pathway.

The sensitivity with respect to parameters $K_{\mathrm{m}\,i}$ follows the opposite trend, with increased sensitivity later in the pathway. This conclusion has more to do with individual kinetics than with the behaviour of the system as a whole. As mentioned, the first reactions process more material and so operate at higher substrate concentrations than those downstream. The saturating nature of the Michaelis-Menten kinetic implies that those reactions operating at high substrate concentrations are less susceptible to variations in K_{m}.

Sensitivity to enzyme weighting

As discussed earlier, the weighting vector α allows the optimization procedure to reflect the relative biosynthetic costs of the enzymes in the pathway. To explore the sensitivity of the optimal activation with respect to the enzyme weighting, we consider the effect of α_i on the activation period Δ_i of enzyme e_i. Changing one enzyme weight at a time, we compute optimal solutions for α_i in the range $\pm 50\%$

of the nominal value with a target flux that is 80% of the limit $\hat{V}$. The optimal activation period normalized with respect to its nominal value is shown in Figure 4.5.
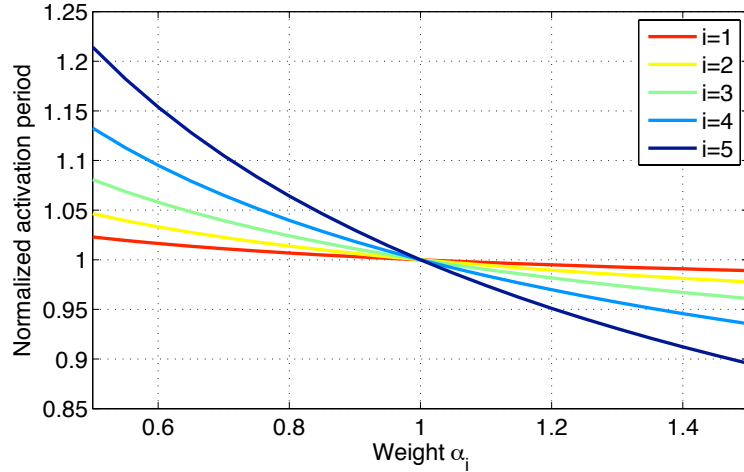
Figure 4.5. Normalized optimal pulse width of each enzyme as a function of the enzyme weight α_i (in units of the nominal weight values).

It can be observed that the activation period decreases as the enzyme is more strongly penalized. The reduction is larger for those enzymes acting close to the end of the pathway. This implies that significant reductions in the use of early enzymes can only be achieved with very large weights, while more freedom is available for the ones toward the end of the pathway. For example, for enzyme e_1 only a marginal reduction can be achieved with a 50% increase in the weight, while for e_5 a reduction over 10% can be attained. This is a consequence of the pathway structure and suggests, as in the previous case study, that the importance of a specific enzyme in the activation dynamics is a decreasing function of its position in the pathway.

4.5.3 Effect of enzyme production dynamics

Throughout this chapter we have considered the enzyme concentrations as control inputs to the metabolic network. As discussed in Chapter 2, enzyme production is controlled by gene expression mechanisms. However, genetic dynamics are not as fast as required by the switching enzyme concentrations of Theorem 4.1, and therefore the solution of Problem 4.1 is unrealistic from a biological viewpoint. A more accurate approach is to extend the metabolic model (4.2.5) to include enzyme

dynamics and to consider the enzyme expression rates as control inputs to the network.

In this section we address the question of whether the sequential behaviour that arises in Problem 4.1 also appears in the optimal activation when the control variables are the enzyme expression rates. As described in Section 2.4, we account for enzyme dynamics with a linear expression/degradation model of the form

$$\dot{e} = r - \mathbf{\Lambda}e, \tag{4.5.10}$$

where $r = \begin{bmatrix} r_0 & r_1 & \cdots & r_n \end{bmatrix}^T$ is the vector of time-dependent expression rates, and $\mathbf{\Lambda} = \mathrm{diag}\,\{\lambda_0, \lambda_1, \ldots, \lambda_n\}$. The constants $\lambda_i > 0$ account for enzyme degradation rate and dilution by cell growth. If the expression rates are regarded as control inputs, then the system can be described by the block diagram in Figure 4.6.
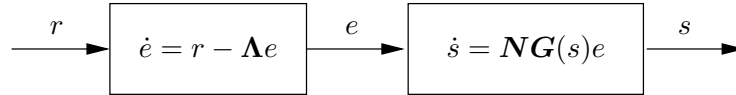
Figure 4.6. Block diagram of metabolic network coupled with enzyme dynamics.

The system in Figure 4.6 is an open-loop version of the feedback scheme for gene regulation shown in Figure 2.5 in Chapter 2. We are interested in an optimal control problem that accounts for metabolic activation (as in Problem 4.1), but where the optimization is carried out directly over the enzyme expression rates. In principle, Problem 4.1 can be recast for the extended system, however, it is not possible to obtain an analytic solution. As an alternative, we consider the numerical solution of a problem that resembles Problem 4.1 and use the example in Section 4.3.3 as a case study.

Consider a reformulation of Problem 4.1 for the metabolic network in (4.2.4) coupled with the enzyme production dynamics in (4.5.10). In this setup the control input to be optimized is the vector of expression rates $r(t) \in \mathbb{R}^m$, whereas the cost function remains unchanged and the constraint on the total enzyme abundance (4.2.9) is replaced by simple box-type constraints of the form $0 \le e_i \le E_{\mathrm{T}}$ and $0 \le r_i \le 1$. In addition, to make the results comparable with those of Problem 4.1, we fix the terminal conditions to match those that solve Problem 4.1.

As an illustration, we revisit the example presented in Section 4.3.3. The un-

branched network is of length $n = 3$ and has Michaelis-Menten kinetics with identical parameters as in Section 4.3.3. The weights in the cost function are chosen as $\alpha_i = 1$ and the degradation rates in (4.5.10) are set to $\lambda_i = 0.5$ for all i. Numerical solutions of this optimal control problem can be obtained with the pseudospectral optimal control solver `Tomlab/PROPT` [86]. The optimal expression rates are shown in Figure 4.7, while the corresponding enzyme and metabolite concentrations are shown in Figure 4.8. To facilitate the comparison with the result of Section 4.3.3, the enzyme profiles of Figure 4.3 are included in dashed lines in Figure 4.8. The optimal expression rates follow a sequential switching pattern that matches the order of the reactions in the network. The enzymes are thus expressed in the same sequence as they act in the network, which leads to an optimal activation that resembles the sequential features of the result in Theorem 4.1. In contrast to Figure 4.3, by including the enzyme production model (4.5.10), the switching behaviour now appears in the optimal expression rates, whereas the enzyme profiles are continuous functions that can indeed be realized by gene expression dynamics. Although these results are purely numerical, their good agreement with the previous theoretical analysis of Problem 4.1 is promising.
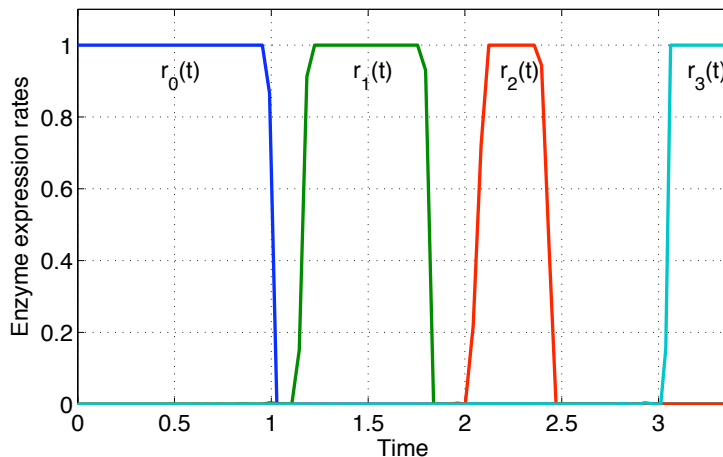
Figure 4.7. Optimal expression rates for network of Section 4.3.3 coupled with enzyme dynamics as in Figure 4.6.

63
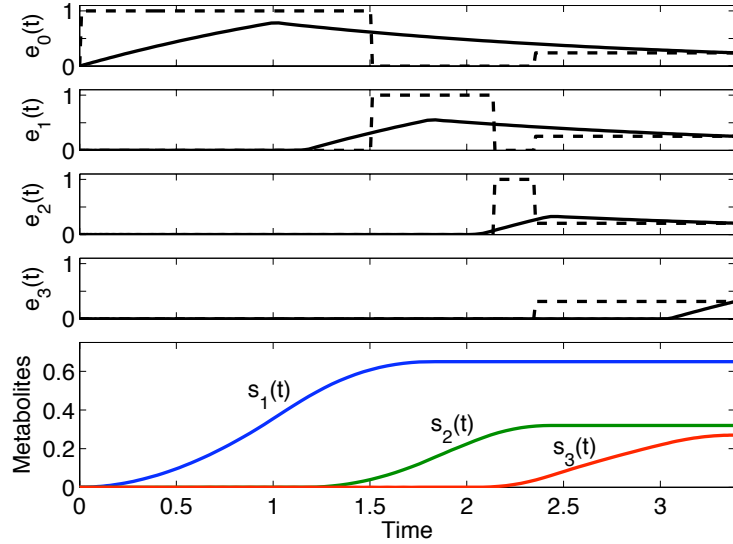
Figure 4.8. Optimal enzyme and metabolite concentrations for network of Section 4.3.3 coupled with enzyme dynamics as in Figure 4.6. The enzyme profiles of Figure 4.3 are shown in dashed line.

4.6 Discussion

The regulation of metabolic activity accommodates resource allocation and product formation in the face of varying external conditions. As discussed in Chapter 2, this regulation is implemented through the genetic control of enzyme expression. We studied such a control policy for the activation of an unbranched metabolic network under the premise that it satisfies an optimality criterion. Under constraints on the total enzyme availability, the objective is to optimize time-dependent enzyme concentrations that drive the pathway from an "off" condition to a target steady state flux. The cost function is a combined measure of the enzyme usage and the duration of the activation process. The duration is measured as the "true" time taken by the network to reach the steady state. This contrasts with other studies in metabolic optimization that consider an averaged quantity known as the *transition time* [28, 82, 83].

As a consequence of the reaction kinetics and network topology, in the optimal solution each enzyme switches between zero and maximum concentration following a temporal sequence that matches the network topology. The analysis is carried out within a control-theoretic framework that allows to prove the optimality of the

activation sequence for a generic class of monomolecular irreversible kinetics. The enzyme kinetics are only required to be monotone in their reactants, and therefore this class includes, for example, the common mass action, Michaelis-Menten and Hill kinetics. The activation sequence is the same as the one reported in [28], and resembles the "just-in-time" activation sequence described in [29]. However, in contrast with those numerical approaches, our main result does not assume specific kinetics or network length, and holds independently of the parameter values. The result thus provides a theoretical justification of the sequential features previously argued in the literature and, in particular, extends the conclusions of [28] to a much broader class of unbranched metabolic networks. This suggests that a sequential pattern in enzyme expression may be a common feature of metabolic regulation that emerges from an underlying optimality principle.

The switching nature of the optimal enzymatic profiles allows us to recast the optimal control problem as a static nonlinear optimization problem which can be solved with standard numerical methods. The decision variables in the equivalent problem are the switching times of each optimal profile, and the optimization is carried out under the positivity constraints in both enzyme and metabolite concentrations. The terminal constraint (4.2.11) defines the set of steady states that are compatible with the enzymatic constraint. In other optimization approaches, such as Flux Balance Analysis [52] and S-system optimization [64], the constraints on steady state concentrations and metabolic fluxes are specified individually. A distinctive feature of a constraint such as (4.2.11) is that in accounting for the limitation in total enzyme abundance, it addresses the steady state of the metabolites and flux simultaneously. As shown by Lemma 4.4, the optimal solution enforces the terminal constraint to be active, which implies that all available enzyme must be allocated to sustain the target flux.

The saturating behaviour of most reaction kinetics imposes an upper bound on the flux that can be achieved by the network. However, because of the constraint on the total enzyme concentration, in steady state it is not possible to allocate all the enzyme to a single reaction. The total enzyme available must then be distributed among the reactions in such a way that the steady state flux is sustained (as expressed by (4.2.10)) and the constraints are not violated. As a consequence, the network flux is limited not only by the saturation rates of the reactions, but also by the enzymatic constraint which imposes a tighter bound to its limiting value (see (4.5.3)). Moreover, the result of Lemma 4.5 implies that the limit flux can only be

reached in an arbitrary large time, since to do so all the reactions need to be driven to saturation.

Despite the ability of our framework to account for more general kinetics than previous efforts [28, 29], we have only been able to complete this analysis with a very simplified description of enzyme dynamics. An improved framework was considered for Michaelis-Menten kinetics in [29] by including genetic feedback in the model. Enzyme levels were set to be dependent on the metabolic product and thus the optimization was carried out over the feedback strengths (more details can be found in Section 3.4.2). In our case the enzyme profiles are considered as independent functions of time and optimized over the class of piecewise continuous functions. This allows switching profiles to be identified as optimal. The result is an activation scheme in which the enzyme concentrations vary more quickly than the metabolite concentrations, when in fact the reverse is a more accurate description of cellular events. This could be addressed by including the rate of change of the enzyme concentrations $\dot{e}(t)$ in the cost function. This is a standard approach in control engineering and has been used for dynamic optimization methods that consider the reaction rates as control inputs [78, 81].

Another way to account for this is by extending the model with enzyme production dynamics. Optimization can then be carried out by finding expression rates that minimize a meaningful metabolic objective. The optimization is not only subject to constraints in enzyme and metabolite levels, but bounds on the expression rates should also be included. As suggested by the example of Section 4.5.3, the optimal activation of the extended model can follow the same temporal pattern as the one obtained from our theoretical analysis. In this extended formulation, the switching behaviour appears in the optimal expression rates required for the activation. Notably, switching expression patterns are consistent with boolean models for genetic networks, which are widely used for the analysis of gene expression dynamics, see e.g. [87]. However, the numerical nature of the solution prevents us from characterizing this behaviour as a general principle. This extended formulation allows the derivation of numerical solutions, but presents major challenges for a general analysis. Similar considerations arise when considering networks with more complicated metabolic interactions such as allosteric feedback regulation (see Section 2.4).

In our efforts to develop a theoretical foundation for the sequential activation of metabolic pathways, the analysis has been limited to unbranched networks. Sequential activation was experimentally shown in [29] for the Arginine pathway in *E.*

coli. It was detected in each branch of the pathway, but no clear relation between the activation of adjacent branches was identified. Extensions of our methodology to branched pathways are not straightforward; in our formulation all the available protein is allocated to a single reaction at a time, which is not realistic when different branches are working simultaneously. It seems that the study of branched pathways should consider different enzymatic constraints and, possibly, a different cost function. Nevertheless, complex topologies are a challenging scenario for other cellular processes in which optimization may play an important role, such as cellular growth [78] and homeostatic regulation [81].

Chapter 5

Optimal expression rates for general networks

5.1 Introduction

In the previous chapter we studied the optimal activation of an unbranched metabolic network from the origin to a prescribed steady state. In that case the structure and kinetics of the network allowed for a rigorous treatment of the optimal control problem. An extension of such analysis to more general scenarios is a challenging problem. This chapter addresses a nonlinear optimal control problem that accounts for a broader class of metabolic networks and more general control objectives.

We consider driving a metabolic network between two arbitrary steady states with time-dependent enzyme expression rates. The network model consists of a metabolic network coupled with dynamics for enzyme synthesis. The problem formulation is general in the sense that no restrictive assumptions on the stoichiometry or enzyme kinetics are imposed. Enzyme synthesis is described as a linear expression/degradation model, where the expression rates are regarded as control inputs to be optimized. The cost function measures the deviation of the species and expression rates from their target steady state values, together with time-derivative of the expression rates. The latter accounts for the genetic "effort" required to drive the network to the new steady state.

In contrast to Chapter 4, the optimization problem does not allow for an analytical solution. Instead we opt for a computational approach and tackle the problem by exploiting the structure of the system dynamics and the quadratic form of the cost function. By introducing a sequence of linear time-variant approximations of the nonlinear system [88], the problem is recast as a sequence of finite horizon Linear Quadratic Tracking (LQT) problems, the solution of which can be obtained with

well-known results [89, 90]. The sequence of LQT problems is solved with an iterative scheme which is shown to converge to a unique suboptimal solution of the original nonlinear problem. Convergence is achieved provided that the time horizon is sufficiently small and the kinetics are globally Lipschitz continuous functions of the metabolite vector. Since the latter condition is satisfied in the positive orthant by many nonlinear kinetics, the convergence result holds for a broad class of metabolic models.

The chapter is organized as follows: the formulation of the optimization problem is presented in Section 5.2 and the solution method in Section 5.3. Convergence of the algorithm is analyzed in Section 5.4, and a numerical example is shown in Section 5.5. A discussion of the results is presented in Section 5.6.

5.2 Problem formulation

We consider a general metabolic network with n metabolites and m reactions described by

$$\dot{s} = \boldsymbol{N}v, \tag{5.2.1}$$

where $\boldsymbol{N} \in \mathbb{Z}^{n \times m}$ is the stoichiometric matrix, $s \in \mathbb{R}^n$ the metabolite vector and $v \in \mathbb{R}^m$ the vector of reaction rates. As in Assumption 2.1 in Chapter 2, each rate is assumed to be linear in the enzyme concentrations. We thus we write $v_i = g_i(s)e_i$, and the network can be described by its kinetic model (see Section 2.3)

$$\dot{s} = \boldsymbol{N}\boldsymbol{G}(s)e, \tag{5.2.2}$$

with the enzyme vector defined as $e \in \mathbb{R}^m$ and $\boldsymbol{G}(s) = \text{diag}\left\{g_1(s), g_2(s), \ldots, g_m(s)\right\}$. As in Section 2.4, the kinetic model is coupled with an expression/degradation model for the enzyme concentrations

$$\dot{e} = r - \boldsymbol{\Lambda}e, \tag{5.2.3}$$

where $r \in \mathbb{R}^m$ is the vector of enzyme expression rates, and $\boldsymbol{\Lambda} = \text{diag}\left\{\lambda_1, \lambda_2, \ldots, \lambda_m\right\}$ with $\lambda_i > 0$ representing the rates of enzymatic degradation and dilution due to cell growth. The time-dependent expression rates are regarded as control inputs that optimally drive the network between two metabolic steady states. The complete model can then be represented by the block diagram of Figure 5.1, which corre-

sponds to an open loop version of the feedback system in Figure 2.5 of Chapter 2. This scheme is the same as the one in Figure 4.6 of the previous chapter, but it is repeated here for consistency.
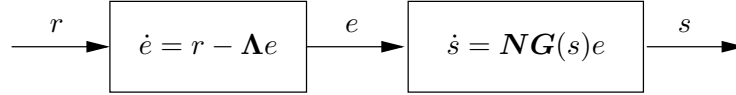
Figure 5.1. Block diagram of a metabolic network coupled with enzyme dynamics.

Initial and target steady states

For $t \leq 0$ the network is assumed to be in an initial steady state given by the triple $(v^i, s^i, e^i) \in \mathbb{R}^m \times \mathbb{R}^n_{>0} \times \mathbb{R}^m_{\geq 0}$. The objective is to drive the network to a prescribed target steady state defined as $(v^f, s^f, e^f) \in \mathbb{R}^m \times \mathbb{R}^n_{>0} \times \mathbb{R}^m_{\geq 0}$. From the enzyme dynamics (5.2.3) it follows that e^i and e^f uniquely specify the steady state expression rates as

$$r^i = \mathbf{\Lambda} e^i, \tag{5.2.4}$$

$$r^f = \mathbf{\Lambda} e^f. \tag{5.2.5}$$

Since (v^i, s^i, e^i) and (v^f, s^f, e^f) define a steady state, they satisfy

$$\mathbf{N} v^i = 0, \qquad\qquad e^i = \mathbf{G}(s^i)^{-1} v^i, \tag{5.2.6}$$

$$\mathbf{N} v^f = 0, \qquad\qquad e^f = \mathbf{G}(s^f)^{-1} v^f. \tag{5.2.7}$$

We aim at finding time-dependent expression rates, $r(t) : [0, t_f] \to \mathbb{R}^m$, that drive the network from (v^i, s^i, e^i) to (v^f, s^f, e^f) while optimizing the cost function described next.

Cost function

In what follows, to shorten the notation, we use the following definition

$$J(z, \mathbf{W}) = \frac{1}{2} \int_0^{t_f} z^T \mathbf{W} z \, \mathrm{d}t, \tag{5.2.8}$$

where $z(t) : [0, t_f] \rightarrow \mathbb{R}^q$ and $\boldsymbol{W} \in \mathbb{R}^{q \times q}$ is a positive semidefinite matrix. The cost function to be minimized is

$$\mathcal{J} = \mathcal{J}_+ + \mathcal{J}_- + \frac{1}{t_f} \mathcal{J}_f, \tag{5.2.9}$$

where

$$\mathcal{J}_+ = J\left(s - s^f, \boldsymbol{W_s}\right) + J\left(e - e^f, \boldsymbol{W_e}\right) + J\left(r - r^f, \boldsymbol{W_r}\right), \tag{5.2.10}$$

$$\mathcal{J}_- = J\left(\dot{r}, \boldsymbol{W_{\dot{r}}}\right), \tag{5.2.11}$$

$$\mathcal{J}_f = J\left(s(t_f) - s^f, \boldsymbol{W_{sf}}\right) + J\left(e(t_f) - e^f, \boldsymbol{W_{ef}}\right) + J\left(r(t_f) - r^f, \boldsymbol{W_{rf}}\right). \tag{5.2.12}$$

The cost $\mathcal{J}_+$ quantifies the deviation of the chemical species and expression rates from their target values, whereas $\mathcal{J}_-$ weighs the time-derivative of the expression rates. Minimization of the total cost $\mathcal{J}$ therefore accounts for the combined optimization of the transition to the target steady state together with the genetic effort allocated to enzyme synthesis. The inclusion of $\mathcal{J}_-$ in the cost function also prevents $\dot{r}$ from taking arbitrary large values, which would lead to discontinuities in the expression rates.

The matrices in the functionals (5.2.10)–(5.2.12) have appropriate dimensions and are assumed to be positive semidefinite, with the exception of $\boldsymbol{W_{\dot{r}}}$ which is assumed to be positive definite. The positive semidefiniteness of the weighting matrices ensures that the integrands in $\mathcal{J}_+$, $\mathcal{J}_-$ and $\mathcal{J}_f$ are nonnegative. The scaling factor $1/t_f$ is included to normalize $\mathcal{J}_f$.

We remark that in this formulation the terminal variables $s(t_f)$, $e(t_f)$ and $r(t_f)$ are not specified *a priori* and their particular values are an outcome of the optimization. This contrasts with the formulation in Chapter 4, where $s(t_f)$ was forced to lie in a given surface. Thus, a possible drawback is that $s(t_f)$, $e(t_f)$ and $r(t_f)$ are distant from s^f, e^f and r^f. This is accounted for by the terminal cost $\mathcal{J}_f$, which prevents them from being too far from their corresponding target values.

As in most optimization problems, the solution is highly dependent on the choice of the weights in $\mathcal{J}$. Intuitively, the solution depends on the norms of the weighting matrices relative to each other. The cost function $\mathcal{J}$ quantifies the cost/benefit relationship between enzyme expression and the transition to the target steady state. A larger weight $\boldsymbol{W_{\dot{r}}}$ implies a stronger penalization on the slope of the expression

rates, and therefore yields a slower transition to the target. Conversely, if the relative norm of the weights $\boldsymbol{W_s}, \boldsymbol{W_e}, \boldsymbol{W_r}$ with respect to $\boldsymbol{W_{\dot{r}}}$ is large, the solution tends to give faster responses. Likewise, choosing large terminal weights $\boldsymbol{W_{sf}}, \boldsymbol{W_{ef}}, \boldsymbol{W_{rf}}$ has a similar role and helps narrowing the gap between the terminal state and the target.

In summary, the optimal control problem reads as follows.

Problem 5.1: *Let (v^i, s^i, e^i) and (v^f, s^f, e^f) be two steady states for the network (5.2.2)–(5.2.3) associated to the steady state expression rates r^i and r^f, respectively. Assume the network is in (v^i, s^i, e^i) for $t \leq 0$. Given weighting matrices $\boldsymbol{W_s}, \boldsymbol{W_{sf}}, \boldsymbol{W_e}, \boldsymbol{W_{ef}}, \boldsymbol{W_r}, \boldsymbol{W_{rf}} \geq 0$ and $\boldsymbol{W_{\dot{r}}} > 0$, find a piecewise continuous control $r(t) : [0, t_f] \to \mathbb{R}^m$ that minimizes*

$$\mathcal{J} = \mathcal{J}_+ + \mathcal{J}_- + \frac{1}{t_f} \mathcal{J}_f. \tag{5.2.13}$$

The solution of Problem 5.1 is a difficult task. Using standard optimal control methods such as Pontryagin's Minimum Principle or the Hamilton-Jacobi-Bellman equation [91] may be successful in special cases (i.e. for specific stoichiometries and kinetics), but the general problem is usually intractable. Our approach to tackle Problem 5.1 follows by exploiting the quadratic form of the cost function (5.2.13) and the structure of the network dynamics.

5.3 Iterative solution procedure

5.3.1 Definitions

Since the cost $\mathcal{J}_-$ weighs the rate of change of the expression rates, we extend the state space with r and consider $\dot{r}$ as the control input. The extended state variable $x \in \mathbb{R}^{n+2m}$ is defined as

$$x = \begin{bmatrix} s \\ e \\ r \end{bmatrix}. \tag{5.3.1}$$

Adopting the standard control-theoretic notation, the control input $u = u(t) \in \mathbb{R}^m$ is given by

$$u = \dot{r}. \tag{5.3.2}$$

We also define the initial and target conditions as

$$x^i = \begin{bmatrix} s^i \\ e^i \\ r^i \end{bmatrix}, \quad x^f = \begin{bmatrix} s^f \\ e^f \\ r^f \end{bmatrix}. \tag{5.3.3}$$

With these definitions, the functionals (5.2.10)–(5.2.12) become

$$\mathcal{J}_+ = J\left(x - x^f, \boldsymbol{Q}\right), \tag{5.3.4}$$

$$\mathcal{J}_- = J\left(u, \boldsymbol{R}\right), \tag{5.3.5}$$

$$\mathcal{J}_f = J\left(x(t_f) - x^f, \boldsymbol{Q_f}\right), \tag{5.3.6}$$

where the weighting matrices $\boldsymbol{Q}, \boldsymbol{Q_f} \geq 0$ and $\boldsymbol{R} > 0$ are

$$\boldsymbol{Q} = \begin{bmatrix} \boldsymbol{W_s} & 0 & 0 \\ 0 & \boldsymbol{W_e} & 0 \\ 0 & 0 & \boldsymbol{W_r} \end{bmatrix}, \quad \boldsymbol{Q_f} = \begin{bmatrix} \boldsymbol{W_{sf}} & 0 & 0 \\ 0 & \boldsymbol{W_{ef}} & 0 \\ 0 & 0 & \boldsymbol{W_{rf}} \end{bmatrix}, \quad \boldsymbol{R} = \boldsymbol{W_{\dot{r}}}. \tag{5.3.7}$$

The dynamics in (5.2.2)–(5.2.3) together with (5.3.2) can be written as

$$\dot{x} = \boldsymbol{A}(x)x + \boldsymbol{B}u, \quad x(0) = x^i, \tag{5.3.8}$$

where $\boldsymbol{A}(x) \in \mathbb{R}^{(n+2m)\times(n+2m)}$ and $\boldsymbol{B} \in \mathbb{R}^{(n+2m)\times m}$ are given by

$$\boldsymbol{A}(x) = \begin{bmatrix} 0 & \boldsymbol{NG}(x) & 0 \\ 0 & -\boldsymbol{\Lambda} & \boldsymbol{I} \\ 0 & 0 & 0 \end{bmatrix}, \quad \boldsymbol{B} = \begin{bmatrix} 0 \\ 0 \\ \boldsymbol{I} \end{bmatrix}, \tag{5.3.9}$$

with $\boldsymbol{G}(x) = \boldsymbol{G}(s)$. The vector x^f can be seen as a signal that has to be tracked by the state variable. The minimization of $\mathcal{J}$ in (5.2.13) for the extended system (5.3.8) corresponds to a nonlinear version of the Linear Quadratic Tracking (LQT) problem presented in Appendix A.2.1. This observation is the basis for the iterative

procedure to be developed in the next section.

5.3.2 Derivation of the algorithm

The idea is to recast the original nonlinear problem as a sequence of standard LQT problems. Assume that $x^{(1)}(t) \in \mathbb{R}^{n+2m}$ and $u^{(1)}(t) \in \mathbb{R}^m$ are given, and define the sequences $\{x^{(k)}\}$ and $\{u^{(k)}\}$ for $k \in \mathbb{N}$, with $x^{(k)} = x^{(k)}(t) \in \mathbb{R}^{n+2m}$ and $u^{(k)} = u^{(k)}(t) \in \mathbb{R}^m$. Consider an approximation of the extended nonlinear system (5.3.8) by the following sequence of linear time-variant systems

$$\dot{x}^{(k)} = \boldsymbol{A}\left(x^{(k-1)}\right)x^{(k)} + \boldsymbol{B}u^{(k)}, \quad x^{(k)}(0) = x^i, \qquad (5.3.10)$$

where each control $u^{(k)}$ minimizes the cost $\mathcal{J}^{(k)} = \mathcal{J}_+^{(k)} + \mathcal{J}_-^{(k)} + (1/t_f)\mathcal{J}_f^{(k)}$, and

$$\mathcal{J}_+^{(k)} = J\left(x^{(k)} - x^f, \boldsymbol{Q}\right), \qquad (5.3.11)$$

$$\mathcal{J}_-^{(k)} = J\left(u^{(k)}, \boldsymbol{R}\right), \qquad (5.3.12)$$

$$\mathcal{J}_f^{(k)} = J\left(x^{(k)}(t_f) - x^f, \boldsymbol{Q_f}\right). \qquad (5.3.13)$$

It is important to note that the state matrix in (5.3.10) is time-dependent, that is, $\boldsymbol{A}\left(x^{(k-1)}\right)$ is a matrix-valued function of time. To avoid confusion in the sequel we write $\boldsymbol{A^{(k)}}(t) = \boldsymbol{A}\left(x^{(k)}\right)$ and (5.3.10) becomes

$$\dot{x}^{(k)}(t) = \boldsymbol{A^{(k-1)}}(t)x^{(k)}(t) + \boldsymbol{B}u^{(k)}(t), \quad x^{(k)}(0) = x^i. \qquad (5.3.14)$$

The approximation of a nonlinear system by a sequence of linear time-variant dynamics such as (5.3.14) has been previously studied in the context of Linear Quadratic optimal control problems [88, 33]. Here we follow a similar approach and use these approximations to build a sequence of LQT problems that can be readily solved for each $k \geq 2$ (the trajectories for $k = 1$ will be discussed later in this section). If $z(t) = x^f$ is regarded as a signal to be tracked by the state variable, then the problem of minimizing $\mathcal{J}^{(k)}$ for the approximate dynamics in (5.3.14) is identical to the finite horizon LQT problem described in Appendix A.2.1. The results in Appendix A.2.1 require the following assumption on the matrix $\boldsymbol{A^{(k)}}(t)$.

Assumption 5.1: *The entries of $\boldsymbol{A^{(k)}}(t)$ are continuous functions of $t \in [0, t_f]$.*

For a broad class of metabolic networks, a sufficient condition for Assumption

5.1 to hold is that $x^{(k-1)}(t)$ lies in the positive orthant for all $t \in [0, t_f]$; this is further discussed in Section 5.6. From the results in Appendix A.2.1, for each $k \geq 2$ the optimal control is given by

$$u^{(k)}(t) = -\boldsymbol{R}^{-1}\boldsymbol{B}^T \left(\boldsymbol{P}^{(k)}(t)x^{(k)}(t) - q^{(k)}(t) \right), \qquad (5.3.15)$$

where $q^{(k)}(t) \in \mathbb{R}^{n+2m}$ is an element of the sequence $\{q^{(k)}\}$ for $k \in \mathbb{N}$, and is the solution of the differential equation

$$\dot{q}^{(k)}(t) = - \left(\boldsymbol{A}^{(k-1)}(t) - \boldsymbol{B}\boldsymbol{R}^{-1}\boldsymbol{B}^T\boldsymbol{P}^{(k)}(t) \right)^T q^{(k)}(t) - \boldsymbol{Q}x^f, \qquad (5.3.16)$$

with terminal condition $q(t_f) = \boldsymbol{Q_f}x^f$. The matrix $\boldsymbol{P}^{(k)}(t) \in \mathbb{R}^{(n+2m)\times(n+2m)}$ belongs to the sequence $\{\boldsymbol{P}^{(k)}\}$ and is the solution of the differential Riccati equation

$$-\dot{\boldsymbol{P}}^{(k)}(t) = \boldsymbol{A}^{(k-1)^T}(t)\boldsymbol{P}^{(k)}(t) + \boldsymbol{P}^{(k)}(t)\boldsymbol{A}^{(k-1)}(t)$$
$$- \boldsymbol{P}^{(k)}(t)\boldsymbol{B}\boldsymbol{R}^{-1}\boldsymbol{B}^T\boldsymbol{P}^{(k)}(t) + \boldsymbol{Q}, \qquad (5.3.17)$$

with $\boldsymbol{P}^{(k)}(t_f) = \boldsymbol{Q_f}$. Equation (5.3.17) can be expanded as

$$-\dot{\boldsymbol{P}}^{(k)}(t) = \left(\boldsymbol{A}^{(k-1)}(t) - \boldsymbol{B}(t)\boldsymbol{R}^{-1}\boldsymbol{B}^T\boldsymbol{P}^{(k)}(t) \right)^T \boldsymbol{P}^{(k)}(t)+$$
$$\boldsymbol{P}^{(k)}(t) \left(\boldsymbol{A}^{(k-1)}(t) - \boldsymbol{B}\boldsymbol{R}^{-1}\boldsymbol{B}^T\boldsymbol{P}^{(k)}(t) \right) +$$
$$\left(\boldsymbol{Q} + \boldsymbol{P}^{(k)}(t)\boldsymbol{B}\boldsymbol{R}^{-1}\boldsymbol{B}^T\boldsymbol{P}^{(k)}(t) \right). \qquad (5.3.18)$$

By defining the matrices

$$\tilde{\boldsymbol{A}}^{(k-1)}(t) = \boldsymbol{A}^{(k-1)}(t) - \boldsymbol{B}\boldsymbol{R}^{-1}\boldsymbol{B}^T\boldsymbol{P}^{(k-1)}(t),$$
$$\tilde{\boldsymbol{Q}}^{(k-1)}(t) = \boldsymbol{Q} + \boldsymbol{P}^{(k-1)}(t)\boldsymbol{B}\boldsymbol{R}^{-1}\boldsymbol{B}^T\boldsymbol{P}^{(k-1)}(t),$$

the solution of (5.3.18) is approximated by that of the differential Lyapunov equation

$$-\dot{\boldsymbol{P}}^{(k)}(t) = \tilde{\boldsymbol{A}}^{(k-1)^T}(t)\boldsymbol{P}^{(k)}(t) + \boldsymbol{P}^{(k)}(t)\tilde{\boldsymbol{A}}^{(k-1)}(t) + \tilde{\boldsymbol{Q}}^{(k-1)}(t), \qquad (5.3.19)$$

with $\boldsymbol{P}^{(k)}(t_f) = \boldsymbol{Q_f}$. The control in (5.3.15) is then approximated by

$$u^{(k)}(t) \approx -\boldsymbol{R}^{-1}\boldsymbol{B}^T \left(\boldsymbol{P}^{(k-1)}(t)x^{(k)}(t) - q^k(t) \right), \qquad (5.3.20)$$

and $q^{(k)}(t)$ in (5.3.16) is approximated as the solution of

$$\dot{q}^{(k)}(t) = -\tilde{A}^{(k-1)^T}(t)q^{(k)}(t) - Qx^f, \qquad (5.3.21)$$

with terminal condition $q^{(k)}(t_f) = Q_f x^f$. Using the approximate system in (5.3.14) and the control (5.3.20), the optimal state trajectory for the kth iteration can be computed from

$$\dot{x}^{(k)}(t) = \tilde{A}^{(k-1)}(t)x^{(k)}(t) + BR^{-1}B^T q^{(k)}(t), \quad x^{(k)}(0) = x^i. \qquad (5.3.22)$$

This procedure allows the computation of a control $u^{(k)}$ that minimizes $\mathcal{J}^{(k)}$ for system (5.3.14) for each value of k. The computation is iterative, with (5.3.19)–(5.3.22) providing a means of computing $u^{(k)}$, $q^{(k)}$, $x^{(k)}$ and $P^{(k)}(t)$ from the previous solutions $x^{(k-1)}(t)$ and $P^{(k-1)}(t)$. The algorithm is summarized next.

Algorithm 5.1: *Consider the statement of Problem 5.1 and the definitions in Section 5.3.1. Assume the initial trajectories $x^{(1)}(t)$ and $P^{(1)}(t)$ are given. Then, for each iteration $k \in \mathbb{N}, k \geq 2$:*

(i) Compute the matrices

$$A^{(k-1)}(t) = A\left(x^{(k-1)}\right), \qquad (5.3.23)$$

$$\tilde{A}^{(k-1)}(t) = A^{(k-1)}(t) - BR^{-1}B^T P^{(k-1)}(t), \qquad (5.3.24)$$

$$\tilde{Q}^{(k-1)}(t) = Q + P^{(k-1)}(t)BR^{-1}B^T P^{(k-1)}(t). \qquad (5.3.25)$$

(ii) Solve the differential equations

$$\dot{q}^{(k)}(t) = -\tilde{A}^{(k-1)^T}(t)q^{(k)}(t) - Qx^f, \qquad (5.3.26)$$

$$-\dot{P}^{(k)}(t) = \tilde{A}^{(k-1)^T}(t)P^{(k)}(t) + P^{(k)}(t)\tilde{A}^{(k-1)}(t) + \tilde{Q}^{(k-1)}(t), \quad (5.3.27)$$

with terminal conditions $q^{(k)}(t_f) = Q_f x^f$ and $P^{(k)}(t_f) = Q_f$.

(iii) Compute the state trajectory and control from

$$\dot{x}^{(k)}(t) = \tilde{A}^{(k-1)}(t)x^{(k)}(t) + BR^{-1}B^T q^{(k)}, \quad x^{(k)}(0) = x^i, \qquad (5.3.28)$$

$$u^{(k)}(t) = -R^{-1}B^T\left(P^{(k-1)}(t)x^{(k)}(t) - q^k(t)\right). \qquad (5.3.29)$$

To compute the initial trajectories $x^{(1)}$ and $\boldsymbol{P^{(1)}}$, we follow the same idea as in the derivation of Algorithm 5.1. By setting $x^{(0)}(t) = x^i$, the approximate system in (5.3.10) for $k = 1$ becomes the linear time invariant system

$$\dot{x}^{(1)} = \boldsymbol{A}\left(x^i\right) x^{(1)} + \boldsymbol{B} u^{(1)}. \tag{5.3.30}$$

Using the results in Appendix A.2.1 the optimal control for $k = 1$ is

$$u^{(1)}(t) = -\boldsymbol{R}^{-1} \boldsymbol{B}^T \left(\boldsymbol{P^{(1)}}(t) x^{(1)}(t) - q^{(1)}(t) \right), \tag{5.3.31}$$

where

$$\dot{q}^{(1)}(t) = -\left(\boldsymbol{A}\left(x^i\right) - \boldsymbol{B} \boldsymbol{R}^{-1} \boldsymbol{B}^T \boldsymbol{P^{(1)}}(t) \right)^T q^{(1)}(t) - \boldsymbol{Q} x^f, \tag{5.3.32}$$

$$-\dot{\boldsymbol{P}}^{(1)}(t) = \boldsymbol{A}^T \left(x^i\right) \boldsymbol{P^{(1)}}(t) + \boldsymbol{P^{(1)}}(t) \boldsymbol{A}\left(x^i\right) - \boldsymbol{P^{(1)}}(t) \boldsymbol{B} \boldsymbol{R}^{-1} \boldsymbol{B}^T \boldsymbol{P^{(1)}}(t) + \boldsymbol{Q}, \tag{5.3.33}$$

with terminal conditions $q^{(1)}(t_f) = \boldsymbol{Q_f} x^f$ and $\boldsymbol{P^{(1)}}(t_f) = \boldsymbol{Q_f}$. The state trajectory $x^{(1)}$ is computed as the solution of

$$\dot{x}^{(1)}(t) = \left(\boldsymbol{A}\left(x^i\right) - \boldsymbol{B} \boldsymbol{R}^{-1} \boldsymbol{B}^T \boldsymbol{P^{(1)}}(t) \right) x^{(1)}(t) + \boldsymbol{B} \boldsymbol{R}^{-1} \boldsymbol{B}^T q^{(1)}(t), \quad x^{(1)}(0) = x^i. \tag{5.3.34}$$

The implementation of Algorithm 5.1 requires solving the three differential equations (5.3.26)–(5.3.28) in each iteration. The equation for $x^{(k)}$ is a standard initial value problem, whereas $q^{(k)}$ and $\boldsymbol{P}^{(k)}$ must be computed by solving (5.3.26)–(5.3.27) backward in time. If the sequences $\{u^{(k)}\}$, $\{x^{(k)}\}$, $\{q^{(k)}\}$ and $\{\boldsymbol{P}^{(k)}\}$ converge to a fixed-point, denoted as $(u^*, x^*, q^*, \boldsymbol{P^*})$, then the species concentrations and enzyme expression rates can be recovered from x^* (recall the definition of the extended state in (5.3.1)). In practice, it is enough to iterate Algorithm 5.1 until $x^{(k)}$ and $x^{(k-1)}$ differ less than a prescribed accuracy. An appropriate stop criterion is

$$\left\lVert x^{(k)} - x^{(k-1)} \right\rVert \leq \varepsilon, \tag{5.3.35}$$

where $\varepsilon > 0$ is a pre-specified tolerance and $\lVert \cdot \rVert$ is the function norm defined in

(B.1.1). In the limit for $k \to \infty$ it holds

$$\lim_{k \to \infty} \left\| \tilde{\boldsymbol{A}}^{\boldsymbol{k}} - \tilde{\boldsymbol{A}}^* \right\| = \lim_{k \to \infty} \left\| \tilde{\boldsymbol{Q}}^{\boldsymbol{k}} - \tilde{\boldsymbol{Q}}^* \right\| = \lim_{k \to \infty} \left\| \boldsymbol{P}^{(k)} - \boldsymbol{P}^* \right\| = \boldsymbol{0}. \qquad (5.3.36)$$

with

$$\tilde{\boldsymbol{A}}^* = \boldsymbol{A}\left(x^*\right) - \boldsymbol{B}\boldsymbol{R}^{-1}\boldsymbol{B}^T\boldsymbol{P}^*, \qquad (5.3.37)$$

$$\tilde{\boldsymbol{Q}}^* = \boldsymbol{Q} - \boldsymbol{P}^*\boldsymbol{B}\boldsymbol{R}^{-1}\boldsymbol{B}^T\boldsymbol{P}^*. \qquad (5.3.38)$$

Using these equations in (5.3.26)–(5.3.29), at the fixed-point the control and state trajectory satisfy

$$u^* = -\boldsymbol{R}^{-1}\boldsymbol{B}^T\left(\boldsymbol{P}^*x^* - q^*\right), \qquad (5.3.39)$$

$$\dot{x}^* = \left(\boldsymbol{A}\left(x^*\right) - \boldsymbol{B}\boldsymbol{R}^{-1}\boldsymbol{B}^T\boldsymbol{P}^*\right)x^* + \boldsymbol{B}\boldsymbol{R}^{-1}\boldsymbol{B}^Tq^*, \quad x^*(0) = x^i, \qquad (5.3.40)$$

where q^* and $\boldsymbol{P}^*$ satisfy

$$\dot{q}^* = -\left(\boldsymbol{A}\left(x^*\right) - \boldsymbol{B}\boldsymbol{R}^{-1}\boldsymbol{B}^T\boldsymbol{P}^*\right)^T q^* - \boldsymbol{Q}x^f, \qquad (5.3.41)$$

$$-\dot{\boldsymbol{P}}^* = \boldsymbol{A}^T\left(x^*\right)\boldsymbol{P}^* + \boldsymbol{P}^*\boldsymbol{A}\left(x^*\right) - \boldsymbol{P}^*\boldsymbol{B}\boldsymbol{R}^{-1}\boldsymbol{B}^T\boldsymbol{P}^* + \boldsymbol{Q}, \qquad (5.3.42)$$

with the terminal conditions $q^*(t_f) = \boldsymbol{Q_f}x^f$ and $\boldsymbol{P}^* = \boldsymbol{Q_f}$. The coupled differential equations (5.3.40)–(5.3.42) can be regarded as a "state-dependent" version of the LQT solution for linear systems presented in Appendix A.2.1. In general, the solution of equations (5.3.39)–(5.3.42) does not satisfy the necessary conditions for optimality provided by Pontryagin's Minimum Principle, and hence Algorithm 5.1 gives a suboptimal solution to the nonlinear optimal control problem.

5.4 Convergence analysis

An iterative procedure such as Algorithm 5.1 is of little use if it is not convergent. As we show next, under some assumptions the algorithm can be shown to converge to a unique fixed-point. To improve readability, the convergence proof is presented separately in Section 5.4.2.

5.4.1 Assumptions and convergence result

We make the following assumption on the enzyme kinetics.

Assumption 5.2: *The turnover rate functions $g_i(s)$ in (5.2.2) are globally Lipschitz continuous, that is, for each $i = 1, 2, \ldots, m$, there exists $\mathcal{K}_i > 0$ such that*

$$|g_i(s_a) - g_i(s_b)| \leq \mathcal{K}_i \, ||s_a - s_b||_E \,, \tag{5.4.1}$$

for all $s_a, s_b \in \mathbb{R}^n$ and with $||\cdot||_E$ denoting the Euclidean norm. The smallest such $\mathcal{K}_i$, denoted as $\mathcal{L}_i$, is the Lipschitz constant of $g_i(s)$.

Since many reaction kinetics have bounded first derivatives for $s \in \mathbb{R}^n_{\geq 0}$, Assumption 5.2 is not restrictive and is met by a broad range of kinetics. This is the case, in particular, of the common Mass Action, Michaelis-Menten, Hill and allosteric kinetics (and, in fact, many sigmoid-shaped kinetics).

Remark 5.1: *It should be pointed out that in most cases enzyme kinetics have bounded derivatives only in the positive orthant $\mathbb{R}^n_{\geq 0}$, and thus strictly speaking, Assumption 5.2 fails to hold. However, the need for Lipschitz continuity in whole $\mathbb{R}^n$ is a consequence of Algorithm 5.1 not accounting for positivity constraints in the state space. Additional discussions on this issue are presented later in Section 5.6.*

The convergence of Algorithm 5.1 is characterized by the next theorem.

Theorem 5.1: *Consider model (5.2.2)–(5.2.3) and the statement of Problem 5.1. If (5.2.2) satisfies Assumption 5.2, there exists a sufficiently small $t_f > 0$ such that Algorithm 5.1 converges to a unique fixed-point.*

Convergence of Algorithm 5.1 is thus guaranteed for a sufficiently small final time t_f. Unfortunately, we cannot provide an estimate of how small t_f must be, and whether a given t_f ensures convergence will depend on the network dynamics, the weighting matrices, and the initial and target conditions. The convergence result is based on a contraction mapping argument (see Section 5.4.2), and hence in the limit the sequence of linear time-variant systems (5.3.14) is a *global* approximation of the nonlinear dynamics. This contrasts with local approximations based on linearization of the dynamics, and implies that the state trajectory x^* in the fixed-point of Algorithm 5.1 is *identical* to that generated by the original nonlinear system (5.3.8) with r^* as control input. This also implies that the convergence result is independent of the initial trajectories $x^{(1)}$ and $\boldsymbol{P^{(1)}}$. Therefore, although in (5.3.33)–(5.3.34) we have specified a way of computing these, faster convergence may be achieved by using other starting trajectories (i.e. those that are closer to the fixed-point). We

also point out that Theorem 5.1 provides a sufficient condition for convergence, and thus it does not preclude convergence under less restrictive conditions.

5.4.2 Proof of Theorem 5.1.

We need to establish conditions under which the sequences $\{u^{(k)}\}$, $\{x^{(k)}\}$, $\{q^{(k)}\}$ and $\{\boldsymbol{P^{(k)}}\}$ in Algorithm 5.1 are convergent. For that purpose we use the fixed-point theorem presented in Appendix B (see also Remark B.1). In the following we use the definitions and notation of Appendix B; let $\mathcal{C}\left([0, t_f], \mathbb{K}\right)$ be the set of continuous functions $f(t): [0, t_f] \to \mathbb{K}$, and define two Banach spaces $\mathbb{B}_1 = \mathcal{C}\left([0, t_f], \mathbb{R}^{n+2m}\right)$, $\mathbb{B}_2 = \mathcal{C}\left([0, t_f], \mathbb{R}^{(n+2m)\times(n+2m)}\right)$ equipped with the function norms defined in (B.1.1) and (B.1.2).

We first note from (5.3.26) and (5.3.29) that convergence of $\{x^{(k)}\}$ and $\{\boldsymbol{P^{(k)}}\}$ is sufficient for $\{q^{(k)}\}$ and $\{u^{(k)}\}$ to be convergent. Therefore, we only prove the convergence of $\{x^{(k)}\}$ and $\{\boldsymbol{P^{(k)}}\}$ and, to that end, we write the iterations in operator form as

$$x^{(k)} = T_1\left(x^{(k-1)}, \boldsymbol{P^{(k-1)}}\right), \tag{5.4.2}$$

$$\boldsymbol{P^{(k)}} = T_2\left(x^{(k-1)}, \boldsymbol{P^{(k-1)}}\right), \tag{5.4.3}$$

where the operators T_1 and T_2 are defined by the solution of the differential equations in (5.3.28) and (5.3.27), respectively, and $x^{(k)} \in \mathbb{B}_1$, $\boldsymbol{P^{(k)}} \in \mathbb{B}_2$ for all $k \in \mathbb{N}$. Using Theorem B.1, the proof follows by finding a matrix $\boldsymbol{M} \in \mathbb{R}^{2\times 2}$ with eigenvalues strictly inside the unit circle such that the inequality

$$\begin{bmatrix} \left|\left|x^{(k+1)} - x^{(k)}\right|\right| \\ \left|\left|\boldsymbol{P^{(k+1)}} - \boldsymbol{P^{(k)}}\right|\right| \end{bmatrix} \leq \boldsymbol{M} \begin{bmatrix} \left|\left|x^{(k)} - x^{(k-1)}\right|\right| \\ \left|\left|\boldsymbol{P^{(k)}} - \boldsymbol{P^{(k-1)}}\right|\right| \end{bmatrix}, \tag{5.4.4}$$

holds component-wise. For the sake of clarity, in the sequel we omit the argument t when it is clear from the context and split the proof in two parts. Firstly, we obtain analytic expressions for the differences $x^{(k+1)} - x^{(k)}$ and $\boldsymbol{P^{(k+1)}} - \boldsymbol{P^{(k)}}$. Secondly, we derive bounds for their norms in terms of $\left|\left|x^{(k)} - x^{(k-1)}\right|\right|$ and $\left|\left|\boldsymbol{P^{(k)}} - \boldsymbol{P^{(k-1)}}\right|\right|$, so as to find an explicit expression for $\boldsymbol{M}$. The argument concludes by showing that with a suitable choice of t_f the eigenvalues of $\boldsymbol{M}$ can be made arbitrarily small.

Part 1:

From the statement of Algorithm 5.1, we have that $x^{(k+1)}$ and $q^{(k+1)}$ are solutions of the inhomogeneous linear time-variant systems

$$\dot{x}^{(k+1)} = \tilde{\boldsymbol{A}}^{\boldsymbol{k}}(t)x^{(k+1)} + \boldsymbol{B}\boldsymbol{R}^{-1}\boldsymbol{B}^T q^{(k+1)}, \quad x^{(k+1)}(0) = x^i, \tag{5.4.5}$$

$$\dot{q}^{(k+1)} = -\tilde{\boldsymbol{A}}^{(\boldsymbol{k})T}q^{(k+1)} - \boldsymbol{Q}x^f, \quad q^{(k+1)}(t_f) = \boldsymbol{Q_f}x^f. \tag{5.4.6}$$

By the variation of constants formula [92], $x^{(k+1)}$ is given by

$$x^{(k+1)}(t) = \boldsymbol{\Phi}^{(\boldsymbol{k+1})}(t,0)x^i + \int_0^t \boldsymbol{\Phi}^{(\boldsymbol{k+1})}(t,\tau)\boldsymbol{B}\boldsymbol{R}^{-1}\boldsymbol{B}^T q^{(k+1)}(\tau)\,\mathrm{d}\tau, \tag{5.4.7}$$

where $\boldsymbol{\Phi}^{(\boldsymbol{k+1})}(t,t_0) \in \mathbb{B}_2$ is the state transition matrix of (5.4.5). A basic property of the transition matrix is

$$\frac{\mathrm{d}}{\mathrm{d}t}\boldsymbol{\Phi}^{(\boldsymbol{k+1})}(t,t_0) = \tilde{\boldsymbol{A}}^{(\boldsymbol{k})}(t)\boldsymbol{\Phi}^{(\boldsymbol{k+1})}(t,t_0). \tag{5.4.8}$$

From this property it can be shown that

$$\frac{\mathrm{d}}{\mathrm{d}t}\boldsymbol{\Phi}^{(\boldsymbol{k+1})^{-1}}(t,t_0) = -\boldsymbol{\Phi}^{(\boldsymbol{k+1})^{-1}}(t,t_0)\tilde{\boldsymbol{A}}^{(\boldsymbol{k})}(t), \tag{5.4.9}$$

$$\frac{\mathrm{d}}{\mathrm{d}t}\boldsymbol{\Phi}^{(\boldsymbol{k+1})^T}(t,t_0) = \boldsymbol{\Phi}^{(\boldsymbol{k+1})^T}(t,t_0)\tilde{\boldsymbol{A}}^{(\boldsymbol{k})^T}(t). \tag{5.4.10}$$

Equation (5.4.9) is obtained by differentiating the identity

$$\boldsymbol{\Phi}^{(\boldsymbol{k+1})}(t,t_0)\boldsymbol{\Phi}^{(\boldsymbol{k+1})^{-1}}(t,t_0) = \boldsymbol{I}, \tag{5.4.11}$$

and then using (5.4.8), whereas (5.4.10) comes simply from transposing (5.4.8). Using the differential equations for $q^{(k)}$ and $x^{(k)}$ in (5.3.26) and (5.3.28) we get

$$\dot{q}^{(k+1)} - \dot{q}^{(k)} = -\tilde{\boldsymbol{A}}^{(\boldsymbol{k})T}\left(q^{(k+1)} - q^{(k)}\right) - \boldsymbol{F_1}^{(\boldsymbol{k})T}q^{(k)}, \tag{5.4.12}$$

$$\dot{x}^{(k+1)} - \dot{x}^{(k)} = \tilde{\boldsymbol{A}}^{(\boldsymbol{k})}\left(x^{(k+1)} - x^{(k)}\right) + \boldsymbol{F_1}^{(\boldsymbol{k})}x^{(k)} + \boldsymbol{B}\boldsymbol{R}^{-1}\boldsymbol{B}^T\left(q^{(k+1)} - q^{(k)}\right), \tag{5.4.13}$$

where $\boldsymbol{F_1^{(k)}} = \boldsymbol{F_1^{(k)}}(t)$ is given by

$$\boldsymbol{F_1^{(k)}} = \tilde{\boldsymbol{A}}^{(k)} - \tilde{\boldsymbol{A}}^{(k-1)}. \tag{5.4.14}$$

We can combine (5.4.9)–(5.4.13) to obtain

$$\frac{\mathrm{d}}{\mathrm{d}t}\left(\boldsymbol{\Phi}^{(k+1)^T}(t,t_0)\left(q^{(k+1)}(t) - q^{(k)}(t)\right)\right) = -\boldsymbol{\Phi}^{(k+1)^T}(t,t_0)\boldsymbol{F_1^{(k)}}(t)q^{(k)}(t), \tag{5.4.15}$$

$$\frac{\mathrm{d}}{\mathrm{d}t}\left(\boldsymbol{\Phi}^{(k+1)^{-1}}(t,t_0)\left(x^{(k+1)}(t) - x^{(k)}(t)\right)\right) = \boldsymbol{\Phi}^{(k+1)^{-1}}(t,t_0)\times$$
$$\left(\boldsymbol{F_1^{(k)}}(t)x^{(k)}(t) + \boldsymbol{B}\boldsymbol{R}^{-1}\boldsymbol{B}^T\left(q^{(k+1)}(t) - q^{(k)}(t)\right)\right). \tag{5.4.16}$$

The right hand sides of (5.4.15) and (5.4.16) do not depend on $q^{(k+1)} - q^{(k)}$ and $x^{(k+1)} - x^{(k)}$, respectively. Hence, these equations can be integrated from $\tau = t_f$ to $\tau = t$ (in the case of (5.4.15)) and from $\tau = 0$ to $\tau = t$ (in the case of (5.4.16)). This gives

$$q^{(k+1)}(t) - q^{(k)}(t) = \boldsymbol{\Phi}^{(k+1)^{-T}}(t,t_0)\int_t^{t_f}\boldsymbol{\Phi}^{(k+1)^T}(\tau,t_0)\boldsymbol{F_1^{(k)}}(\tau)q^{(k)}(\tau)\,\mathrm{d}\tau, \tag{5.4.17}$$

$$x^{(k+1)}(t) - x^{(k)}(t) = \boldsymbol{\Phi}^{(k+1)}(t,t_0)\int_0^t\boldsymbol{\Phi}^{(k+1)^{-1}}(\tau,t_0)\left(\boldsymbol{F_1^{(k)}}(\tau)x^{(k)}(\tau)\right.$$
$$\left. + \boldsymbol{B}\boldsymbol{R}^{-1}\boldsymbol{B}^T\left(q^{(k+1)}(\tau) - q^{(k)}(\tau)\right)\right)\,\mathrm{d}\tau, \tag{5.4.18}$$

where we used the facts that $q^{(k+1)}(t_f) = q^{(k)}(t_f)$ and $x^{(k+1)}(0) = x^{(k)}(0)$. Equations (5.4.17)–(5.4.18) are explicit expressions for the differences $q^{(k+1)} - q^{(k)}$ and $x^{(k+1)} - x^{(k)}$. With a similar approach, an expression for $\boldsymbol{P}^{(k+1)} - \boldsymbol{P}^{(k)}$ can also be derived. From the differential Lyapunov equation (5.3.27) it follows that

$$\frac{\mathrm{d}}{\mathrm{d}t}\left(\boldsymbol{P}^{(k+1)} - \boldsymbol{P}^{(k)}\right) = -\tilde{\boldsymbol{A}}^{(k)^T}\left(\boldsymbol{P}^{(k+1)} - \boldsymbol{P}^{(k)}\right) -$$
$$\left(\boldsymbol{P}^{(k+1)} - \boldsymbol{P}^{(k)}\right)\tilde{\boldsymbol{A}}^{(k)} - \boldsymbol{F_2^{(k)}}, \tag{5.4.19}$$

where $\boldsymbol{F_2^{(k)}} = \boldsymbol{F_2^{(k)}}(t)$ is given by

$$\boldsymbol{F_2^{(k)}} = \boldsymbol{F_1^{(k)}}^T\boldsymbol{P}^{(k)} + \boldsymbol{P}^{(k)}\boldsymbol{F_1^{(k)}} + \left(\tilde{\boldsymbol{Q}}^{(k)} - \tilde{\boldsymbol{Q}}^{(k-1)}\right). \tag{5.4.20}$$

From (5.4.19) it follows

$$\frac{\mathrm{d}}{\mathrm{d}t}\left(\mathbf{\Phi}^{(k+1)^T}(t,t_0)\left(\boldsymbol{P}^{(k+1)}(t)-\boldsymbol{P}^{(k)}(t)\right)\mathbf{\Phi}^{(k+1)}(t,t_0)\right)=$$
$$-\mathbf{\Phi}^{(k+1)^T}(t,t_0)\boldsymbol{F_2}^{(k)}\mathbf{\Phi}^{(k+1)}(t,t_0). \tag{5.4.21}$$

Equation (5.4.21) follows upon differentiation of the product and then using (5.4.8), (5.4.10) and (5.4.19) (the intermediate steps are omitted for brevity). Integration of (5.4.21) from $\tau=t_f$ to $\tau=t$ gives

$$\boldsymbol{P}^{(k+1)}(t)-\boldsymbol{P}^{(k)}(t)=\mathbf{\Phi}^{(k+1)^{-T}}(t,t_0)\times$$
$$\left(\int_t^{t_f}\mathbf{\Phi}^{(k+1)^T}(\tau,t_0)\boldsymbol{F_2}^{(k)}(\tau)\mathbf{\Phi}^{(k+1)}(\tau,t_0)\,\mathrm{d}\tau\right)\mathbf{\Phi}^{(k+1)^{-1}}(t,t_0), \tag{5.4.22}$$

where we used $\boldsymbol{P}^{(k+1)}(t_f)=\boldsymbol{P}^{(k)}(t_f)$.

Part 2:

The proof now proceeds by estimating the norms $\left|\left|x^{(k+1)}-x^{(k)}\right|\right|$ and $\left|\left|\boldsymbol{P}^{(k+1)}-\boldsymbol{P}^{(k)}\right|\right|$ from their corresponding expressions in (5.4.17), (5.4.18) and (5.4.22). We first present the following simple result.

Lemma 5.1: *Let $h\in\mathbb{B}_1$ or $h\in\mathbb{B}_2$, then the following bounds hold*

$$\left|\left|\int_0^t h(\tau)\,\mathrm{d}\tau\right|\right|\leq t_f\left|\left|h\right|\right|, \tag{5.4.23}$$

$$\left|\left|\int_t^{t_f} h(\tau)\,\mathrm{d}\tau\right|\right|\leq t_f\left|\left|h\right|\right|, \tag{5.4.24}$$

where $\left|\left|\cdot\right|\right|$ is the function norm defined in (B.1.1) and (B.1.2).

Proof:

From the definition of $\left|\left|\cdot\right|\right|$ and standard norm properties it follows that

$$\left|\left|\int_0^t h(\tau)\,\mathrm{d}\tau\right|\right|\leq\sup_{t\in[0,t_f]}\int_0^t\left|\left|h(\tau)\right|\right|_E\,\mathrm{d}\tau. \tag{5.4.25}$$

The integrand in the right hand side of (5.4.25) is nonnegative, hence the integral is a non-decreasing function of t. Its supremum is attained at $t = t_f$ and thus

$$\left|\left| \int_0^t h(\tau)\,\mathrm{d}\tau \right|\right| \leq \int_0^{t_f} ||h(\tau)||_E \,\mathrm{d}\tau, \tag{5.4.26}$$

$$\leq t_f \sup_{t\in[0,t_f]} ||h(t)||_E, \tag{5.4.27}$$

$$\leq t_f \,||h||. \tag{5.4.28}$$

The proof for (5.4.24) and the case $h \in \mathbb{B}_2$ follow similarly.

□□□

Lemma 5.1 and the Cauchy-Schwarz inequality can be used in the differences in (5.4.17), (5.4.18) and (5.4.22) to get

$$\left|\left| q^{(k+1)} - q^{(k)} \right|\right| \leq t_f \left|\left| \boldsymbol{\Phi}^{(k+1)^{-T}} \right|\right| \left|\left| \boldsymbol{\Phi}^{(k+1)^T} \right|\right| \left|\left| \boldsymbol{F_1^{(k)}} \right|\right| \left|\left| q^{(k)} \right|\right|, \tag{5.4.29}$$

$$\left|\left| x^{(k+1)} - x^{(k)} \right|\right| \leq t_f \gamma_1 \left(\left|\left| \boldsymbol{F_1^{(k)}} \right|\right| \left|\left| x^{(k)} \right|\right| + ||\boldsymbol{BR}^{-1}\boldsymbol{B}^T|| \left|\left| q^{(k+1)} - q^{(k)} \right|\right| \right), \tag{5.4.30}$$

$$\left|\left| \boldsymbol{P^{(k+1)}} - \boldsymbol{P^{(k)}} \right|\right| \leq t_f \gamma_1^2 \left|\left| \boldsymbol{F_2^{(k)}} \right|\right|, \tag{5.4.31}$$

where

$$\gamma_1 = \left|\left| \boldsymbol{\Phi}^{(k+1)^{-1}} \right|\right| \left|\left| \boldsymbol{\Phi}^{(k+1)} \right|\right|. \tag{5.4.32}$$

Note that in (5.4.29)–(5.4.30) we have also used the fact that the matrix and vector euclidean norms $||\cdot||_E$ are compatible, i.e. $||\boldsymbol{A}z||_E \leq ||\boldsymbol{A}||_E \,||z||_E$ for all $\boldsymbol{A} \in \mathbb{R}^{n+2m}$ and $z \in \mathbb{R}^{n+2m}$. In addition, since $||\boldsymbol{A}||_E = \left|\left| \boldsymbol{A}^T \right|\right|_E$ we can write (5.4.29) as

$$\left|\left| q^{(k+1)} - q^{(k)} \right|\right| \leq t_f \gamma_1 \left|\left| \boldsymbol{F_1^{(k)}} \right|\right| \left|\left| q^{(k)} \right|\right|. \tag{5.4.33}$$

Substitution of (5.4.33) in (5.4.30) and noting that $||\boldsymbol{BR}^{-1}\boldsymbol{B}^T|| = \left|\left| \boldsymbol{R}^{-1} \right|\right|$ (recall the definition of $\boldsymbol{B}$ in (5.3.9)) yields

$$\left|\left| x^{(k+1)} - x^{(k)} \right|\right| \leq t_f \gamma_1 \left(\gamma_2 + t_f \gamma_1 \gamma_3 \right) \left|\left| \boldsymbol{F_1^{(k)}} \right|\right|, \tag{5.4.34}$$

where

$$\gamma_2 = \left|\left|x^{(k)}\right|\right|, \tag{5.4.35}$$

$$\gamma_3 = \left|\left|\boldsymbol{R}^{-1}\right|\right|\left|\left|q^{(k)}\right|\right|. \tag{5.4.36}$$

The definitions of $\boldsymbol{F}_1^{(k)}$ and $\boldsymbol{F}_2^{(k)}$ in (5.4.14) and (5.4.20) imply

$$\left|\left|\boldsymbol{F}_1^{(k)}\right|\right| = \left|\left|\tilde{\boldsymbol{A}}^{(k)} - \tilde{\boldsymbol{A}}^{(k-1)}\right|\right|, \tag{5.4.37}$$

$$\left|\left|\boldsymbol{F}_2^{(k)}\right|\right| \leq 2\left|\left|\boldsymbol{P}^{(k)}\right|\right|\left|\left|\boldsymbol{F}_1^{(k)}\right|\right| + \left|\left|\tilde{\boldsymbol{Q}}^{(k)} - \tilde{\boldsymbol{Q}}^{(k-1)}\right|\right|. \tag{5.4.38}$$

Substituting (5.4.37)–(5.4.38) in (5.4.31) and (5.4.34) and arranging the terms in matrix form, we can write

$$\begin{bmatrix} \left|\left|x^{(k+1)} - x^{(k)}\right|\right| \\ \left|\left|\boldsymbol{P}^{(k+1)} - \boldsymbol{P}^{(k)}\right|\right| \end{bmatrix} \leq t_f \begin{bmatrix} \gamma_1\left(\gamma_2 + t_f\gamma_1\gamma_3\right) & 0 \\ \gamma_1^2\gamma_4 & \gamma_1^2 \end{bmatrix} \begin{bmatrix} \left|\left|\tilde{\boldsymbol{A}}^{(k)} - \tilde{\boldsymbol{A}}^{(k-1)}\right|\right| \\ \left|\left|\tilde{\boldsymbol{Q}}^{(k)} - \tilde{\boldsymbol{Q}}^{(k-1)}\right|\right| \end{bmatrix}, \tag{5.4.39}$$

where the inequality is understood in a component-wise sense and

$$\gamma_4 = 2\left|\left|\boldsymbol{P}^{(k)}\right|\right|. \tag{5.4.40}$$

Moreover, $\tilde{\boldsymbol{A}}^{(k)}$ in (5.3.24) implies

$$\left|\left|\tilde{\boldsymbol{A}}^{(k)} - \tilde{\boldsymbol{A}}^{(k-1)}\right|\right| \leq \left|\left|\boldsymbol{A}^{(k)} - \boldsymbol{A}^{(k-1)}\right|\right| + \left|\left|\boldsymbol{R}^{-1}\right|\right|\left|\left|\boldsymbol{P}^{(k)} - \boldsymbol{P}^{(k-1)}\right|\right|. \tag{5.4.41}$$

A bound for $\left|\left|\boldsymbol{A}^{(k)} - \boldsymbol{A}^{(k-1)}\right|\right|$ follows directly from Assumption 5.2. This is stated in the next lemma.

Lemma 5.2: *Consider the network (5.2.2) satisfying Assumption 5.2. Let*

$$\mathcal{L}_A = \left(\sum_{i=1}^{n}\sum_{j=1}^{m}|N_{ij}|^2\,\mathcal{L}_j^2\right)^{\frac{1}{2}}, \tag{5.4.42}$$

where N_{ij} is the $(i,j)-$entry of $\boldsymbol{N}$ and $\mathcal{L}_j$ is the Lipschitz constant of $g_j(s)$, then

$$\left|\left|\boldsymbol{A}^{(k)} - \boldsymbol{A}^{(k-1)}\right|\right| \leq \mathcal{L}_A\left|\left|x^{(k)} - x^{(k-1)}\right|\right|. \tag{5.4.43}$$

Proof:

Since $\boldsymbol{G}(s)$ in the kinetic model (5.2.2) is diagonal, it can be shown that

$$||\boldsymbol{NG}(s_a) - \boldsymbol{NG}(s_b)||_E^2 = \sum_{i=1}^{n}\sum_{j=1}^{m} |N_{ij}|^2 |g_j(s_a) - g_j(s_b)|^2, \qquad (5.4.44)$$

for all $s_a, s_b \in \mathbb{R}^n$. Using Assumption 5.2 in each term in the right hand side of (5.4.44) yields

$$||\boldsymbol{NG}(s_a) - \boldsymbol{NG}(s_b)||_E \leq \mathcal{L}_A \, ||s_a - s_b||_E. \qquad (5.4.45)$$

Using the definition of $\boldsymbol{A}(x)$ in (5.3.9) we get

$$||\boldsymbol{A}(x_a) - \boldsymbol{A}(x_b)||_E = ||\boldsymbol{NG}(x_a) - \boldsymbol{NG}(x_b)||_E, \qquad (5.4.46)$$

for all $x_a, x_b \in \mathbb{R}^{n+2m}$. By definition $\boldsymbol{G}(s) = \boldsymbol{G}(x)$ with $x = \begin{bmatrix} s^T & e^T & r^T \end{bmatrix}^T$, and thus we can combine (5.4.45)–(5.4.46) to get

$$||\boldsymbol{A}(x_a) - \boldsymbol{A}(x_b)||_E \leq \mathcal{L}_A \, ||x_a - x_b||_E. \qquad (5.4.47)$$

If x_a and x_b depend on time so that $x_a, x_b \in \mathbb{B}_1$, then we can take the supremum in (5.4.47) so that $||\boldsymbol{A}(x_a) - \boldsymbol{A}(x_b)|| \leq \mathcal{L}_A \, ||x_a - x_b||$ for all $x_a, x_b \in \mathbb{B}_1$. The result follows by recalling that $\boldsymbol{A}^{(k)} = \boldsymbol{A}\left(x^{(k)}\right)$ and taking $x_a = x^{(k)}$ and $x_b = x^{(k-1)}$.

$\square\square\square$

Lemma 5.2 can be used to write the bound in (5.4.41) as

$$\left|\left|\tilde{\boldsymbol{A}}^{(k)} - \tilde{\boldsymbol{A}}^{(k-1)}\right|\right| \leq \mathcal{L}_A \left|\left|x^{(k)} - x^{(k-1)}\right|\right| + ||\boldsymbol{R}^{-1}|| \left|\left|\boldsymbol{P}^{(k)} - \boldsymbol{P}^{(k-1)}\right|\right|. \qquad (5.4.48)$$

In addition, a bound for $\left|\left|\tilde{\boldsymbol{Q}}^{(k)} - \tilde{\boldsymbol{Q}}^{(k-1)}\right|\right|$ can be obtained from the expression for $\tilde{\boldsymbol{Q}}^{(k-1)}$ in (5.3.25). We write

$$\tilde{\boldsymbol{Q}}^{(k)} - \tilde{\boldsymbol{Q}}^{(k-1)} = \left(\boldsymbol{P}^{(k)} + \boldsymbol{P}^{(k-1)}\right)\boldsymbol{B}\boldsymbol{R}^{-1}\boldsymbol{B}^T\left(\boldsymbol{P}^{(k)} - \boldsymbol{P}^{(k-1)}\right), \qquad (5.4.49)$$

which follows by noting that both $\boldsymbol{P^{(k-1)}}$ and $\boldsymbol{P^{(k)}}$ are symmetric, and hence $\boldsymbol{P^{(k)}BR^{-1}B^T P^{(k-1)}}$ also is. Thus, we have that

$$\left|\left|\tilde{\boldsymbol{Q}}^{(k)} - \tilde{\boldsymbol{Q}}^{(k-1)}\right|\right| \leq \gamma_5 \left|\left|\boldsymbol{R}^{-1}\right|\right| \left|\left|\boldsymbol{P}^{(k)} - \boldsymbol{P}^{(k-1)}\right|\right|, \tag{5.4.50}$$

where $\gamma_5 = \left|\left|\boldsymbol{P}^{(k)} + \boldsymbol{P}^{(k-1)}\right|\right|$.

The bounds in (5.4.48) and (5.4.50) can be written as the following component-wise inequality

$$\begin{bmatrix} \left|\left|\tilde{\boldsymbol{A}}^{(k)} - \tilde{\boldsymbol{A}}^{(k-1)}\right|\right| \\ \left|\left|\tilde{\boldsymbol{Q}}^{(k)} - \tilde{\boldsymbol{Q}}^{(k-1)}\right|\right| \end{bmatrix} \leq \begin{bmatrix} \mathcal{L}_A & \left|\left|\boldsymbol{R}^{-1}\right|\right| \\ 0 & \gamma_5 \left|\left|\boldsymbol{R}^{-1}\right|\right| \end{bmatrix} \begin{bmatrix} \left|\left|x^{(k)} - x^{(k-1)}\right|\right| \\ \left|\left|\boldsymbol{P}^{(k)} - \boldsymbol{P}^{(k-1)}\right|\right| \end{bmatrix}. \tag{5.4.51}$$

Substitution of (5.4.51) in (5.4.39) gives

$$\begin{bmatrix} \left|\left|x^{(k+1)} - x^{(k)}\right|\right| \\ \left|\left|\boldsymbol{P}^{(k+1)} - \boldsymbol{P}^{(k)}\right|\right| \end{bmatrix} \leq \boldsymbol{M} \begin{bmatrix} \left|\left|x^{(k)} - x^{(k-1)}\right|\right| \\ \left|\left|\boldsymbol{P}^{(k)} - \boldsymbol{P}^{(k-1)}\right|\right| \end{bmatrix}, \tag{5.4.52}$$

with

$$\boldsymbol{M} = t_f \begin{bmatrix} \gamma_1 \left(\gamma_2 + t_f \gamma_1 \gamma_3\right) \mathcal{L}_A & \gamma_1 \left(\gamma_2 + t_f \gamma_1 \gamma_3\right) \left|\left|\boldsymbol{R}^{-1}\right|\right| \\ \gamma_1^2 \gamma_4 \mathcal{L}_A & \left(\gamma_1^2 \gamma_4 + \gamma_1^2 \gamma_5\right) \left|\left|\boldsymbol{R}^{-1}\right|\right| \end{bmatrix} \tag{5.4.53}$$

Assumption 5.1 implies that the entries of $\boldsymbol{A^{(k)}}(t)$ in $[0, t_f]$ are bounded in $[0, t_f]$ and thus the norms in $\gamma_1, \gamma_2, \ldots, \gamma_5$ are finite. Hence, by choosing t_f sufficiently small, the eigenvalues of $\boldsymbol{M}$ can be made arbitrarily small, which by Theorem B.1 implies that the sequences $\{x^{(k)}\}$ and $\{\boldsymbol{P^{(k)}}\}$ converge to a unique fixed-point. This completes the proof.

□□□

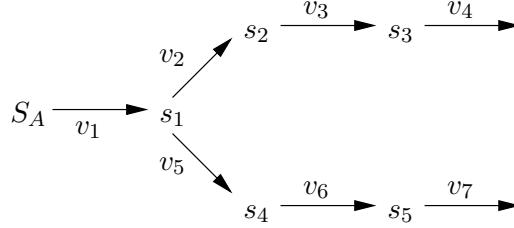## 5.5 Example

Consider the metabolic network of Figure 5.2.

Figure 5.2. Example metabolic network with $n = 5$ metabolites and $m = 7$ reactions.

The stoichiometric matrix of this network is

$$N = \begin{bmatrix} 1 & -1 & 0 & 0 & -1 & 0 & 0 \\ 0 & 1 & -1 & 0 & 0 & 0 & 0 \\ 0 & 0 & 1 & -1 & 0 & 0 & 0 \\ 0 & 0 & 0 & 0 & 1 & -1 & 0 \\ 0 & 0 & 0 & 0 & 0 & 1 & -1 \end{bmatrix}. \tag{5.5.1}$$

The enzyme kinetics are written as $v_i = g_i(s)e_i$ and are assumed to be of Michaelis-Menten type:

$$g_1 = \frac{k_{\text{cat}\,1}S_A}{K_{\text{m}\,1} + S_A}, \tag{5.5.2}$$

$$g_2 = \frac{k_{\text{cat}\,2}s_1}{K_{\text{m}\,2} + s_1}, \qquad g_5 = \frac{k_{\text{cat}\,5}s_1}{K_{\text{m}\,5} + s_1},$$

$$g_3 = \frac{k_{\text{cat}\,3}s_2}{K_{\text{m}\,3} + s_2}, \qquad g_6 = \frac{k_{\text{cat}\,6}s_4}{K_{\text{m}\,6} + s_4},$$

$$g_4 = \frac{k_{\text{cat}\,4}s_3}{K_{\text{m}\,4} + s_3}, \qquad g_7 = \frac{k_{\text{cat}\,7}s_5}{K_{\text{m}\,7} + s_5}.$$

The parameter values for the enzyme kinetics are given in Table 5.1. All the enzymes are assumed to have an equal degradation constant $\lambda = 1$ and the external substrate is assumed constant $S_A = 1$.

Reaction	v_1	v_2	v_3	v_4	v_5	v_6	v_7
$k_{\text{cat}\,i}$	1	2	1	3	4	1	2
$K_{\text{m}\,i}$	1	1	1	1	1	1	1

Table 5.1. Parameters values for the metabolic network in Figure 5.2.

The weighting matrices are chosen as $W_s = 10I$ and $W_e = W_r = W_{\dot{r}} = 10I$.

We also choose nonzero terminal weights $\boldsymbol{W_{sf}} = 10\boldsymbol{I}$ and $\boldsymbol{W_{ef}} = \boldsymbol{W_{ef}} = \boldsymbol{W_{rf}} = 10\boldsymbol{I}$ so as to force the terminal state to be close to the target. For $t \leq 0$ the network is assumed to be in the initial steady state

$$s^i = \begin{bmatrix} 1 & 1 & 1 & 1 \end{bmatrix}^T, \tag{5.5.3}$$

$$v^i = \begin{bmatrix} 1 & 0.5 & 0.5 & 0.5 & 0.5 & 0.5 & 0.5 \end{bmatrix}^T. \tag{5.5.4}$$

As the target steady state we consider a 50% increase in the fluxes and metabolite concentrations, i.e. $v^f = 1.5v^i$ and $s^f = 1.5s^i$. Note that the steady state enzyme levels (e^i and e^f) and expression rates (r^i and r^f) can be computed directly from (5.2.4)–(5.2.7). In this example solving Problem 5.1 requires the optimization of seven control inputs for a nonlinear system with twelve state variables. We use the iterative procedure of Algorithm 5.1 to compute the suboptimal responses in the interval $[0, 8]$ and a tolerance of $\varepsilon = 10^{-4}$. The tolerance is reached after 165 iterations and the results for the final iteration are shown in Figures 5.3–5.4. The trajectories show that the chosen horizon t_f is large enough for the network to approach the target steady state and yield satisfactory results.
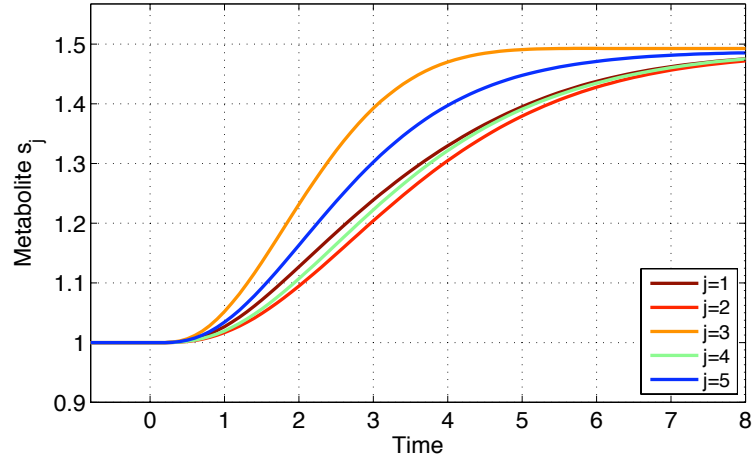

Figure 5.3. Metabolite concentrations for the network in Figure 5.2.
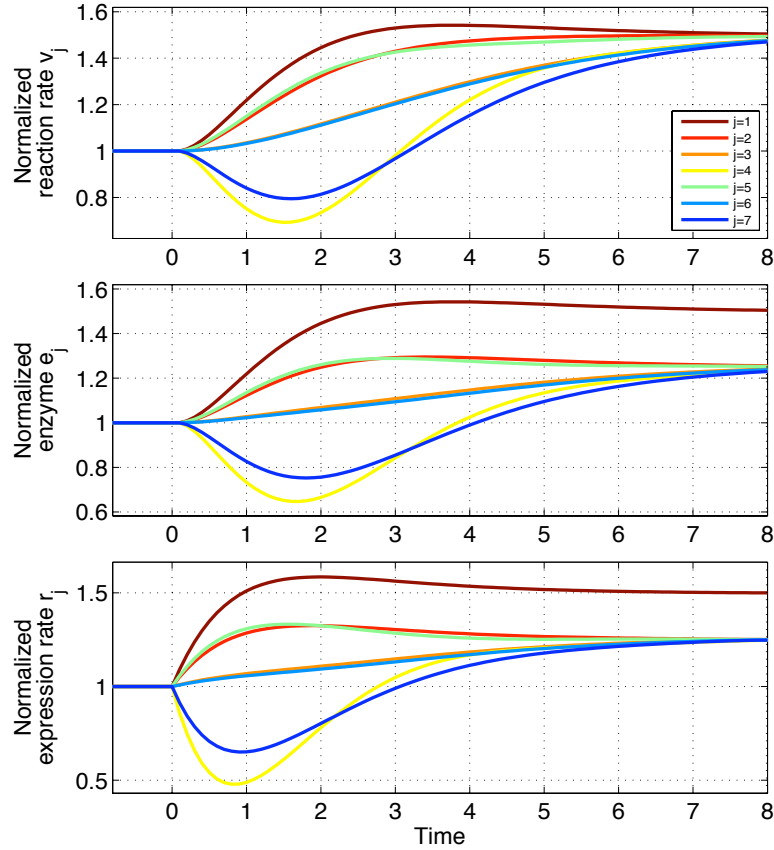
Figure 5.4. Reaction rates, enzyme concentrations and their expression rates for the network in Figure 5.2. The variables are normalized with respect to their initial values v_j^i, e_j^i and r_j^i, respectively.

5.6 Discussion

This chapter deals with the problem of determining time-dependent enzyme expression rates that drive a metabolic network between two different steady states while satisfying an optimality criterion. The dynamical system under consideration is composed of a nonlinear model for the metabolic network coupled with a linear expression/degradation model for enzyme synthesis. In this setup the enzyme expression rates are regarded as control inputs and we formulate Problem 5.1 as a way of accounting for the combined minimization of the effort needed for enzyme synthesis (as measured by the rate of change of the expression rates), together with the devi-

90

ation of the species and expression rates from their target steady state values. No restrictive assumptions are made on the stoichiometry and reaction kinetics, so the formulation can include highly nonlinear networks with a large number of metabolites and reactions. In addition, since the reaction rates are allowed to depend on any number of metabolites, nonlinear regulatory phenomena such as allostery (see Chapter 2) can also be accounted for.

Solving this optimal control problem is not easy, as standard theoretical approaches such as Pontryagin's Minimum Principle or the Hamilton-Jacobi-Bellman equation [91] yield problems that may be explicitly solved for particular cases, but the general case with arbitrary stoichiometries and kinetics does not admit a general solution. Numerical solutions can also be tried, but since metabolic networks usually have a large number of metabolites and reactions, the effectiveness of numerical techniques can be impaired. This is aggravated by the fact that the metabolic network is extended with a model for enzyme synthesis. Thus, for a network with n metabolites and m reactions, the optimization problem involves m control inputs and $n + m$ state variables.

We formulate Algorithm 5.1 as an iterative procedure for computing suboptimal solutions of the optimization problem. The algorithm is based on the observation that the dynamics can be written in the following linear-like form

$$\dot{x} = \boldsymbol{A}(x)x + \boldsymbol{B}u. \qquad (5.6.1)$$

From this representation one can build a sequence of linear time-variant approximations of the dynamics by evaluating $\boldsymbol{A}(x)$ along the state trajectory computed at a previous iteration. The cost function is quadratic and has the same form as those used in finite horizon Linear Quadratic optimal control. Moreover, the target steady state can be regarded as an external signal to be tracked by the state variable, and hence the original problem can be recast as a sequence of finite horizon LQT problems. This kind of approximation technique has been used previously in the literature for the optimal control of bilinear systems [93, 94], polynomial systems [95], and general nonlinear systems [88, 33]. All these approaches result in iterative algorithms for computing the suboptimal solution and, with the exception of [94], they rely on the solution of a differential Riccati equation at each iteration. A possible drawback is that, since the Riccati equation is quadratic, it may become computationally expensive for high-dimensional systems. Instead we opt for an ap-

proach similar to [94] and build the iterative scheme in a way that only the solution of a differential Lyapunov equation is required in each iteration. This equation is linear and computationally less demanding, which makes it better suited for the high-dimensional case. In this view, the method presented here corresponds to an extension of the approach in [94] for more general nonlinear systems.

The algorithm is shown to converge provided that the optimization horizon t_f is sufficiently small and the kinetics are globally Lipschitz continuous functions of the metabolites. Many common enzyme kinetics (such as Michaelis-Menten, Hill and allosteric kinetics) are globally Lipschitz continuous in the positive orthant $\mathbb{R}^n_{\geq 0}$. Hence, convergence can be guaranteed for a quite general class of networks, both in terms of stoichiometry and reaction kinetics. A limitation of this result is that for some problems one may need to use a prohibitively small t_f to ensure convergence. This can lead to unsatisfactory solutions that do not drive the network close to the target steady state. Although we cannot estimate *a priori* how small the horizon must be, a possible way of avoiding the problem is to adjust the weights in the cost function so as to generate faster responses that reach the target in a shorter time interval.

A shortcoming of our method is that the optimization does not account for constraints on the chemical species and expression rates. This can yield unrealistic responses since in a real network concentrations and expression rates can only have positive values and are also subject to upper bounds. Another consequence of this is related to the solution of the sequence of LQT problems. Many reaction kinetics have singularities for negative metabolite concentrations. For example, the irreversible Michaelis-Menten kinetics

$$\frac{k_{\mathrm{cat}}s}{K_{\mathrm{m}} + s}e, \tag{5.6.2}$$

have a singularity at $s = -K_{\mathrm{m}}$, and the same applies to other common cases such as Hill or allosteric kinetics (see Chapter 2). These singularities also appear in $\boldsymbol{A}(x)$ (recall is definition in (5.3.9)), and therefore in the absence of constraints the sequence of LQT problems may involve a linear time-variant system with a discontinuous state matrix, so that Assumption 5.1 fails to hold and this precludes the use of the standard LQT solution.

The above discussion stresses the need to extend these kind of optimization problems to account for constraints. The analysis presented in this chapter suggests

that the use of linear time-variant approximations for nonlinear systems may prove useful in this respect. They have the advantage of providing a global approximation of the dynamics and, at the same time, give access to the extensive machinery developed for linear systems, including constrained optimal control methods.

Chapter 6

Optimal expression rates under stoichiometric constraints

6.1 Introduction

It has been observed that large variations in metabolic fluxes can be accompanied by comparatively small changes in the steady state metabolite concentrations [27]. In this chapter we study the limiting case of this scenario and address the optimal transition between two steady states under *constant* metabolite concentrations.

The optimal control problem can be regarded as a special case of the nonlinear problem treated in the previous chapter. We consider the optimization of an infinite horizon version of the cost function of Chapter 5 and impose the additional constraint of constant metabolite concentrations along the whole optimization interval. The resulting problem is linear and can be solved with the well-known results for the infinite horizon Linear Quadratic Regulator (LQR) problem.

The steady state constraint on the metabolites translates into algebraic constraints on the enzyme trajectories and expression rates. These are related to the network topology and can be regarded as a *stoichiometric constraint* on the linear model for enzyme expression/degradation. The problem can thus be treated within the LQR framework for a linear Differential-Algebraic Equation (DAE) system. By exploiting the structure of the DAE system, the problem can be recast as a standard LQR problem for a lower-dimensional linear system without algebraic constraints, which can be readily solved via the classic LQR theory.

The chapter is organized as follows: the problem is stated in Section 6.2 and its solution is developed in Section 6.3. The results are illustrated with a simple numerical example in Section 6.4. We conclude with a discussion of the results in Section 6.5.

6.2 Problem formulation

The formulation of the optimal control problem is essentially a special case of that presented in the previous chapter (Problem 5.1). For completeness, we briefly recall the notation and definitions from Section 5.2.

A metabolic network coupled with its enzyme dynamics can be described by

$$\dot{s} = \boldsymbol{N}\boldsymbol{G}(s)e, \tag{6.2.1}$$

$$\dot{e} = r - \boldsymbol{\Lambda}e, \tag{6.2.2}$$

where $\boldsymbol{N} \in \mathbb{Z}^{n \times m}$ is the stoichiometric matrix, $s \in \mathbb{R}^n$ the metabolite vector, $e \in \mathbb{R}^m$ the vector of enzyme concentrations, and $r \in \mathbb{R}^m$ the vector of enzyme expression rates. The matrix $\boldsymbol{\Lambda} = \mathrm{diag}\,\{\lambda_1, \lambda_2, \ldots, \lambda_m\}$ with $\lambda_i > 0$ accounts for linear enzymatic degradation, and $\boldsymbol{G}(s) = \mathrm{diag}\,\{g_1(s), g_2(s), \ldots, g_m(s)\}$ comprises the enzyme turnover rates and relates to the reaction rates $v \in \mathbb{R}^m$ by

$$v = \boldsymbol{G}(s)e. \tag{6.2.3}$$

The complete model is represented by the block diagram of Figure 5.1. We are interested in finding optimal enzyme expression rates that drive the network between two steady states under constant metabolite concentrations.

Initial and target steady states

Consider the constraint

$$s(t) = s^i, \tag{6.2.4}$$

for all $t \geq 0$, where $s^i \in \mathbb{R}^n_{>0}$ is a vector of metabolite concentrations such that $\boldsymbol{G_i} = \boldsymbol{G}\left(s^i\right)$ is nonsingular. Under this constraint, the initial and target steady states can be specified solely in terms of the network fluxes: Given an initial flux $v^i \in \mathbb{R}^m$ and target flux $v^f \in \mathbb{R}^m$, from (6.2.1)–(6.2.2) the corresponding steady state enzyme concentrations and expression rates can be computed from

$$e^i = \boldsymbol{G_i}^{-1}v^i, \qquad\qquad e^f = \boldsymbol{G_i}^{-1}v^f, \tag{6.2.5}$$

$$r^i = \boldsymbol{\Lambda}e^i, \qquad\qquad r^f = \boldsymbol{\Lambda}e^f. \tag{6.2.6}$$

Note that nonsingularity of $\boldsymbol{G_i}$ is required for e^i and e^f to be well defined.

Cost function

Consider an infinite horizon version of $J(z, \boldsymbol{W})$ defined in (5.2.8):

$$J(z, \boldsymbol{W}) = \frac{1}{2} \int_0^\infty z^T \boldsymbol{W} z \, \mathrm{d}t, \tag{6.2.7}$$

where $z(t) : [0, \infty) \rightarrow \mathbb{R}^q$ and $\boldsymbol{W} \in \mathbb{R}^{q \times q}$ is a positive semidefinite matrix. We consider the minimization of

$$\mathcal{J} = \mathcal{J}_+ + \mathcal{J}_-, \tag{6.2.8}$$

where

$$\mathcal{J}_+ = J\left(e - e^f, \boldsymbol{W_e}\right) + J\left(r - r^f, \boldsymbol{W_r}\right), \tag{6.2.9}$$

$$\mathcal{J}_- = J\left(\dot{r}, \boldsymbol{W_{\dot{r}}}\right). \tag{6.2.10}$$

The matrices in the functionals (6.2.9)–(6.2.10) have appropriate dimensions and are assumed to satisfy $\boldsymbol{W_e}, \boldsymbol{W_r} \geq 0$ and $\boldsymbol{W_{\dot{r}}} > 0$. The cost $\mathcal{J}$ in (6.2.8) is an infinite horizon version of the one used in Chapter 5. Its interpretation and the effect of the weighting matrices are, therefore, the same as those discussed in Section 5.2. Note that, in contrast to the previous chapter, it is not necessary to include a weight on the terminal state in the definition of $\mathcal{J}$. This is because for $J(z, \boldsymbol{W})$ to be finite, it is necessary that $\lim_{t \to \infty} z(t) = 0$. Thus, if there exists an optimal $r(t)$, it must drive the state exactly to the target, i.e.

$$\lim_{t \to \infty} e(t) = e^f, \tag{6.2.11}$$

$$\lim_{t \to \infty} r(t) = r^f. \tag{6.2.12}$$

The optimization problem can be summarized as follows.

Problem 6.1: *Let $v^i, v^f \in \mathbb{R}^m$ be two steady state fluxes for the network (6.2.1)–(6.2.2) and let $s^i \in \mathbb{R}^n_{>0}$ be a metabolite concentration vector such that $\boldsymbol{G_i}$ is non-singular. Assume that the network is in steady state with $s(t) = s^i$, $e(t) = e^i$ and $r(t) = r^i$ for all $t \leq 0$, with e^i and r^i given in (6.2.5)–(6.2.6). Given weight matrices $\boldsymbol{W_e}, \boldsymbol{W_r} \geq 0$ and $\boldsymbol{W_{\dot{r}}} > 0$, find a piecewise continuous control $r(t) : [0, \infty) \rightarrow \mathbb{R}^m$*

that minimizes

$$\mathcal{J} = \mathcal{J}_+ + \mathcal{J}_-, \tag{6.2.13}$$

subject to $s(t) = s^i$ for all $t \geq 0$.

Problem 6.1 has a considerable simpler structure as compared to the nonlinear problem studied in the previous chapter. In fact, the nonlinearities in system (6.2.1)–(6.2.2) only appear in the matrix function $\boldsymbol{G}(s)$, and hence the system is linear under the constraint of constant metabolites. Unlike the finite horizon case, the solution of Problem 6.1 must also guarantee asymptotic stability of (6.2.1)–(6.2.2) under the optimal control. As we show in the next section, however, Problem 6.1 can be recast as a Linear Quadratic Regulator problem and stability can be directly accounted for.

6.3 Equivalent problem and solution

6.3.1 Differential-Algebraic system

The following lemma provides a useful characterization of the constraint $s(t) = s^i$ in Problem 6.1. This will allow us to recast the enzyme dynamics in (6.2.2) as a linear Differential-Algebraic system.

Lemma 6.1: *Consider the metabolic network (6.2.1) with $s(t) = s^i \in \mathbb{R}^n_{>0}$ for all $t \leq 0$ and such that $\boldsymbol{G_i}$ is nonsingular. Define $\boldsymbol{T_1} = \boldsymbol{G_i}^{-1}\boldsymbol{K} \in \mathbb{R}^{m \times (m-d)}$ where the columns of $\boldsymbol{K} \in \mathbb{R}^{m \times (m-d)}$ form a basis for the nullspace of $\boldsymbol{N}$, i.e. $\boldsymbol{NK} = 0$ with $d = \mathrm{rank}\{\boldsymbol{N}\}$. Then, $s(t) = s^i$ for all $t \geq 0$ if and only if e satisfies the stoichiometric constraint*

$$e = \boldsymbol{T_1}\phi, \tag{6.3.1}$$

for all $\phi = \phi(t) \in \mathbb{R}^{m-d}$.

Proof:

Sufficiency follows by substituting (6.3.1) in the metabolic dynamics (6.2.1), which yields

$$\dot{s} = \boldsymbol{N}\boldsymbol{G}(s)\boldsymbol{G_i}^{-1}\boldsymbol{K}\phi. \tag{6.3.2}$$

Evaluation of (6.3.2) at $t = 0$ implies that $\dot{s}(0) = \boldsymbol{NK}\phi = 0$ for all ϕ and hence $s(t) = s^i$ for all $t \geq 0$. Necessity can be proven by noting that in (6.2.1), $\dot{s} = 0$ holds only when

$$\boldsymbol{G}(s)e = 0, \ \forall t \geq 0, \tag{6.3.3}$$

or

$$e(t) \in \ker \left\{ \boldsymbol{N}\boldsymbol{G}(s) \right\}, \ \forall t \geq 0. \tag{6.3.4}$$

Equation (6.3.3) holds if $e = 0$ (the trivial case) or $\boldsymbol{G}(s) = 0$ for all $t \geq 0$, which can be discarded because $\boldsymbol{G}(s)$ is nonsingular at least for $t = 0$ (recall that $\boldsymbol{G_i}$ is nonsingular). Moreover, $s(t) = s^i$ for all $t \geq 0$ implies that (6.3.4) only holds when $e(t) \in \ker \left\{ \boldsymbol{NG_i} \right\}$, which is equivalent to (6.3.1) because the columns of $\boldsymbol{T_1}$ form a basis for the nullspace of $\boldsymbol{NG_i}$.

$\square\square\square$

The stoichiometric constraint in (6.3.1) parameterizes the enzyme vector $e \in \mathbb{R}^m$ to guarantee the constraint $s(t) = s^i$ to be satisfied. Substitution of (6.3.1) in the enzyme dynamics (6.2.2) yields

$$\boldsymbol{T_1}\dot{\phi} = -\boldsymbol{\Lambda}\boldsymbol{T_1}\phi + r. \tag{6.3.5}$$

The matrices $\boldsymbol{T_1}$ and $\boldsymbol{\Lambda}\boldsymbol{T_1}$ are rectangular, and thus the above system is a nonregular linear Differential-Algebraic Equation (DAE) system. The term "nonregular" is used to distinguish the DAE system from cases in which $\boldsymbol{T_1}$ and the state matrix are square and $\boldsymbol{T_1}$ is singular [96, 97]. The DAE system in (6.3.5) is overdetermined, since it contains m differential equations and only $m - d$ state variables. The d algebraic constraints in ϕ can be satisfied by constraining d degrees of freedom in e and r, and leaving the remaining $(m - d)$ as variables to be optimized.

Before proceeding with this approach, we note that the cost $\mathcal{J}$ includes a weight on $\dot{r}$ and so we extend the state space of (6.2.2) and consider $\dot{r}$ as the control input (this is the same idea we used for the nonlinear problem in Section 5.3). Define the extended state variable $x \in \mathbb{R}^{2m}$ as

$$x = \begin{bmatrix} e \\ r \end{bmatrix}, \tag{6.3.6}$$

with initial and target values

$$x^i = \begin{bmatrix} e^i \\ r^i \end{bmatrix}, \quad x^f = \begin{bmatrix} e^f \\ r^f \end{bmatrix}. \tag{6.3.7}$$

If $u = \dot{r}$ is regarded as the control input, from the enzyme dynamics in (6.2.2) we can describe the extended system as

$$\dot{x} = \begin{bmatrix} -\boldsymbol{\Lambda} & \boldsymbol{I} \\ \boldsymbol{0} & \boldsymbol{0} \end{bmatrix} x + \begin{bmatrix} \boldsymbol{0} \\ \boldsymbol{I} \end{bmatrix} u, \quad x(0) = x^i. \tag{6.3.8}$$

It is convenient to work with an *incremental* state variable

$$\bar{x} = x - x^f. \tag{6.3.9}$$

Using the steady state condition in (6.2.5), the system (6.3.8) becomes

$$\dot{\bar{x}} = \begin{bmatrix} -\boldsymbol{\Lambda} & \boldsymbol{I} \\ \boldsymbol{0} & \boldsymbol{0} \end{bmatrix} \bar{x} + \begin{bmatrix} \boldsymbol{0} \\ \boldsymbol{I} \end{bmatrix} u, \quad \bar{x}(0) = x^i - x^f. \tag{6.3.10}$$

The cost $\mathcal{J}$ in (6.2.13) can then be written as

$$\mathcal{J} = \frac{1}{2} \int_0^\infty \left(\bar{x}^T \bar{\boldsymbol{Q}} \bar{x} + u^T \boldsymbol{W_{\dot{r}}} u \right) \, \mathrm{d}t, \tag{6.3.11}$$

where

$$\bar{\boldsymbol{Q}} = \begin{bmatrix} \boldsymbol{W_e} & \boldsymbol{0} \\ \boldsymbol{0} & \boldsymbol{W_r} \end{bmatrix}. \tag{6.3.12}$$

The minimization of $\mathcal{J}$ for the dynamics in (6.3.10) corresponds to an infinite horizon Linear Quadratic Regulator (LQR) problem. This is a considerable advantage since it enables us to apply the well-known results presented in Appendix A.2.2.

We mentioned that, as a consequence of the stoichiometric constraint, the enzyme concentrations, e, and expression rates, r, have only $(m - d)$ degrees of freedom. This implies that the extended state $\bar{x} \in \mathbb{R}^{2m}$ and control $u = \dot{r} \in \mathbb{R}^m$ have $2(m - d)$ and $(m - d)$ degrees of freedom, respectively. Thus any $\bar{x}$ that satisfies the

stoichiometric constraint must be of the form

$$\bar{x} = \boldsymbol{E}z, \tag{6.3.13}$$

where $\boldsymbol{E} \in \mathbb{R}^{2m \times 2(m-d)}$ and $z \in \mathbb{R}^{2(m-d)}$. Note that in this case $\bar{x}$ has exactly rank $\{\boldsymbol{E}\}$ degrees of freedom, and so in order to avoid introducing further constraints on $\bar{x}$, the matrix $\boldsymbol{E}$ needs to have full column rank.

The form of the incremental model (6.3.10) and the stoichiometric constraint can be exploited to choose the state transformation $\boldsymbol{E}$ such that the solution of Problem 6.1 can be explicitly computed in terms of the system matrices $(\boldsymbol{N}, \boldsymbol{G_i}, \boldsymbol{\Lambda})$ and weights $(\boldsymbol{W_e}, \boldsymbol{W_r}, \boldsymbol{W_{\dot{r}}})$. Define the matrix $\boldsymbol{T_2} = \boldsymbol{\Lambda T_1} \in \mathbb{R}^{m \times (m-d)}$ and pick $\boldsymbol{E}$ as

$$\boldsymbol{E} = \begin{bmatrix} \boldsymbol{T_1} & \boldsymbol{0} \\ \boldsymbol{T_2} & \boldsymbol{T_1} \end{bmatrix}. \tag{6.3.14}$$

The matrix $\boldsymbol{E}$ has full column rank and we substitute $\bar{x} = \boldsymbol{E}z$ in (6.3.10) to obtain

$$\boldsymbol{E}\dot{z} = \boldsymbol{A}z + \boldsymbol{B}u, \quad z(0) = \boldsymbol{E}^+ \left(x^i - x^f \right), \tag{6.3.15}$$

with $\boldsymbol{A} \in \mathbb{R}^{2m \times 2(m-d)}$ and $\boldsymbol{B} \in \mathbb{R}^{2m \times m}$ defined as

$$\boldsymbol{A} = \begin{bmatrix} \boldsymbol{0} & \boldsymbol{T_1} \\ \boldsymbol{0} & \boldsymbol{0} \end{bmatrix}, \quad \boldsymbol{B} = \begin{bmatrix} \boldsymbol{0} \\ \boldsymbol{I} \end{bmatrix}, \tag{6.3.16}$$

and $\boldsymbol{E}^+ = \left(\boldsymbol{E}^T \boldsymbol{E} \right)^{-1} \boldsymbol{E}^T$ is the Moore-Penrose pseudoinverse of $\boldsymbol{E}$. In next section we use the structure of $\boldsymbol{E}$ to explicitly decouple the algebraic and differential parts of the DAE system in (6.3.15).

6.3.2 Equivalent problem

Define the matrix $\boldsymbol{E^*} \in \mathbb{R}^{2m \times 2m}$ as

$$\boldsymbol{E^*} = \begin{bmatrix} \boldsymbol{E}^{\perp} \\ \boldsymbol{E}^+ \end{bmatrix}, \tag{6.3.17}$$

where $\boldsymbol{E}^{\perp} \in \mathbb{R}^{2d \times 2m}$ is defined as

$$\boldsymbol{E}^{\perp} = \begin{bmatrix} \boldsymbol{NG_i} & \boldsymbol{0} \\ -\boldsymbol{N\Lambda G_i} & \boldsymbol{NG_i} \end{bmatrix}. \tag{6.3.18}$$

Note that $\boldsymbol{E}^{\perp}\boldsymbol{E} = \boldsymbol{0}$ and $\boldsymbol{E}^{\perp}\boldsymbol{E}^{+T} = \boldsymbol{0}$, which implies that the rows of $\boldsymbol{E}^{\perp}$ are orthogonal to the ones of $\boldsymbol{E}^{+}$, and hence $\boldsymbol{E}^{*}$ is nonsingular. Multiplication of the DAE system in (6.3.15) by $\boldsymbol{E}^{*}$ yields the equalities

$$0 = \boldsymbol{E}^{\perp}\boldsymbol{A}z + \boldsymbol{E}^{\perp}\boldsymbol{B}u, \tag{6.3.19}$$

$$\dot{z} = \boldsymbol{E}^{+}\boldsymbol{A}z + \boldsymbol{E}^{+}\boldsymbol{B}u. \tag{6.3.20}$$

The above equations are the algebraic and differential parts of the DAE system: (6.3.19) consists of $2d$ algebraic equations, whereas (6.3.20) comprises $2(m - d)$ differential equations in z. Equation (6.3.19) can be used to explicitly find the class of controls that satisfy the stoichiometric constraint. The products $\boldsymbol{E}^{\perp}\boldsymbol{A}$ and $\boldsymbol{E}^{\perp}\boldsymbol{B}$ are given by

$$\boldsymbol{E}^{\perp}\boldsymbol{A} = \begin{bmatrix} \boldsymbol{0} & \boldsymbol{0} \\ \boldsymbol{0} & -\boldsymbol{NG_i T_2} \end{bmatrix}, \quad \boldsymbol{E}^{\perp}\boldsymbol{B} = \begin{bmatrix} \boldsymbol{0} \\ \boldsymbol{NG_i} \end{bmatrix}, \tag{6.3.21}$$

and thus (6.3.19) reduces to only d nontrivial equations

$$\boldsymbol{NG_i}\left(-\boldsymbol{T_u}z + u\right) = 0, \tag{6.3.22}$$

where $\boldsymbol{T_u} \in \mathbb{R}^{m \times 2(m-d)}$ is given by $\boldsymbol{T_u} = \begin{bmatrix} \boldsymbol{0} & \boldsymbol{T_2} \end{bmatrix}$. Equation (6.3.22) implies that if a control u satisfies the algebraic constraint, then it also satisfies

$$(-\boldsymbol{T_u}z + u) \in \ker\{\boldsymbol{NG_i}\}. \tag{6.3.23}$$

The columns of $\boldsymbol{T_1}$ span the nullspace of $\boldsymbol{NG_i}$, and thus any u satisfying (6.3.23) has the form

$$u = \boldsymbol{T_u}z + \boldsymbol{T_1}\omega, \tag{6.3.24}$$

for some $\omega \in \mathbb{R}^{m-d}$. We have obtained a parameterization of the original control u in terms of a lower-dimensional control ω which guarantees that the stoichiometric

constraint is satisfied (and hence it ensures constant metabolite concentrations). The dynamics for z can be rewritten in terms of ω by substituting the parameterization (6.3.24) in (6.3.20)

$$
\begin{aligned}
\dot{z} &= \boldsymbol{E}^{+}\left(\boldsymbol{A}+\boldsymbol{B}\boldsymbol{T_u}\right)z + \boldsymbol{E}^{+}\boldsymbol{B}\boldsymbol{T_1}\omega, \\
&= \boldsymbol{E}^{+}\begin{bmatrix} \boldsymbol{0} & \boldsymbol{T_1} \\ \boldsymbol{0} & \boldsymbol{T_2} \end{bmatrix} z + \boldsymbol{E}^{+}\begin{bmatrix} \boldsymbol{0} \\ \boldsymbol{T_1} \end{bmatrix}\omega, \\
&= \underbrace{\boldsymbol{E}^{+}\boldsymbol{E}\begin{bmatrix} \boldsymbol{0} & \boldsymbol{I} \\ \boldsymbol{0} & \boldsymbol{0} \end{bmatrix}}_{\boldsymbol{A_z}} z + \underbrace{\boldsymbol{E}^{+}\boldsymbol{E}\begin{bmatrix} \boldsymbol{0} \\ \boldsymbol{I} \end{bmatrix}}_{\boldsymbol{B_z}}\omega, \\
&= \boldsymbol{A_z}z + \boldsymbol{B_z}\omega, \quad\quad\quad\quad\quad\quad\quad\quad\quad\quad\quad\quad (6.3.25)
\end{aligned}
$$

where $\boldsymbol{A_z} \in \mathbb{R}^{2(m-d)\times 2(m-d)}$ and $\boldsymbol{B_z} \in \mathbb{R}^{2(m-d)\times(m-d)}$. Since the constraint $s(t) = s^i$ for all $t \geq 0$ is satisfied for any ω, the solution of Problem 6.1 can be obtained by optimizing ω for system (6.3.25) without algebraic constraints. To that end, we rewrite the cost $\mathcal{J}$ in (6.3.11) in terms of the new state z and control ω. Substituting $\bar{x} = \boldsymbol{E}z$ and (6.3.24) in the cost (6.3.11) yields

$$
\mathcal{J} = \frac{1}{2}\int_0^\infty \left(z^T\boldsymbol{Q}z + \omega^T\boldsymbol{R}\omega + 2z^T\boldsymbol{S}\omega\right)\,\mathrm{d}t, \quad\quad (6.3.26)
$$

where

$$
\boldsymbol{Q} = \boldsymbol{E}^T\bar{\boldsymbol{Q}}\boldsymbol{E} + \boldsymbol{T_u}^T\boldsymbol{W_{\dot{r}}}\boldsymbol{T_u}, \quad \boldsymbol{R} = \boldsymbol{T_1}^T\boldsymbol{W_{\dot{r}}}\boldsymbol{T_1}, \quad \boldsymbol{S} = \boldsymbol{T_u}^T\boldsymbol{W_{\dot{r}}}\boldsymbol{T_1}. \quad (6.3.27)
$$

The minimization of $\mathcal{J}$ in (6.3.26) for the linear system (6.3.25) has the standard form of the LQR problem presented in Appendix A.2.2. It is worth noting that the algebraic constraint on u in (6.3.24) translates into $\mathcal{J}$ having a *mixed* term that weighs the product between state and control (via the weight matrix $\boldsymbol{S} \in \mathbb{R}^{2(m-d)\times(m-d)}$). We also see that the dynamics of z in (6.3.25) are unstable, since all the eigenvalues of $\boldsymbol{A_z}$ are located at the origin. Therefore, in order to use the LQR solution of Lemma A.2 we need to guarantee that the stabilizability and detectability conditions in Assumption A.1 are satisfied. Next lemma tackles this issue and gives the solution to Problem 6.1.

Lemma 6.2: *Consider $\boldsymbol{A_z}$ and $\boldsymbol{B_z}$ defined in (6.3.25) and $\boldsymbol{Q}$, $\boldsymbol{R}$, and $\boldsymbol{S}$ defined in (6.3.27). Then:*

(i) the pair $(\boldsymbol{A_z}, \boldsymbol{B_z})$ is stabilizable,

(ii) $\boldsymbol{R} > 0$,

(iii) $\boldsymbol{W_e}, \boldsymbol{W_r} > 0$ implies that $\tilde{\boldsymbol{Q}} = \boldsymbol{Q} - \boldsymbol{S}\boldsymbol{R}^{-1}\boldsymbol{S}^T > 0$.

Provided that $\boldsymbol{W_e}, \boldsymbol{W_r} > 0$, the solution $x^* = \begin{bmatrix} e^* \\ r^* \end{bmatrix}$ of Problem 6.1 is therefore given by

$$x^* = \boldsymbol{E}z^* + x^f, \tag{6.3.28}$$

where z^* satisfies

$$\dot{z}^* = \left(\tilde{\boldsymbol{A}}_{\boldsymbol{z}} - \boldsymbol{B_z}\boldsymbol{R}^{-1}\boldsymbol{B_z}^T\boldsymbol{P} \right) z^*, \quad z^*(0) = \boldsymbol{E}^+ \left(x^i - x^f \right), \tag{6.3.29}$$

and $\boldsymbol{P} \in \mathbb{R}^{2(m-d) \times 2(m-d)}$ is the solution of the algebraic Riccati equation

$$\tilde{\boldsymbol{A}}_{\boldsymbol{z}}^T \boldsymbol{P} + \boldsymbol{P}\tilde{\boldsymbol{A}}_{\boldsymbol{z}} - \boldsymbol{P}\boldsymbol{B_z}\boldsymbol{R}^{-1}\boldsymbol{B_z}\boldsymbol{P} + \tilde{\boldsymbol{Q}} = 0, \tag{6.3.30}$$

with $\tilde{\boldsymbol{A}}_{\boldsymbol{z}} = \boldsymbol{A_z} - \boldsymbol{B_z}\boldsymbol{R}^{-1}\boldsymbol{S}^T$.

Proof:

To prove claim (i), we recall the definitions of $\boldsymbol{A_z}$ and $\boldsymbol{B_z}$ in (6.3.25) to check that

$$\begin{bmatrix} \boldsymbol{B_z} & \boldsymbol{A_z}\boldsymbol{B_z} & \cdots & \boldsymbol{A_z}^{2(m-d)-1}\boldsymbol{B_z} \end{bmatrix} = \begin{bmatrix} \boldsymbol{0} & \boldsymbol{I} & \boldsymbol{0} & \cdots & \boldsymbol{0} \\ \boldsymbol{I} & \boldsymbol{0} & \boldsymbol{0} & \cdots & \boldsymbol{0} \end{bmatrix}, \tag{6.3.31}$$

and so

$$\text{rank}\left\{ \begin{bmatrix} \boldsymbol{B_z} & \boldsymbol{A_z}\boldsymbol{B_z} & \cdots & \boldsymbol{A_z}^{2(m-d)-1}\boldsymbol{B_z} \end{bmatrix} \right\} = 2(m-d), \tag{6.3.32}$$

which means that the pair $(\boldsymbol{A_z}, \boldsymbol{B_z})$ is completely controllable and therefore stabilizable (see Definition A.1).

Claim (ii) follows by noting that $\boldsymbol{T_1}$ has full column rank, and so $\boldsymbol{W_{\dot{r}}} > 0$ implies $\boldsymbol{R} = \boldsymbol{T_1}^T\boldsymbol{W_{\dot{r}}}\boldsymbol{T_1} > 0$ (see e.g. [98, p. 399]).

To prove claim (iii) we note that, provided that $\boldsymbol{W_e}, \boldsymbol{W_r} > 0$, we have $\bar{\boldsymbol{Q}} > 0$ and so $\boldsymbol{E}^T\bar{\boldsymbol{Q}}\boldsymbol{E} > 0$, which implies that $\boldsymbol{Q} = \boldsymbol{E}^T\bar{\boldsymbol{Q}}\boldsymbol{E} + \boldsymbol{T_u}^T\boldsymbol{W_{\dot{r}}}\boldsymbol{T_u} > 0$ (note that $\boldsymbol{T_u}^T\boldsymbol{W_{\dot{r}}}\boldsymbol{T_u} \geq 0$). Using Schur's complement (see e.g. [98, p. 472]), this implies that

$\tilde{Q} = Q - SR^{-1}S^T > 0$ if and only if

$$\tilde{Q}' = \begin{bmatrix} Q & S \\ S^T & R \end{bmatrix} > 0. \tag{6.3.33}$$

From the definitions of Q, R and S in (6.3.27) we get

$$\tilde{Q}' = \begin{bmatrix} E^T \bar{Q} E + T_u{}^T W_{\dot{r}} T_u & T_u{}^T W_{\dot{r}} T_1 \\ T_1{}^T W_{\dot{r}} T_u & T_1{}^T W_{\dot{r}} T_1 \end{bmatrix} > 0. \tag{6.3.34}$$

Let $y = \begin{bmatrix} y_a \\ y_b \end{bmatrix}$ with $y_a \in \mathbb{R}^{2(m-d)}$ and $y_b \in \mathbb{R}^{m-d}$, then

$$\begin{aligned} y^T \tilde{Q}' y &= (E y_a)^T \bar{Q} (E y_a) + (T_u y_a)^T W_{\dot{r}} (T_u y_a) + (T_1 y_b)^T W_{\dot{r}} (T_1 y_b) \\ &\quad + 2 (T_u y_a)^T W_{\dot{r}} (T_1 y_b), \\ &= (E y_a)^T \bar{Q} (E y_a) + (T_u y_a + T_1 y_b)^T W_{\dot{r}} (T_u y_a + T_1 y_b). \end{aligned} \tag{6.3.35}$$

Since E has full column rank, $E y_a = 0$ only for $y_a = 0$, so that $\bar{Q} > 0$ implies $(E y_a)^T \bar{Q} (E y_a) > 0$ for all $y_a \neq 0$. Moreover, $W_{\dot{r}} > 0$ implies that the second term in (6.3.35) is nonnegative, and hence we conclude that $y^T \tilde{Q}' y > 0$ for all $y \neq 0$. This implies $\tilde{Q}' > 0$ and hence claim (iii) follows.

Claims (i)-(iii) imply that Assumption A.1 holds, and therefore the optimal solution is given by Lemma A.2. The result (6.3.29) is a direct consequence of (A.2.14) in Lemma A.2, whereas (6.3.28) follows from $\bar{x} = Ez$ and the definition $\bar{x} = x - x^f$.

□□□

Lemma 6.2 gives the solution to Problem 6.1 provided that $W_e, W_r > 0$. This is a sufficient condition for the matrix $\tilde{Q}$ to be positive definite, which in turn guarantees that the detectability condition for the LQR solution of Lemma A.2 is satisfied. This enables us to compute a stabilizing solution to Problem 6.1 using the classic LQR results [90].

6.4 Example

We illustrate the result of Lemma 6.2 with the metabolic network in Figure 6.1.
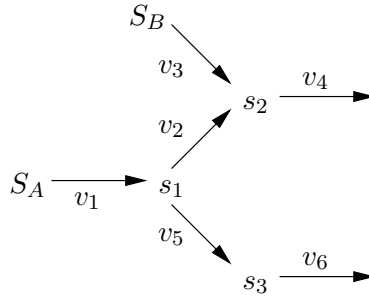
Figure 6.1. Metabolic network with $n = 3$ metabolites and $m = 6$ reactions.

The stoichiometric matrix of this network is

$$N = \begin{bmatrix} 1 & -1 & 0 & 0 & -1 & 0 \\ 0 & 1 & 1 & -1 & 0 & 0 \\ 0 & 0 & 0 & 0 & 1 & -1 \end{bmatrix}. \qquad (6.4.1)$$

The enzyme kinetics are written as $v_i = g_i(s)e_i$ (recall Assumption 2.1 in Chapter 2) and are assumed to be of Michaelis-Menten type:

$$g_1 = \frac{k_{\text{cat}\,1}S_A}{K_{\text{m}\,2} + S_A}, \qquad\qquad g_4 = \frac{k_{\text{cat}\,4}s_2}{K_{\text{m}\,4} + s_2},$$

$$g_2 = \frac{k_{\text{cat}\,2}s_1}{K_{\text{m}\,2} + s_1}, \qquad\qquad g_5 = \frac{k_{\text{cat}\,5}s_1}{K_{\text{m}\,5} + s_1},$$

$$g_3 = \frac{k_{\text{cat}\,3}S_B}{K_{\text{m}\,3} + S_B}, \qquad\qquad g_6 = \frac{k_{\text{cat}\,6}s_3}{K_{\text{m}\,6} + s_3}.$$

The parameter values of the enzyme kinetics are given in Table 6.1. All enzymes are assumed to have the same degradation constant $\lambda = 0.1$ and the external substrates are assumed constant with $S_A = S_B = 1$.

Reaction	v_1	v_2	v_3	v_4	v_5	v_6
$k_{\text{cat}\,i}$	4	2	1	3	4	2
$K_{\text{m}\,i}$	1	1	1	1	1	1

Table 6.1. Parameter values of the metabolic network in Figure 6.1.

The weights are chosen as $\boldsymbol{W_{\dot{r}}} = \boldsymbol{I}$ and

$$\boldsymbol{W_e} = \boldsymbol{W_r} = \begin{bmatrix} 1 & 0 & 0 & 0 & 0 & 0 \\ 0 & 1 & 0 & 0 & 0 & 0 \\ 0 & 0 & 1 & 0 & 0 & 0 \\ 0 & 0 & 0 & 10 & 0 & 0 \\ 0 & 0 & 0 & 0 & 1 & 0 \\ 0 & 0 & 0 & 0 & 0 & 10 \end{bmatrix}. \tag{6.4.2}$$

This choice accounts for the need of fast transient responses in the "output" rates of the network (v_4 and v_6). The metabolite vector is chosen as $s^i = \begin{bmatrix} 1 & 1 & 1 \end{bmatrix}^T$, and the initial and target fluxes are

$$v^i = \begin{bmatrix} 2 & 1.5 & 1 & 2.5 & 0.5 & 0.5 \end{bmatrix}^T,$$
$$v^f = \begin{bmatrix} 3 & 2 & 1.5 & 3.5 & 1 & 1 \end{bmatrix}^T.$$

The enzyme concentrations (e^i and e^f) and the expression rates (r^i and r^f) can be computed directly from (6.2.5)–(6.2.6). Figure 6.2 depicts the optimal enzyme concentrations and expression rates as given by Lemma 6.2. The corresponding reaction rates can be computed from $v = \boldsymbol{G_i} e$ and satisfy $\dot{s} = \boldsymbol{N} v = 0$ for all $t \geq 0$, thus ensuring that the constraint of constant metabolite concentrations is satisfied.

6.5 Discussion

The nonlinearities in the model (6.2.1)–(6.2.2) appear only in the enzyme kinetics contained in the matrix $\boldsymbol{G}(s)$. As a consequence, under the constraint of constant metabolite concentrations the system is linear. This constraint is of stoichiometric nature and is equivalent to parameterizing the enzyme vector in terms of a lower-dimensional state variable. This can be used to recast the optimization as a LQR problem for a nonregular linear DAE system. Linear DAE systems are also known as *descriptor* systems in the control community [99, 100], and have been studied extensively, see e.g. [96, 97]. The LQR problem for regular DAE systems was originally treated in [101, 102], whereas the nonregular case has recently gathered interest, see e.g. [103, 104] and the references therein. The idea behind these methods is essentially to "regularize" the dynamics by introducing suitable state transformations that render a standard lower-dimensional system without algebraic constraints
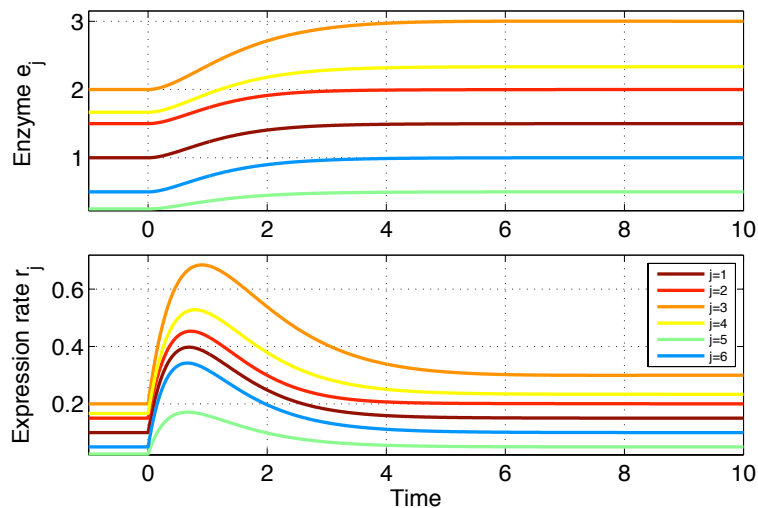
Figure 6.2. Optimal enzyme concentrations and their expression rates for the network in Figure 6.1.

[105].

Here we follow a similar approach and use a state transformation to split the algebraic and differential parts of the DAE system. The advantage is that in our case, the structure of the problem allows us to build the state transformation explicitly in terms of the nullspace of the stoichiometric matrix $\boldsymbol{N}$, the kinetics in $\boldsymbol{G}(s)$, and the matrix of degradation constants $\boldsymbol{\Lambda}$. From the algebraic part, we can parameterize every control input that satisfies the stoichiometric constraint, and thus reduce the problem to an LQR problem for a purely differential lower-dimensional linear system. The solution of this equivalent problem can be readily computed with the classic results presented in Appendix A.2.2. Since we have not made any restrictive assumption on the stoichiometry and reaction kinetics, the solution procedure can be applied to a broad class of metabolic models.

The key step in our derivation is the parameterization of the enzyme vector so as to ensure that the metabolic network (6.2.1) remains in equilibrium (see Lemma 6.1). This parameterization has been used before in the context of the "universal method" for metabolic interventions proposed in [106]. Although a number of extensions to this idea have been described in the literature, see e.g. [107], to our best knowledge these applications have only dealt with static problems. These aim at determining constant enzyme concentrations associated to a prescribed metabolic

flux in the network. Our results extend this idea to a dynamic context, whereby enzyme trajectories guarantee constant metabolites for all $t \geq 0$ and, at the same time, can be optimized so as to drive the network between two given fluxes.

In this view, our approach may be combined with static optimization techniques such as Flux Balance Analysis [52]. Such integration can be thought of as a two-stage optimization process: Once optimal initial and target fluxes are identified via Linear Programming (see Chapter 3), the transition between both can be realized by time-dependent enzyme expression rates that are computed as solutions to Problem 6.1. In order to obtain meaningful solutions, however, the results presented here should be extended to account for positivity and upper bound constraints on the enzyme concentrations and expression rates.

Chapter 7

Summary and outlook

7.1 Framework

Most approaches to dynamic optimization of metabolic networks are based on the stoichiometric model

$$\dot{s} = \boldsymbol{N} v.$$

In this model the vector of metabolite concentrations s is the state variable, and the reaction rates v are regarded as control inputs. Although the linearity of the stoichiometric model is favourable for the formulation and solution of optimal control problems, this description overlooks the dependency of the reaction rates on the metabolites. The reaction rates are typically linear in the enzyme concentration and nonlinear in the concentrations of the metabolites. They can thus be generally written as

$$v_i(s) = g_i(s) e_i,$$

with the nonlinear function $g_i(s)$ describing the saturable behaviour of enzyme e_i. The standard approach for studying metabolic dynamics assumes that the enzyme concentration in the above equation is *constant*, see Chapter 2. In this thesis we have considered *time-dependent* enzyme concentrations by describing the metabolic network as the *nonlinear control-affine system*

$$\dot{s} = \boldsymbol{N}\boldsymbol{G}(s) e,$$

where the nonlinearities of the enzyme kinetics are contained in the diagonal matrix

$$\boldsymbol{G}(s) = \operatorname{diag}\left\{g_1(s), g_2(s), \ldots, g_m(s)\right\}.$$

By regarding the enzyme vector e as a control input to the network, this model is appropriate for carrying out control-theoretic analyses of metabolic networks. To our surprise, although this description of a metabolic network offers certain advantages, it has not been used elsewhere in the literature. Throughout the thesis we used this nonlinear model and exploited its form to pose and solve optimal control problems associated with metabolic dynamics.

7.2 Results and open questions

In Chapter 4 we solved a nonlinear optimal control problem for unbranched networks. The problem statement accounts for the optimal activation of the network from the origin to a prescribed steady state flux under simplex-type constraints on the enzyme concentrations. The optimal enzyme inputs minimize an integral cost that quantifies enzyme usage and the duration of the activation. The cost is linear in the control, and thus the bang-bang form of the solution can be derived from geometric properties of the associated Hamiltonian. Two key elements in this analysis are the network topology and the monotonicity of $g_i(s_i)$ with respect to s_i. These allowed us to show that, for a whole class of monomolecular reaction kinetics, each optimal enzyme input is a single square pulse between zero and the maximum concentration and, moreover, the pulses occur one after another following the same order as the reactions appear in the network.

Previous studies have suggested the optimality of this temporal pattern for specific reaction kinetics [28, 29]. Our results suggest that sequential activation may also appear in more general unbranched networks. From a biological viewpoint, however, switching enzyme concentrations can only be realized by infinitely fast gene expression, and thus a realistic analysis must also take enzyme dynamics into account.

Consequently, we further considered an extended system by coupling the nonlinear model with a linear model for enzyme dynamics

$$\dot{e} = r - \boldsymbol{\Lambda}e.$$

This model accounts for the balance between enzyme expression and degradation, with gene expression represented by a time-dependent vector of expression rates (r), and the degradation assumed proportional to the enzyme concentrations ($\boldsymbol{\Lambda}$ is a diagonal matrix formed by the degradation constants). In the last part of Chapter 4 we explored the optimization of r under box-type constraints via a numerical method for a particular case study. The optimal solution exhibits the same sequential pattern, but its numerical nature does not allow for generalizations. The analytic treatment of this extended problem is an interesting topic for future research. In addition, the analysis has been limited to unbranched networks, and whether other temporal patterns can be identified in more complex topologies remains an open question that deserves further investigation.

In Chapters 5 and 6 we addressed more general topologies and kinetics by considering a different class of optimal control problems. In Chapter 5 we considered the optimization of enzyme expression rates for a quadratic integral cost accounting for the transition between two arbitrary metabolic steady states. The cost function weighs the deviation of metabolites, enzymes and expression rates from their prescribed target values. In contrast to Chapter 4, the problem formulation does not include restrictive assumptions on the stoichiometry and enzyme kinetics. This problem does not admit general solutions, but since the nonlinear model is affine in the enzyme vector, the dynamics of the full model can be written as

$$\dot{x} = \boldsymbol{A}(x)x + \boldsymbol{B}u.$$

Since the cost function also weighs the time-derivative of the expression rates, it is convenient to choose the control as $u = \dot{r}$ and define an extended state variable x composed of the metabolites, enzymes and expression rates. We exploited the form of the above system and introduced a sequence of linear time-variant approximations of the nonlinear dynamics. If the sequence converges, the fixed-point provides a global approximation of the dynamics, which is a considerable improvement over traditional linearization methods. This technique has been used elsewhere for the optimal control of nonlinear systems [33]. In that approach, for each element of the sequence the problem is recast as a Linear Quadratic Tracking (LQT) problem, the solution of which can be obtained by means of a differential Riccati equation. We developed a modified version of this method by approximating the solution of the Riccati equation with that of a differential Lyapunov equation, which is better suited

for high-dimensional systems. The Lyapunov equation approach was proposed in [94] for bilinear systems, and therefore our results extend this idea to a more general class of nonlinear systems.

The sequence of LQT solutions was shown to converge to a suboptimal solution of the original problem. Convergence is ensured for a quite general class of kinetics provided that the optimization horizon is sufficiently small. Unfortunately, in some cases one may need a prohibitively small horizon in order to achieve convergence. An open question is whether this limitation can be overcome by using receding horizon optimization (such as Model Predictive Control techniques [108]) for each linear time-variant system. A receding horizon approach would also allow the inclusion of constraints on the state and control variables, the lack of which is one of the shortcomings of our approach. Nevertheless, we find this approximation method promising for metabolic optimization, since it provides a global approximation and, at the same time, allows the application of methods from linear systems theory.

A special case of the nonlinear problem was addressed in Chapter 6. Under the additional constraint of constant metabolite concentrations and with an infinite time horizon, the problem was recast as a Linear Quadratic Regulator problem for a differential-algebraic equation (DAE) system. This is realized by exploiting the rank deficiency of the stoichiometric matrix, where we can explicitly identify the class of enzyme trajectories that satisfy the constraint. With an appropriate state transformation, the DAE system can be written as a purely differential system in terms of lower-dimensional state and control variables. The solution is then readily available with the classic results for the LQR problem. As in Chapter 5, the lack of hard constraints on the state and control is a drawback of the method, and their inclusion is a promising target for future research.

7.3 Concluding remarks

In this thesis we employed analytic methods from optimal control theory to tackle dynamic optimization problems for metabolic networks. As opposed to numerical approaches, an analytic treatment allows the identification of the solution properties as inherent features of the network, rather than a consequence of fine-tuning the model parameters. This is particularly evident in the results on metabolic activation in Chapter 4, where the sequential behaviour was identified for a whole class of networks.

The application of optimal control methods to the nonlinear model for metabolic dynamics typically yields problems that are analytically intractable for many cases of practical importance. Explicit solutions may be sought using classic formulations such as Pontryagin's Minimum Principle or the Hamilton-Jacobi-Bellman equation. Even if they can be posed as tractable problems, however, this would normally imply constraining the network stoichiometry and kinetics to a few special cases.

We tackled this difficulty by exploiting properties of the model and cost functions so as to recast the problems into tractable formulations. For example, the monotonicity of the enzyme kinetics and the linearity of the cost are key aspects for the results of Chapter 1. Likewise, the control-affine property of the nonlinear model is the basis for Chapter 5, and we took advantage of its stoichiometric structure in Chapter 6.

Apart from kinetic and structural properties, we believe that time-scale separation can also be useful in tackling metabolic optimization problems, because enzyme dynamics operate on comparatively slower time-scales than their metabolic counterpart. This idea has been the basis for optimization problems under *constant* enzyme concentrations, like Flux Balance Analysis or the S-system formulation (see Chapter 3). We remark, however, that the time-scale separation can be used in the reverse direction for *dynamic* optimization: one can pose an optimization problem for the enzyme dynamics and approximate the fast metabolic dynamics by an algebraic function of the enzyme trajectories. In this setup, one needs to optimize the linear model for enzyme dynamics, and the metabolite trajectories can be computed as solutions of the system of nonlinear algebraic equations

$$\boldsymbol{N}\boldsymbol{G}(s)e = 0.$$

It must also be pointed out that, given the large scale of real metabolic networks, the use of dynamic optimization as a practical tool still requires the development of appropriate numerical techniques that can efficiently cope with high-dimensional problems, perhaps in the spirit of recent work in the field [78, 109]. Moreover, since numerical methods typically allow for constraints in the optimization problems, their development will probably become increasingly important for the design of metabolic intervention strategies.

We conclude by observing that the use of Systems and Control ideas in biochemical networks is accompanied by a number of difficulties, among which are the lack of

plant/controller separation and knowledge of the control objectives. In this respect, metabolic networks are amenable to control-theoretic analyses, as their dynamics can be identified as a "plant" that is controlled by the enzyme concentrations. In addition, evolutionary principles suggest optimality as a sensible choice for an underlying control objective. We therefore believe that metabolic optimization is a promising framework for new developments in optimal control theory and may, at the same time, help in understanding biological design principles.

Appendix A

Classical optimal control methods

A.1 Pontryagin's Minimum Principle

In this section we present the necessary conditions for optimality provided by Pontryagin's Minimum Principle [84]. These results can be found in standard textbooks on optimal control theory, e.g. [91]. Consider the system

$$\dot{x} = f\left(x, u\right), \quad x(0) = x^0, \tag{A.1.1}$$

with $x \in \mathbb{R}^n$ and $u \in \mathcal{U} \subseteq \mathbb{R}^m$. Assume that the state has to be driven to $x(t_f) \in \mathcal{S} \subseteq \mathbb{R}^n$ in the time interval $[0, t_f]$. A general optimal control problem is to find a piecewise continuous control $u^* : [0, t_f] \to \mathcal{U}$ that minimizes the cost

$$\mathcal{J} = \int_0^{t_f} L\left(x, u\right) \, \mathrm{d}t, \quad L\left(x, u\right) > 0. \tag{A.1.2}$$

Define the *Hamiltonian* as

$$\mathcal{H}\left(x, u, p\right) = L\left(x, u\right) + p^T f\left(x, u\right), \tag{A.1.3}$$

where $p \in \mathbb{R}^n$ is the co-state vector. Pontryagin's Minimum Principle states that, if an optimal u^* exists, then there exist nontrivial trajectories x^* and p^* such that:

(a) They satisfy the two-point boundary value problem

$$\dot{x}^* = \frac{\partial}{\partial p} \mathcal{H}\left(x^*, u^*, p^*\right), \tag{A.1.4}$$

$$\dot{p}^* = -\frac{\partial}{\partial x} \mathcal{H}\left(x^*, u^*, p^*\right), \tag{A.1.5}$$

subject to the boundary conditions $x^*(0) = x^0$ and $x^*(t_f) \in \mathcal{S}$.

(b) The Hamiltonian is minimized by the optimal control for all $t \in [t_0, t_f]$, i.e.

$$\mathcal{H}\left(x^*(t), u^*(t), p^*(t)\right) = \min_{u \in \mathcal{U}} \mathcal{H}\left(x^*(t), u(t), p^*(t)\right), \quad \forall t \in [t_0, t_f]. \qquad \text{(A.1.6)}$$

(c) The co-state vector is transversal to $\mathcal{S}$ in the final time, i.e.

$$p^{*T}(t_f)\left(q - x^*(t_f)\right) = 0, \quad \forall q \in \mathcal{M}\left(x^*(t_f)\right) \qquad \text{(A.1.7)}$$

where $\mathcal{M}\left(x^*(t_f)\right)$ is the tangent hyper-plane of $\mathcal{S}$ at $x^*(t_f)$.

(d) The Hamiltonian evaluated at the optimal trajectory is constant for all $t \in [0, t_f]$, i.e.

$$\mathcal{H}\left(x^*(t), u^*(t), p^*(t)\right) = C, \quad \forall t \in [0, t_f] \qquad \text{(A.1.8)}$$

Moreover, if the final time t_f is not specified *a priori*, but instead is an outcome of the optimization then $C = 0$ in (A.1.8).

A.2 Linear Quadratic optimization

In this section we briefly present some results on Linear Quadratic optimal control. These are classic results available in standard textbooks on optimal control, e.g. [89, 91, 90].

A.2.1 Finite horizon Linear Quadratic Tracking (LQT) problem

Consider the linear time-variant system

$$\dot{x}(t) = \boldsymbol{A}(t)x(t) + \boldsymbol{B}(t)u(t), \quad x(0) = x^0, \qquad \text{(A.2.1)}$$

$$y(t) = \boldsymbol{C}(t)x(t), \qquad \text{(A.2.2)}$$

where $x(t) \in \mathbb{R}^n$, $u(t) \in \mathbb{R}^m$, $y(t) \in \mathbb{R}^p$, $\boldsymbol{A}(t) \in \mathbb{R}^{n \times n}$, $\boldsymbol{B}(t) \in \mathbb{R}^{n \times m}$, and $\boldsymbol{C}(t) \in \mathbb{R}^{p \times n}$. The entries of $\boldsymbol{A}(t)$, $\boldsymbol{B}(t)$ and $\boldsymbol{C}(t)$ are assumed to be continuous. In the finite horizon LQT problem one seeks for a control $u^*(t)$, $t \in [0, t_f]$, that minimizes the cost

$$\mathcal{J} = \frac{1}{2}\tilde{x}^T(t_f)\boldsymbol{Q_f}\tilde{x}(t_f) + \frac{1}{2}\int_0^{t_f}\left(\tilde{x}^T\boldsymbol{Q}\tilde{x} + u^T\boldsymbol{R}u\right)\,\mathrm{d}t, \qquad \text{(A.2.3)}$$

where $\boldsymbol{Q_f} \in \mathbb{R}^{n\times n}$, $\boldsymbol{Q} = \boldsymbol{Q}(t) \in \mathbb{R}^{n\times n}$, $\boldsymbol{R} = \boldsymbol{R}(t) \in \mathbb{R}^{m\times m}$. The variable $\tilde{x} = y - z$ is the deviation of the output with respect to a signal z that needs to be tracked.

Lemma A.1: *Assume that* $\boldsymbol{Q_f}, \boldsymbol{Q}(t) \geq 0$, $\boldsymbol{R}(t) > 0$ *for all* $t \in [0, t_f]$. *The optimal control* u^* *is given by the linear state feedback*

$$u^*(t) = -\boldsymbol{R}^{-1}(t)\boldsymbol{B}^T(t)\left(\boldsymbol{P}(t)x(t) - q(t)\right), \tag{A.2.4}$$

where $\boldsymbol{P}(t) \in \mathbb{R}^{n\times n}$ *is the solution of the differential Riccati equation*

$$-\dot{\boldsymbol{P}}(t) = \boldsymbol{A}^T(t)\boldsymbol{P}(t) + \boldsymbol{P}(t)\boldsymbol{A}(t) - \boldsymbol{P}(t)\boldsymbol{B}(t)\boldsymbol{R}^{-1}(t)\boldsymbol{B}^T(t)\boldsymbol{P}(t) + \boldsymbol{C}^T(t)\boldsymbol{Q}(t)\boldsymbol{C}(t), \tag{A.2.5}$$

with the terminal condition $\boldsymbol{P}(t_f) = \boldsymbol{C}^T(t_f)\boldsymbol{Q_f}\boldsymbol{C}(t_f)$. *The vector* $q(t) \in \mathbb{R}^n$ *is a feedforward term computed as the solution of the differential equation*

$$\dot{q}(t) = -\left(\boldsymbol{A}(t) - \boldsymbol{B}(t)\boldsymbol{R}^{-1}(t)\boldsymbol{B}^T(t)\boldsymbol{P}(t)\right)^T q(t) - \boldsymbol{C}^T(t)\boldsymbol{Q}(t)z(t), \tag{A.2.6}$$

with the terminal condition $q(t_f) = \boldsymbol{C}^T(t_f)\boldsymbol{Q_f}z(t_f)$. *The optimal state trajectory* x^* *is then the solution of the inhomogeneous system*

$$\dot{x}(t) = \left(\boldsymbol{A}(t) - \boldsymbol{B}(t)\boldsymbol{R}^{-1}(t)\boldsymbol{B}^T(t)\boldsymbol{P}(t)\right)x(t) + \boldsymbol{B}(t)\boldsymbol{R}^{-1}(t)\boldsymbol{B}^T(t)q(t), \quad x(0) = x^0. \tag{A.2.7}$$

A.2.2 Infinite horizon Linear Quadratic Regulator (LQR) problem

Consider the linear time-invariant system

$$\dot{x} = \boldsymbol{A}x + \boldsymbol{B}u, \quad x(0) = x^0, \tag{A.2.8}$$

where $x \in \mathbb{R}^n$, $u \in \mathbb{R}^m$, $\boldsymbol{A} \in \mathbb{R}^{n\times n}$, and $\boldsymbol{B} \in \mathbb{R}^{n\times m}$. In the infinite horizon LQR problem one seeks for a control $u^* : [0, \infty) \to \mathbb{R}^m$, that minimizes the quadratic cost

$$\mathcal{J} = \frac{1}{2}\int_0^\infty \left(x^T\boldsymbol{Q}x + u^T\boldsymbol{R}u + 2x^T\boldsymbol{S}u\right)\,\mathrm{d}t, \tag{A.2.9}$$

where $\boldsymbol{Q} \in \mathbb{R}^{n\times n}$, $\boldsymbol{S} \in \mathbb{R}^{n\times m}$, and $\boldsymbol{R} \in \mathbb{R}^{m\times m}$. This problem can be seen as a special case of the finite horizon LQT problem of the previous section (by taking $z = 0$ and

letting $t_f \rightarrow \infty$). In the infinite horizon case, however, the optimal solution must also ensure asymptotic stability of (A.2.8) under the optimal control. This can be done by imposing additional assumptions on the systems and weighting matrices. To that end we need the following standard definitions.

Definition A.1: *Let $\boldsymbol{A} \in \mathbb{R}^{n \times n}$, $\boldsymbol{B} \in \mathbb{R}^{n \times p}$, and $\boldsymbol{C} \in \mathbb{R}^{q \times n}$.*

(a) The pair $(\boldsymbol{A}, \boldsymbol{B})$ is completely controllable *if and only if*

$$\text{rank}\left\{ \begin{bmatrix} \boldsymbol{B} & \boldsymbol{AB} & \cdots & \boldsymbol{A}^{n-1}\boldsymbol{B} \end{bmatrix} \right\} = n. \tag{A.2.10}$$

Likewise, the pair $(\boldsymbol{A}, \boldsymbol{C})$ is completely observable *if and only if $(\boldsymbol{A}^T, \boldsymbol{C}^T)$ is completely controllable.*

(b) If $(\boldsymbol{A}, \boldsymbol{B})$ is not completely controllable, then every $\lambda \in \mathbb{R}$ such that

$$\text{rank}\left\{ \begin{bmatrix} \lambda\boldsymbol{I} - \boldsymbol{A} & \boldsymbol{B} \end{bmatrix} \right\} < n, \tag{A.2.11}$$

is an uncontrollable mode *of $(\boldsymbol{A}, \boldsymbol{B})$. The* unobservable modes *of the pair $(\boldsymbol{A}, \boldsymbol{C})$ are defined analogously.*

(c) The pair $(\boldsymbol{A}, \boldsymbol{B})$ is stabilizable *if and only if every uncontrollable mode is stable ($\text{Re}\lambda < 0$), and $(\boldsymbol{A}, \boldsymbol{C})$ is* detectable *if and only if, every unobservable mode is stable ($\text{Re}\lambda < 0$). Note that complete controllability (observability) implies stabilizability (detectability).*

Assumption A.1: *Define $\tilde{\boldsymbol{A}} = \boldsymbol{A} - \boldsymbol{B}\boldsymbol{R}^{-1}\boldsymbol{S}^T$ and $\tilde{\boldsymbol{Q}} = \boldsymbol{Q} - \boldsymbol{S}\boldsymbol{R}^{-1}\boldsymbol{S}^T$:*

(a) $\boldsymbol{R} > 0$ and $\tilde{\boldsymbol{Q}} \geq 0$.

(b) The pair $(\boldsymbol{A}, \boldsymbol{B})$ is stabilizable.

(c) The pair $(\tilde{\boldsymbol{A}}, \tilde{\boldsymbol{Q}}^{\frac{1}{2}})$ is detectable, where $\tilde{\boldsymbol{Q}}^{\frac{1}{2}}$ is such that $\tilde{\boldsymbol{Q}}^{\frac{1}{2}^T}\tilde{\boldsymbol{Q}}^{\frac{1}{2}} = \tilde{\boldsymbol{Q}}$.

Note that if $\tilde{\boldsymbol{Q}} > 0$, (c) is automatically satisfied.

Lemma A.2: *Under Assumption A.1, the optimal control u^* is stabilizing and given by the linear state feedback*

$$u^* = -\boldsymbol{R}^{-1}\left(\boldsymbol{B}^T\boldsymbol{P} + \boldsymbol{S}^T \right)x, \tag{A.2.12}$$

where the matrix $\boldsymbol{P} \in \mathbb{R}^{n \times n}$ is the non-negative solution of the algebraic Riccati equation

$$\tilde{\boldsymbol{A}}^T \boldsymbol{P} + \boldsymbol{P} \tilde{\boldsymbol{A}} - \boldsymbol{P} \boldsymbol{B} \boldsymbol{R}^{-1} \boldsymbol{B}^T \boldsymbol{P} + \tilde{\boldsymbol{Q}} = 0. \tag{A.2.13}$$

The optimal state trajectory x^* is then the solution of the homogeneous system

$$\dot{x} = \left(\tilde{\boldsymbol{A}} - \boldsymbol{B} \boldsymbol{R}^{-1} \boldsymbol{B}^T \boldsymbol{P} \right) x, \quad x(0) = x^0. \tag{A.2.14}$$

Appendix B

Fixed-point theorem

In this appendix we present a fixed-point theorem that is used to study the convergence properties of Algorithm 5.1 in Chapter 5. Let $\mathcal{C}\left([0, t_f], \mathbb{K}\right)$ be the set of continuous functions $f(t) : [0, t_f] \to \mathbb{K}$, and define two Banach spaces $\mathbb{B}_1 = \mathcal{C}\left([0, t_f], \mathbb{R}^p\right)$, $\mathbb{B}_2 = \left([0, t_f], \mathbb{R}^{p \times p}\right)$ with the submultiplicative function norms

$$||f|| = \sup_{t \in [0, t_f]} ||f(t)||_E, \, f \in \mathbb{B}_1, \tag{B.1.1}$$

$$||\boldsymbol{F}|| = \sup_{t \in [0, t_f]} ||\boldsymbol{F}(t)||_E, \, \boldsymbol{F} \in \mathbb{B}_2, \tag{B.1.2}$$

where $||\cdot||_E$ denotes the Euclidean norm for vectors, $||f(t)||_E = \left(\operatorname{tr}\left\{f^T(t)f(t)\right\}\right)^{\frac{1}{2}}$, or matrices $, ||\boldsymbol{F}(t)||_E = \left(\operatorname{tr}\left\{\boldsymbol{F}^T(t)\boldsymbol{F}(t)\right\}\right)^{\frac{1}{2}}$. We define the operators

$$T_1 : \mathbb{B}_1 \times \mathbb{B}_2 \to \mathbb{B}_1, \tag{B.1.3}$$

$$(x, \boldsymbol{P}) \to T_1(x, \boldsymbol{P}),$$

$$T_2 : \mathbb{B}_1 \times \mathbb{B}_2 \to \mathbb{B}_2, \tag{B.1.4}$$

$$(x, \boldsymbol{P}) \to T_2(x, \boldsymbol{P}), \tag{B.1.5}$$

and the following properties.

Definition B.1:

(a) The subsets $\mathbb{D}_1 \subseteq \mathbb{B}_1$ and $\mathbb{D}_2 \subseteq \mathbb{B}_2$ are called invariant under T_1 and T_2 *if*

$$T_1(x, \boldsymbol{P}) \in \mathbb{D}_1, \tag{B.1.6}$$

$$T_2(x, \boldsymbol{P}) \in \mathbb{D}_2, \tag{B.1.7}$$

for all $x \in \mathbb{D}_1$ and $\boldsymbol{P} \in \mathbb{D}_2$.

(b) The operators T_1 and T_2 are called contractive in $\mathbb{B}_1 \times \mathbb{B}_2$ *if there exists $\boldsymbol{M} \in \mathbb{R}^{2 \times 2}$ with eigenvalues $|\lambda_i| < 1$, $i = 1, 2$, such that the following inequality holds component-wise*

$$
\begin{bmatrix} ||T_1(x_1, \boldsymbol{P_1}) - T_1(x_2, \boldsymbol{P_2})|| \\ ||T_2(x_1, \boldsymbol{P_1}) - T_2(x_2, \boldsymbol{P_2})|| \end{bmatrix} \leq \boldsymbol{M} \begin{bmatrix} ||x_1 - x_2|| \\ ||\boldsymbol{P_1} - \boldsymbol{P_2}|| \end{bmatrix}, \tag{B.1.8}
$$

for all $x_1, x_2 \in \mathbb{B}_1$ and $\boldsymbol{P_1}, \boldsymbol{P_2} \in \mathbb{B}_2$.

Theorem B.1: *Consider the two operators T_1 and T_2 and assume that there exist sets $\mathbb{D}_1$, $\mathbb{D}_2$ that are invariant under T_1 and T_2. Let $x^{(0)} \in \mathbb{D}_1$ and $\boldsymbol{P^{(0)}} \in \mathbb{D}_2$. Then, if T_1 and T_2 are contractive in $\mathbb{B}_1 \times \mathbb{B}_2$, the iteration*

$$
x^{(k+1)} = T_1 \left(x^{(k)}, \boldsymbol{P^{(k)}} \right), \tag{B.1.9}
$$

$$
\boldsymbol{P^{(k+1)}} = T_2 \left(x^{(k)}, \boldsymbol{P^{(k)}} \right), \tag{B.1.10}
$$

is convergent and the sequences $\left\{ x^{(k)} \right\}$, $\left\{ \boldsymbol{P^{(k)}} \right\}$ converge to a unique fixed-point $(x^*, \boldsymbol{P^*}) \in \mathbb{D}_1 \times \mathbb{D}_2$, i.e.

$$
\lim_{k \to \infty} \left|\left| x^{(k)} - x^* \right|\right| = 0, \qquad T_1 \left(x^*, \boldsymbol{P^*} \right) = x^*, \tag{B.1.11}
$$

$$
\lim_{k \to \infty} \left|\left| \boldsymbol{P^{(k)}} - \boldsymbol{P^*} \right|\right| = 0, \qquad T_2 \left(x^*, \boldsymbol{P^*} \right) = \boldsymbol{P^*}. \tag{B.1.12}
$$

Proof:

The proof can be found in [93].

$\square\square\square$

Remark B.1: *For completeness, Theorem B.1 has been stated exactly as in the original source [93]. However, for our purposes it suffices to take $\mathbb{D}_1 = \mathbb{B}_1$ and $\mathbb{D}_2 = \mathbb{B}_2$, which by definition are the image sets of T_1 and T_2, and hence invariant. In this case we can use Theorem B.1 without checking the existence of invariant sets.*

Nomenclature

$\mathbf{0}$ Zero matrix of appropriate dimensions.

$\mathbf{\Lambda}$ Diagonal matrix of enzyme degradation constants.

$\boldsymbol{A} > 0$ Positive definite matrix.

$\boldsymbol{A} \geq 0$ Positive semidefinite matrix.

$\boldsymbol{A}^+$ Moore-Penrose pseudoinverse of $\boldsymbol{A}$.

$\boldsymbol{G}(s)$ Diagonal matrix of enzyme turnover rates.

$\boldsymbol{I}$ Identity matrix of appropriate dimensions.

$\boldsymbol{K}$ Matrix with columns spanning the nullspace of $\boldsymbol{N}$.

$\boldsymbol{N}$ Stoichiometric matrix of a metabolic network.

$\ker\{\boldsymbol{A}\}$ Nullspace of $\boldsymbol{A}$.

λ_i Degradation constant of enzyme e_i.

$\mathbb{R}^{n \times m}$ Set of $n \times m$ matrices with real entries.

$\mathbb{R}^n$ Set of n-dimensional vectors with real components.

$\mathbb{R}^n_{>0}$ Set of n-dimensional vectors with real positive components.

$\mathbb{R}^n_{\geq 0}$ Set of n-dimensional vectors with real nonnegative components.

$\mathbb{Z}^{n \times m}$ Set of $n \times m$ matrices with integer entries.

$\operatorname{tr}\{\boldsymbol{A}\}$ Trace of matrix $\boldsymbol{A}$.

$||\boldsymbol{A}||_E$ Euclidean norm of matrix $\boldsymbol{A}$.

$||x||_E$ Euclidean norm of vector x.

$||\boldsymbol{F}||$ Norm of a matrix-valued function $\boldsymbol{F}(t)$, see (B.1.2).

$||f||$ Norm of a vector-valued function $f(t)$, see (B.1.1).

e Enzyme vector of a metabolic network.

g_i Enzyme turnover rate of reaction v_i.

r Vector of enzyme expression rates.

s Metabolite vector of a metabolic network.

v Reaction rate vector of a metabolic network.

References

[1] J. Stelling, U. Sauer, Z. Szallasi, F. Doyle, and J. Doyle, "Robustness of cellular functions," *Cell*, vol. 118, pp. 675–685, 2004.

[2] N. Wiener, *Cybernetics*. Wiley, 1948.

[3] E. D. Sontag, "Molecular systems biology and control," *European Journal of Control*, vol. 11, pp. 1–40, 2005.

[4] P. Wellstead, E. Bullinger, D. Kalamatianos, O. Mason, and M. Verwoerd, "The role of control and systems theory in systems biology," *Annual reviews in control*, vol. 32, pp. 33–47, 2008.

[5] P. A. Iglesias and B. P. Ingalls, Eds., *Control Theory and Systems Biology*. MIT Press, 2009.

[6] E. Andrianantoandro, S. Basu, D. Karig, and R. Weiss, "Synthetic biology: new engineering rules for an emerging discipline," *Molecular Systems Biology*, vol. 2, 2006.

[7] L. von Bertalanffy, "The theory of open systems in physics and biology," *Science*, vol. 111, no. 2872, pp. 23–29, 1950.

[8] M. D. Mesarović, *Systems theory and biology*. Springer-Verlag, 1968.

[9] E. D. Sontag, "Some new directions in control theory inspired by systems biology," *Systems Biology*, vol. 1, pp. 9–18, 2004.

[10] M. E. Csete and J. C. Doyle, "Reverse engineering of biological complexity," *Science*, vol. 295, no. 5560, pp. 1664–1669, 2002.

[11] H. Kitano, "Systems biology: a brief overview," *Science*, vol. 295, no. 5560, pp. 1662–1664, 2002.

[12] U. Alon, *An introduction to systems biology: design principles of biological circuits.* Chapman & Hall/CRC, 2006.

[13] G. A. Parker and J. M. Smith, "Optimality theory in evolutionary biology," *Nature*, vol. 348, pp. 27–33, 1990.

[14] J. M. Smith, "Optimization theory in evolution," *Annual Review of Ecology and Systematics*, vol. 9, pp. 31–56, 1978.

[15] R. Rosen, *Optimality principles in biology.* Butterworth, 1967.

[16] R. M. Alexander, *Optima for animals.* Princeton University Press, Princeton, 1996.

[17] W. J. Sutherland, "The best solution," *Nature*, vol. 435, p. 569, 2005.

[18] R. Heinrich, S. Schuster, and H.-G. Holzhütter, "Mathematical analysis of enzymatic reaction systems using optimization principles," *European Journal of Biochemistry*, vol. 201, pp. 1–21, 1991.

[19] A. Lehninger, D. L. Nelson, and M. M. Cox, *Principles of Biochemistry*, 5th ed. W. H. Freeman, 2008.

[20] B. Alberts, J. Wilson, A. Johnson, J. Hunt, M. Raff, and K. Roberts, *Molecular biology of the cell*, 5th ed. Garland Science, 2007.

[21] M. A. Savageau, "A theory of alternative designs for biochemical control systems," *Biomedica Biochimica Acta*, vol. 44, no. 6, pp. 875–880, 1985.

[22] ——, *Biochemical Systems Analysis: a Study of Function and Design in Molecular Biology.* Addison-Wesley, Reading, MA, 1976.

[23] R. Heinrich and S. Schuster, "The modelling of metabolic systems. structure, control and optimality," *BioSystems*, vol. 47, pp. 61–77, 1998.

[24] H.-G. Holzhütter, "The principle of flux minimization and its application to estimate stationary fluxes in metabolic networks," *European Journal of Biochemistry*, vol. 271, pp. 2905–2922, 2004.

[25] A. Cornish-Bowden, *The Pursuit of Perfection: Aspects of Biochemical Evolution.* Oxford University Press, USA, 2004.

[26] P. Smolen, D. A. Baxter, and J. H. Byrne, "Modeling transcriptional control in gene networks—methods, recent results, and future directions," *Bulletin of Mathematical Biology*, vol. 62, pp. 247–292, 2000.

[27] D. Fell, *Understanding the Control of Metabolism*, ser. Frontiers in Metabolism 2, K. Snell, Ed. Portland Press, London, 1997.

[28] E. Klipp, R. Heinrich, and H. G. Holzhütter, "Prediction of temporal gene expression : metabolic optimization by re-distribution of enzyme activities," *European Journal of Biochemistry*, vol. 269, pp. 5406–5413, 2002.

[29] A. Zaslaver, A. Mayo, R. Rosenberg, P. Bashkin, H. Sberro, M. Tsalyuk, M. Surette, and U. Alon, "Just-in-time transcription program in metabolic pathways," *Nature Genetics*, vol. 36, no. 5, pp. 486–491, May 2004.

[30] D. Ropers, H. de Jong, M. Page, D. Schneider, and J. Geiselmann, "Qualitative simulation of the carbon starvation response in *Escherichia coli*," *BioSystems*, vol. 84, pp. 124–152, 2006.

[31] R. Ibarra, J. Edwards, and B. Palsson, "*Escherichia coli* K-12 undergoes adaptive evolution to achieve in silico predicted optimal growth." *Nature*, vol. 420, pp. 186–189, 2002.

[32] K. Bettenbrock, S. Fischer, A. Kremling, K. Jahreis, T. Sauter, and E. Gilles, "A quantitative approach to catabolite repression in *Escherichia coli*," *Journal of Biological Chemistry*, vol. 281, no. 5, pp. 2578–2584, 2006.

[33] T. Çimen and S. P. Banks, "Nonlinear optimal tracking control with application to super-tankers for autopilot design," *Automatica*, vol. 40, pp. 1845–1863, 2004.

[34] B. Meibohm, *Pharmacokinetics and Pharmacodynamics of Biotech Drugs: Principles and Case Studies in Drug Development.* Wiley VCH, 2006.

[35] B.-F. Krippendorff, Ph.D. dissertation, National University of Ireland Maynooth, 2009.

[36] R. Heinrich and S. Schuster, *The regulation of cellular systems.* Chapman & Hall, 1996.

[37] E. Klipp, R. Herwig, A. Kowald, C. Wierling, and H. Lehrach, *Systems Biology in Practice: Concepts, Implementation and Application*. Wiley-Vch, 2005.

[38] T. E. Turner, S. Schnell, and K. Burrage, "Stochastic approaches for modelling in vivo reactions," *Computational Biology and Chemistry*, vol. 28, pp. 165–178, 2004.

[39] A. Cornish-Bowden, *Fundamentals of Enzyme Kinetics*, 3rd ed. Portland Press, 2004.

[40] E. Meléndez-Hevia, N. Torres, and J. Sicilia, "A generalization of metabolic control analysis to conditions of no proportionality between activity and concentrations of enzymes." *Journal of Theoretical Biology*, vol. 142, pp. 443–451, 1990.

[41] B. Palsson, *Systems Biology: Properties of reconstructed networks*. Cambridge University Press, 2006.

[42] H. de Jong, "Modeling and simulation of genetic regulatory systems: a literature review," *Journal of Computational Biology*, vol. 9, pp. 67–103, 2002.

[43] M. Ronen, R. Rosenberg, B. Shraiman, and U. Alon, "Assigning numbers to the arrows: parameterizing a gene regulation network by using accurate expression kinetics," *Proceedings of the National Academy of Sciences*, vol. 99, pp. 10 555–10 560, 2002.

[44] D. Lebiedz, "Exploiting optimal control for target-oriented manipulation of (bio)chemical systems: A model-based approach to specific modification of self-organized dynamics," *International Journal of Modern Physics B*, vol. 19, no. 25, pp. 3763–3798, 2005.

[45] J. R. Banga, "Optimization in computational systems biology," *BMC Systems Biology*, vol. 2, no. 47, 2008.

[46] G. Stephanopoulos, A. Aristidou, and J. Nielsen, *Metabolic Engineering. Principles and Methodologies*. Academic Press, 1998.

[47] N. Torres and E. Voit, *Pathway analysis and Optimization in Metabolic Engineering*. Cambridge University Press, 2002.

[48] J. E. Bailey, "Toward a science of metabolic engineering," *Science*, vol. 252, no. 5013, pp. 1668–1675, 1991.

[49] "Metabolic engineering in the post genomic era," B. N. Kholodenko and H. V. Westerhoff, Eds. Horizon Biosciences, Norfolk, England, 2004.

[50] W. Wiechert, "Modeling and simulation: tools for metabolic engineering," *Journal of Biotechnology*, vol. 94, pp. 37–63, 2002.

[51] A. P. Burgard, P. Pharkya, and C. D. Maranas, "Optknock: A bilevel programming framework for identifying gene knockout strategies for microbial strain optimization," *Biotechnology and Bioengineering*, vol. 84, no. 6, pp. 647–657, 2003.

[52] A. Varma and B. Palsson, "Metabolic flux balancing: Basic concepts, scientific and practical use," *Bio/Technology*, vol. 12, pp. 994–998, 1994.

[53] J. M. Savinell and B. O. Palsson, "Network analysis of intermediary metabolism using linear optimization. I. Development of mathematical formalism." *Journal of Theoretical Biology*, vol. 154, no. 4, pp. 421–454, 1992.

[54] I. Famili, J. Förster, J. Nielsen, and B. O. Palsson, "*Saccharomyces cerevisiae* phenotypes can be predicted by using constraint-based analysis of a genome–scale reconstructed metabolic network," *Proceedings of the National Academy of Sciences*, vol. 100, no. 23, pp. 13 134–13 139, 2003.

[55] R. Schuetz, L. Kuepfer, and U. Sauer, "Systematic evaluation of objective functions for predicting intracellular fluxes in *Escherichia coli*," *Molecular Systems Biology*, vol. 3, no. 119, 2007.

[56] J. Nielsen, "Principles of optimal network operation," *Molecular Systems Biology*, vol. 3, no. 126, 2007.

[57] S. Schuster, T. Pfeiffer, and D. Fell, "Is maximization of molar yield in metabolic networks favoured by evolution?" *Journal of Theoretical Biology*, vol. 252, no. 3, pp. 497–504, 2008.

[58] J. S. Edwards, R. U. Ibarra, and B. O. Palsson, "*In silico* predictions of *Escherichia coli* metabolic capabilities are consistent with experimental data," *Nature Biotechnology*, vol. 19, pp. 125–130, 2001.

[59] T. F. Cooper, D. E. Rozen, and R. E. Lenski, "Parallel changes in gene expression after 20,000 generations of evolution in *Escherichia coli*," *Proceedings of the National Academy of Sciences*, vol. 100, no. 3, pp. 1072–1077, 2003.

[60] A. Varma and B. O. Palsson, "Stoichiometric flux balance models quantitatively predict growth and metabolic by-product secretion in wild-type *Escherichia coli* W3110," *Applied Environmental Microbiology*, vol. 60, no. 10, pp. 3724–3731, 1994.

[61] K. J. Kauffman, P. Prakash, and J. S. Edwards, "Advances in flux balance analysis," *Current Opinion in Biotechnology*, vol. 14, pp. 491–496, 2003.

[62] E. O. Voit, *Computational Analysis of Biochemical Systems. A Practical Guide for Biochemists and Molecular Biologists.* Cambridge University Press, 2000.

[63] V. Hatzimanikatis, C. A. Floudas, and J. E. Bailey, "Optimization of regulatory architectures in metabolic reaction networks," *Biotechnology and Bioengineering*, vol. 52, no. 4, pp. 485 – 500, 1996.

[64] J. Vera, P. de Atauri, M. Cascante, and N. Torres, "Multicriteria optimization of biochemical systems by linear programming: application to production of ethanol by *Saccharomyces cerevisiae*," *Biotechnology and Bioengineering*, vol. 83, pp. 335–343, 2003.

[65] E. Klipp and R. Heinrich, "Competition for enzymes in metabolic pathways: Implications for optimal distributions of enzyme concentrations and for the distribution of flux control," *BioSystems*, vol. 54, pp. 1–14, 1999.

[66] G. Pettersson, "Effect of evolution on the kinetic properties of enzymes," *European Journal of Biochemistry*, vol. 184, pp. 561–566, 1989.

[67] E. Klipp and R. Heinrich, "Evolutionary optimisation of enzyme kinetic parameters: the effect of constraints," *Journal of Theoretical Biology*, vol. 171, pp. 309–323, 1994.

[68] B. S. Adiwijaya, P. I. Barton, and B. Tidor, "Biological network design strategies: discovery through dynamic optimization," *Molecular BioSystems*, vol. 2, pp. 650–659, 2006.

[69] G. Brown, "Total cell protein concentration as an evolutionary constraint on the metabolic control distribution in cells," *Journal of Theoretical Biology*, vol. 153, pp. 195–203, 1991.

[70] E. Dekel and U. Alon, "Optimality and evolutionary tuning of the expression level of a protein," *Nature*, vol. 436, pp. 588–592, 2005.

129

[71] N. Campbell, "Timing is everything," *Nature Reviews Genetics*, vol. 5, p. 405, 2004.

[72] J. Ou, T. Yamada, K. Nagahis, T. Hirasawa, C. Furusawa, T. Yomo, and H. Shimizu, "Dynamic change in promoter activation during lysine biosynthesis in *Escherichia coli* cells," *Molecular BioSystems*, vol. 4, pp. 128–134, 2008.

[73] S. Kalir, J. McClure, K. Pabbaraju, C. Southward, M. Ronen, S. Leibler, M. G. Surette, and U. Alon, "Ordering genes in a flagella pathway by analysis of expression kinetics from living bacteria," *Science*, vol. 292, pp. 2080–2083, 2001.

[74] X. Leng and H.-G. Müller, "Time ordering of gene coexpression," *Biostatistics*, vol. 7, no. 4, pp. 569–584, 2006.

[75] M. Giuseppin and N. van Riel, "Metabolic modeling of *Saccharomyces cerevisiae* using the optimal control of homeostasis: A cybernetic model definition." *Metabolic Engineering*, vol. 2, pp. 14–33, 2000.

[76] N. van Riel, M. Giuseppin, and C. Verrips, "Dynamic optimal control of homeostasis: an integrative systems approach for modeling of the central nitrogen metabolism in *Saccharomyces cerevisiae*," *Metabolic Engineering*, vol. 2, pp. 14–33, 2000.

[77] J. Varner and D. Ramkrishna, "Metabolic engineering from a cybernetic perspective.1. Theoretical preliminaries," *Biotechnology Progress*, vol. 15, pp. 407–425, 1999.

[78] R. Mahadevan, J. Edwards, and F. Doyle, "Dynamic flux balance analysis of diauxic growth in *Escherichia coli*," *Biophysical Journal*, vol. 83, pp. 1331–1340, 2002.

[79] J. E. Cuthrell and L. T. Biegler, "On the optimization of differential algebraic process systems," *AIChE Journal*, vol. 33, pp. 1257–1270, 1987.

[80] K. Uygun and Y. L. Huang, "A dynamic cybernetic approach: Optimal control for predicting regulatory metabolism actions," in *Proceedings of the AIChE Annual National Meeting, San Franciso, CA*, 2003, pp. 16–21.

[81] K. Uygun, H. Matthew, and Y. Huang, "DFBA-LQR: An optimal control approach to flux balance analysis," *Industrial & Engineering Chemical Research*, vol. 45, pp. 8554–8564, 2006.

[82] M. Lloréns, J. Nuno, Y. Rodríguez, E. Meléndez-Hevia, and F. Montero, "Generalization of the theory of transition times in metabolic pathways: a geometrical approach," *Biophysical Journal*, vol. 77, pp. 22–36, 1999.

[83] N. Torres, "Application of the transition time of metabolic systems as a criterion for optimization of metabolic processes," *Biotechnology and Bioengineering*, vol. 44, pp. 291–296, 1994.

[84] L. S. Pontryagin, V. Boltyanskii, R. Gamkrelidze, and F. Mischenko, *The Mathematical Theory of Optimal Processes*, L. Neustadt, Ed. New York: Wiley, 1962, (transl. by K.N. Tririgoff).

[85] D. Oyarzún, B. Ingalls, and D. Kalamatianos, "Optimal metabolic regulation by time varying enzyme activities: a control theoretic approach," in *Proceedings of Foundations of Systems Biology & Engineering, Stuttgart, Germany*, 2007.

[86] P. Rutquist and M. Edvall, *PROPT - Matlab Optimal Control Software*, Tomlab Optimization Inc., 260 SE Bishop Blvd Ste E, Pullman, WA 99163, USA, February 2009.

[87] M. Chaves, R. Albert, and E. Sontag, "Robustness and fragility of Boolean models for genetic regulatory network," *Journal of Theoretical Biology*, vol. 235, pp. 431–449, 2005.

[88] S. P. Banks and K. Dinesh, "Approximate optimal control and stability of nonlinear finite- and infinite-dimensional systems," *Annals of Operations Research*, vol. 98, pp. 19–44, 2000.

[89] M. Athans and P. Falb, *Optimal Control*. McGraw Hill Book Company, 1966.

[90] B. Anderson and J. Moore, *Optimal Control: Linear Quadratic Methods*. Englewood Cliffs, New Jersey: Prentice Hall, 1989.

[91] D. Kirk, *Optimal control theory: an introduction*. Prentice-Hall Englewood Cliffs, New Jersey, USA., 1970.

[92] T. Kailath, *Linear Systems*. Englewood Cliffs, New Jersey: Prentice-Hall, 1980.

[93] E. Hofer and B. Tibken, "An iterative method for the finite-time bilinear-quadratic control problem," *Journal of Optimization Theory and Applications*, vol. 57, pp. 411–427, 1988.

[94] Z. Aganovic and Z. Gajic, "The successive approximation procedure for finite-time optimal control of bilinear systems," *IEEE Transactions on Automatic Control*, vol. 39, no. 9, pp. 1932–1935, 1994.

[95] X. Xu and S. K. Agrawal, "Finite-time optimal control of polynomial systems using successive suboptimal approximations," *Journal of Optimization Theory and Applications*, vol. 105, no. 2, pp. 477–489, May 2000.

[96] S. L. Campbell, *Singular systems of differential equations.* Pitman, Boston, 1980.

[97] P. Kunkel and V. Mehrmann, *Differential-algebraic equations: analysis and numerical solution.* European Mathematical Society, 2006.

[98] R. A. Horn and C. R. Johnson, *Matrix Analysis.* Cambridge University Press, 1990.

[99] D. Luenberger, "Dynamic equations in descriptor form," *IEEE Transactions on Automatic Control*, vol. 22, no. 3, pp. 312–321, 1977.

[100] F. L. Lewis, "A survey of linear singular systems," *Circuits, Systems, and Signal Processing*, vol. 5, no. 1, pp. 3–36, 1986.

[101] D. Cobb, "Descriptor variable systems and optimal state regulation," *IEEE Transactions on Automatic Control*, vol. 28, no. 5, pp. 601–611, 1983.

[102] D. J. Bender and A. J. Laub, "The linear-quadratic optimal regulator for descriptor systems," *IEEE Transactions on Automatic Control*, vol. 32, no. 8, pp. 672–688, 1987.

[103] P. Kunkel and V. Mehrmann, "The linear quadratic optimal control problem for linear descriptor systems with variable coefficients," *Mathematics of Control, Signals, and Systems*, vol. 10, no. 3, pp. 247–264, 1997.

[104] J. Zhu, S. Ma, and Z. Cheng, "Singular LQ problem for nonregular descriptor systems," *IEEE Transactions on Automatic Control*, vol. 47, no. 7, pp. 1128–1133, 2002.

[105] R. Byers, P. Kunkel, and V. Mehrmann, "Regularization of linear descriptor systems with variable coefficients," *SIAM Journal on Control and Optimization*, vol. 35, no. 1, pp. 117–133, 1997.

[106] H. Kacser and L. Acerenza, "A universal method for achieving increases in metabolite production," *Eur. J. Biochem*, vol. 216, pp. 361–367, 1993.

[107] B. N. Kholodenko, M. Cascante, J. B. Hoek, , H. V. Westerhoff, and J. Schwaber, "Metabolic design: how to engineer a living cell to desired metabolite concentrations and fluxes," *Biotechnology and Bioengineering*, vol. 59, pp. 239–247, 1998.

[108] E. F. Camacho and C. Bordons, *Model Predictive Control*. Springer, 2004.

[109] T. Hirmajer, E. Balsa-Canto, and J. R. Banga, "DOTcvpSB, a software toolbox for dynamic optimization in systems biology," *BMC Bioinformatics*, vol. 10:199, 2009.